Drew University

College of Liberal Arts

Functional Analysis of the TunG Protein in the Biosynthetic Pathway of Tunicamycin

A Thesis in Biology

by

John H. Lewis

Submitted in Partial Fulfillment

of the Requirements

for the Degree of

Bachelor of Science

With Specialized Honors in Biology

May 2026

Abstract

Antimicrobial resistance (AMR) poses a critical and escalating threat to global public health. This necessitates the discovery of new antibiotics and a deeper understanding of existing biosynthetic pathways. Tunicamycin is a nucleoside antibiotic that inhibits bacterial cell wall biosynthesis by targeting the essential enzyme MraY. However, its clinical utility has historically been limited by toxicity. Recent development of tunicamycin derivatives with reduced cytotoxicity has renewed interest in elucidating the tunicamycin biosynthetic pathway, particularly the roles of poorly characterized enzymes. One such enzyme is the TunG protein, hypothesized to function early in the pathway through nucleotide processing.

This study aimed to characterize experimentally the biochemical activity of the TunG protein using heterologous expression in *Escherichia coli* (*E. coli*). The *tunG* gene was codon-optimized, cloned into a T7 promoter-based expression vector, and expressed in *E. coli* BL21(DE3) cells. The TunG protein was purified via nickel-affinity chromatography and analyzed by SDS-PAGE. This confirmed successful expression but revealed co-purification of endogenous *E. coli* proteins. Enzymatic activity was assessed using High-Performance Liquid Chromatography (HPLC) to monitor reactions with a range of nucleotide substrates, including uridine monophosphate (UMP), adenosine monophosphate (AMP), thymidine monophosphate (TMP), and higher-order uridine nucleotides under varying reaction conditions.

HPLC analyses revealed nucleotide turnover across multiple substrates; however, comparable activity was observed in both TunG-expressing and control samples lacking the *tunG* gene. Metal ion dependence, substrate specificity, and reaction condition profiles were consistent with known *E. coli* nucleotidases, particularly YfbR and SurE, rather than a TunG-specific

activity. Diphosphate and triphosphate substrates, including UDP, UTP, and UDP-GlcNAc, remained largely unprocessed after extended incubation, further suggesting that the endogenous *E. coli* enzymes do not function as a general nucleotide phosphatase.

Collectively, these results indicate that the observed enzymatic activity arises from endogenous *E. coli* enzymes rather than the TunG protein itself. However, this work narrows the range of plausible biochemical functions for TunG and highlights the challenges of characterizing pathway-specific enzymes outside their native biosynthetic context. Future studies will focus on improved purification, alternative substrates, and pathway reconstitution will be essential to fully define the role of the TunG protein in tunicamycin biosynthesis.

Acknowledgements

This thesis is dedicated to those working to confront the growing global threat of antimicrobial resistance, and to the continued pursuit of innovative solutions that may extend the effectiveness of life-saving antibiotics. I would like to express my deepest gratitude to Dr. Anderson for his mentorship, guidance, and unwavering support throughout this project. His insight, patience, and encouragement allowed me to grow not only as a researcher but as a scientist capable of independent thought and problem-solving. I would also like to thank the RISE Fellows program at Drew University for providing the opportunity to engage in extensive, independent research. The experience and resources offered through this program were instrumental in the completion of this work. I am especially grateful to my fellow RISE researchers for their collaboration, feedback, and shared dedication to scientific inquiry. Additionally, I would like to acknowledge the support of the Dean Paolo Cucchi Student Research Grant for helping to fund this project and make this work possible. Finally, I would like to thank the faculty of the Chemistry and Biology departments at Drew University for fostering an environment of curiosity, rigor, and interdisciplinary thinking. Their teaching and mentorship have played a significant role in shaping my academic journey and passion for scientific research.

Table of Contents

I. Introduction

The “golden age” of antibiotics, which transformed medicine in the mid-twentieth century, is widely considered to be over. The widespread and often indiscriminate use of these drugs has accelerated the emergence of antimicrobial resistance (AMR), reducing the effectiveness of many once-reliable treatments. Today, AMR represents one of the most significant global public health challenges of the twenty-first century. The most comprehensive global analysis to date estimates that antibiotic-resistant infections were directly responsible for approximately 1.27 million deaths worldwide in 2019 and associated with nearly 5 million deaths overall.[56] Although global surveillance remains limited, more recent modeling suggests that this burden persists at a comparable scale, with an estimated 1.14 million deaths directly attributable to antimicrobial resistance in 2021.[67]

Despite this growing crisis, the discovery of novel antibiotics has slowed considerably, necessitating alternative approaches such as the modification and optimization of existing antimicrobial scaffolds. One promising candidate is tunicamycin, a nucleoside antibiotic with a well-defined mechanism of action but historically limited clinical utility due to toxicity. Recent advances in tunicamycin-derived compounds have renewed interest in understanding its biosynthetic pathway at the molecular level. In particular, the TunG protein has been proposed to function as a nucleotide-processing enzyme early in this pathway, although its precise biochemical role remains uncharacterized. The objective of this study is to experimentally characterize the enzymatic activity of the TunG protein and define its role within the tunicamycin biosynthetic pathway. By clarifying the function of this enzyme, this work aims to

contribute to a broader effort to enable biosynthetic engineering of tunicamycin and the development of improved antimicrobial compounds.

This thesis begins by establishing the historical context of antibiotic discovery in order to frame the current antimicrobial resistance crisis. The first section provides an overview of what antibiotics are and how they were discovered and developed during the early and mid-twentieth century. Its primary focus is on historical and review literature describing the "golden age" of antibiotic discovery and the rise of natural-product drug screening.[48,50] This section demonstrates how early antibiotic discovery relied heavily on microbial metabolites and fermentation-based screening approaches.

The second section examines how bacteria respond to antibiotic exposure by evolving resistance mechanisms. Using foundational microbiology research on the evolution of antimicrobial resistance, this section explains how mutations, horizontal gene transfer, and selective pressure allow resistant strains to emerge and spread within microbial populations.[51,52] These studies provide the biological basis for understanding why antibiotic effectiveness inevitably declines after widespread clinical use.

After establishing the evolutionary mechanisms behind resistance, the third section evaluates the scale of the antimicrobial resistance crisis today. This portion of the thesis draws on epidemiological reports from organizations such as the World Health Organization and the Centers for Disease Control and Prevention, as well as large-scale global burden studies, to demonstrate the magnitude of resistant infections worldwide and the public health threat they pose.[55,57] These sources illustrate the growing medical and economic consequences of antibiotic resistance.

The fourth section then explores previous attempts to address antimicrobial resistance and explains why many strategies have proven insufficient. Using recent reviews of the antibiotic development pipeline and global policy reports, this section discusses limitations in current antibiotic discovery efforts, including the slowdown in novel antibiotic discovery and the challenges associated with developing new antimicrobial drugs.[48,60]

The fifth section introduces tunicamycin and explains why it represents a promising scaffold for antibiotic development. The first portion provides a biochemical overview of nucleosides and nucleotide-derived molecules to establish the structural basis of nucleoside antibiotics (Figure 4). This background is then used to explain the chemical architecture of tunicamycin itself, highlighting the uridyl nucleoside core, carbohydrate linkage, and variable lipid tail that define the compound's molecular structure (Figure 5).

The next section examines the antibacterial mechanism of tunicamycin. Using schematic and microscopic representations of bacterial cell lysis, this portion illustrates how disruption of peptidoglycan synthesis compromises cell wall integrity and ultimately leads to bacterial death (Figure 6). The molecular basis of this effect is then explored through analysis of the MraY enzyme, a membrane-associated catalyst responsible for forming the lipid-linked peptidoglycan intermediate Lipid I (Figure 7). This step is positioned within the broader peptidoglycan biosynthetic pathway to demonstrate how tunicamycin interrupts an early and essential stage of bacterial cell wall construction (Figure 8). Structural differences between Gram-positive and Gram-negative bacteria are then discussed to explain why tunicamycin exhibits stronger activity against organisms lacking an outer membrane barrier (Figure 9).

Following this mechanistic overview, the discussion shifts to the therapeutic potential of tunicamycin derivatives. Although native tunicamycin displays cytotoxicity in eukaryotic cells, structural modifications of the molecule have produced derivatives with reduced toxicity that still retain antibacterial activity. These modifications, particularly within the lipid chain and nucleobase components, illustrate how rational redesign of the tunicamycin scaffold can decouple antibacterial potency from host toxicity (Figures 10-11). Experimental validation of these derivatives in vivo is then examined through the zebrafish infection model, which enables direct visualization of bacterial burden and host response during treatment (Figure 12). Complementary studies in murine and bovine models further support these findings, demonstrating that tunicamycin derivatives such as TunR2 exhibit improved pharmacokinetic properties, including increased systemic persistence, reduced toxicity, and effective distribution across higher-order organisms (Figure 13).

After establishing tunicamycin as a promising antibiotic scaffold, the focus shifts to the biosynthetic processes responsible for its production in bacteria. An overview of bacterial biosynthetic pathways introduces the concept of gene clusters encoding enzyme networks that assemble complex natural products. This framework leads into a detailed examination of the tunicamycin biosynthetic gene cluster, whose conserved organization across multiple actinomycete species suggests a shared enzymatic strategy for assembling the antibiotic molecule (Figure 14).

The current model of tunicamycin biosynthesis is then presented, outlining the proposed enzymatic sequence that converts nucleotide precursors into lipid-tailed tunicamycin homologs (Figure 15). While this model provides a valuable framework, several enzymatic steps remain

experimentally unverified. In particular, the biochemical activity of the TunG protein remains uncertain despite strong bioinformatic evidence suggesting a nucleotide-processing role.

The final sections therefore focus on evaluating potential catalytic functions of the TunG protein. Sequence homology analysis strongly supports a dephosphorylase model in which the TunG protein converts uridine 5′-monophosphate into uridine during early stages of the pathway (Figure 16). Alternative functional hypotheses, including phosphate rearrangement via mutase activity (Figure 17) and cyclic nucleotide formation through cyclase activity (Figure 18), are considered but appear less consistent with available bioinformatic evidence.

Together, these sections establish the biochemical context necessary to understand tunicamycin biosynthesis and highlight the importance of experimentally characterizing pathway enzymes such as the TunG protein. By clarifying the catalytic role of the TunG protein within this pathway, this work contributes to a broader effort to understand and engineer tunicamycin biosynthesis for the development of improved antimicrobial compounds.

II. Background

The Discovery and Development of Antibiotics

Antibiotics are chemical compounds that inhibit the growth of bacteria or kill them outright, allowing the immune system to clear infections that would otherwise be fatal. These compounds can be produced naturally by microorganisms, chemically synthesized, or derived from natural scaffolds through semi-synthetic modification. The majority of historically important antibiotics were originally discovered as natural products produced by soil bacteria and fungi, particularly members of the genus Streptomyces.[48] These organisms produce antimicrobial compounds as part of ecological competition, and early antibiotic discovery efforts relied heavily on screening environmental microbes for these natural metabolites.[48,49]

The modern antibiotic era began in 1928 when Alexander Fleming discovered penicillin, a compound produced by the fungus *Penicillium notatum*. Although Fleming observed its antibacterial activity, it was not until the early 1940s that penicillin was purified and mass-produced for clinical use during World War II.[50] The success of penicillin triggered an intense period of antibiotic discovery known as the "golden age" of antibiotics between the 1940s and 1960s (Figure 1). During this time, scientists isolated numerous antibiotic classes including streptomycin, tetracyclines, macrolides, and glycopeptides through systematic screening of microbial fermentation products.[48] Over time, antibiotic discovery has evolved from the passive identification of naturally occurring antimicrobial compounds to more targeted strategies that exploit microbial biosynthetic machinery, enabling the modification and optimization of these compounds to generate new antibiotics.

These discoveries revolutionized medicine. Diseases that had once been major causes of death, such as bacterial pneumonia, tuberculosis, and septicemia, became treatable with relatively simple drug therapies. Antibiotics also made modern medical procedures possible, including complex surgeries, chemotherapy treatments, and organ transplantation, all of which depend on reliable infection control.[55]

However, despite the extraordinary success of antibiotics during the twentieth century, the rate of discovery of entirely new antibiotic classes has declined significantly since the late 1960s. Many pharmaceutical companies shifted away from antibiotic research because of economic and regulatory challenges, and modern drug discovery approaches have struggled to identify novel antibacterial scaffolds at the same rate as earlier natural product screening programs.[48] This slowdown in antibiotic discovery has become increasingly problematic as bacterial pathogens continue to evolve mechanisms that render existing antibiotics ineffective.

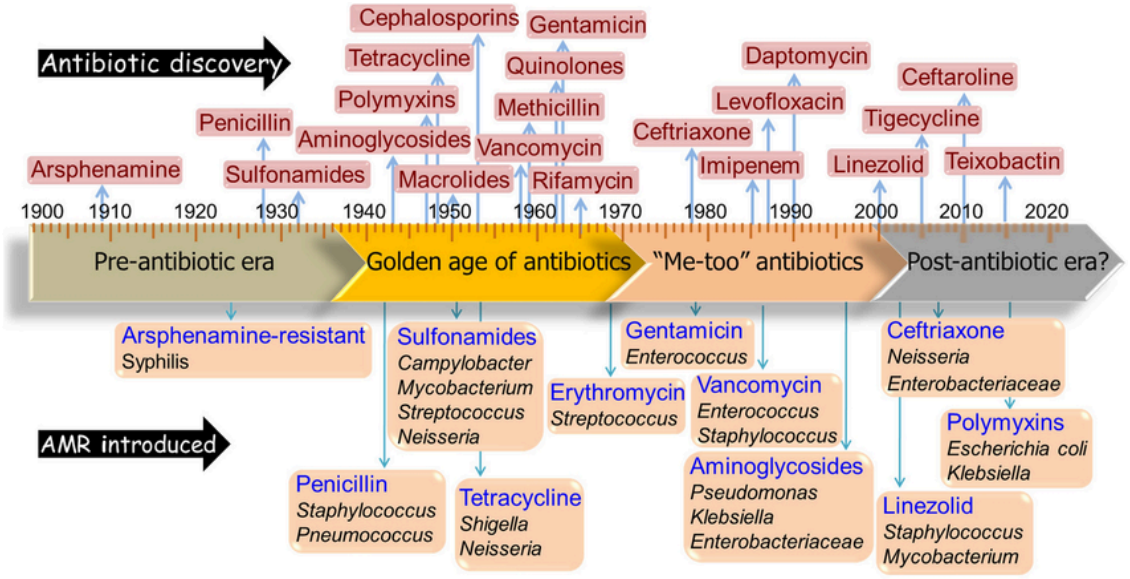

Figure 1: Timeline illustrating key milestones in antibiotic discovery, including the discovery of penicillin and the subsequent "golden age" of antibiotic discovery during the mid-twentieth century.[48,50]

The Emergence of Antimicrobial Resistance

Although antibiotics initially appeared to offer a permanent solution to bacterial infections, microorganisms rapidly demonstrated the ability to evolve resistance. Antimicrobial resistance (AMR) occurs when bacteria develop mechanisms that allow them to survive exposure to antibiotics that would normally inhibit or kill them. These mechanisms can arise through spontaneous genetic mutations or through horizontal gene transfer, in which bacteria acquire resistance genes from other microorganisms through plasmids, transposons, or bacteriophages.[51]

When antibiotics are introduced into an environment, they impose strong selective pressure on bacterial populations. Susceptible bacteria are eliminated, while those with resistance mechanisms survive and reproduce. Over time, resistant strains become dominant within the population. This evolutionary process explains why resistance often appears soon after a new antibiotic is introduced into clinical practice (Figure 2). For example, penicillin-resistant strains of *Staphylococcus aureus* were reported only a few years after penicillin entered widespread medical use.[51]

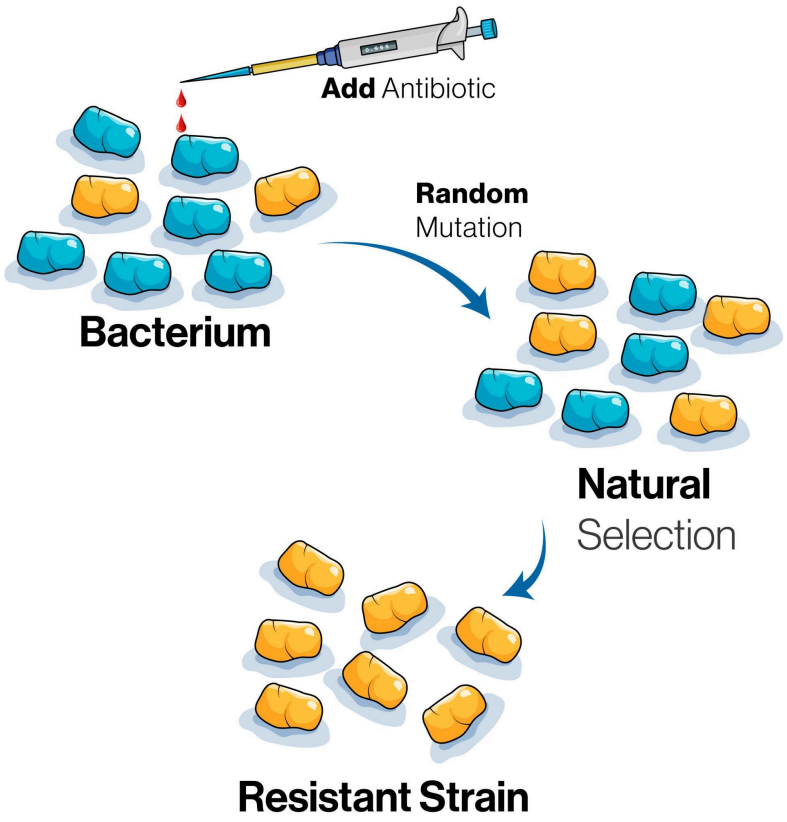

Figure 2: Diagram showing the natural selection of antibiotic pressure on bacterial agents.[51,52]

The Global Impact of Antimicrobial Resistance

Antimicrobial resistance has become one of the most significant global health challenges of the twenty-first century. Resistant infections compromise the effectiveness of existing treatments and increase the risk of complications, prolonged hospital stays, and mortality. A comprehensive global analysis estimated that antimicrobial resistance was directly responsible for approximately 1.27 million deaths worldwide in 2019 and associated with nearly 5 million deaths overall.[56] These numbers place antimicrobial resistance among the leading causes of death globally.

In addition to its direct health impact, AMR poses a major economic burden. Resistant infections require longer treatment durations, more expensive medications, and increased healthcare resources (Figure 3). The World Health Organization has identified antimicrobial resistance as a critical threat to modern medicine, warning that continued increases in resistance could undermine routine medical procedures that depend on effective antibiotics.[55]

In the United States alone, the Centers for Disease Control and Prevention estimates that more than 2.8 million antibiotic-resistant infections occur each year, resulting in over 35,000 deaths.[57] The problem has been further exacerbated by factors such as inappropriate antibiotic use, global travel, agricultural antibiotic usage, and disruptions to healthcare systems.[64]

Taken together, these trends indicate that antimicrobial resistance is not simply an emerging problem but a rapidly expanding crisis that threatens the continued effectiveness of one of medicine's most important therapeutic tools.

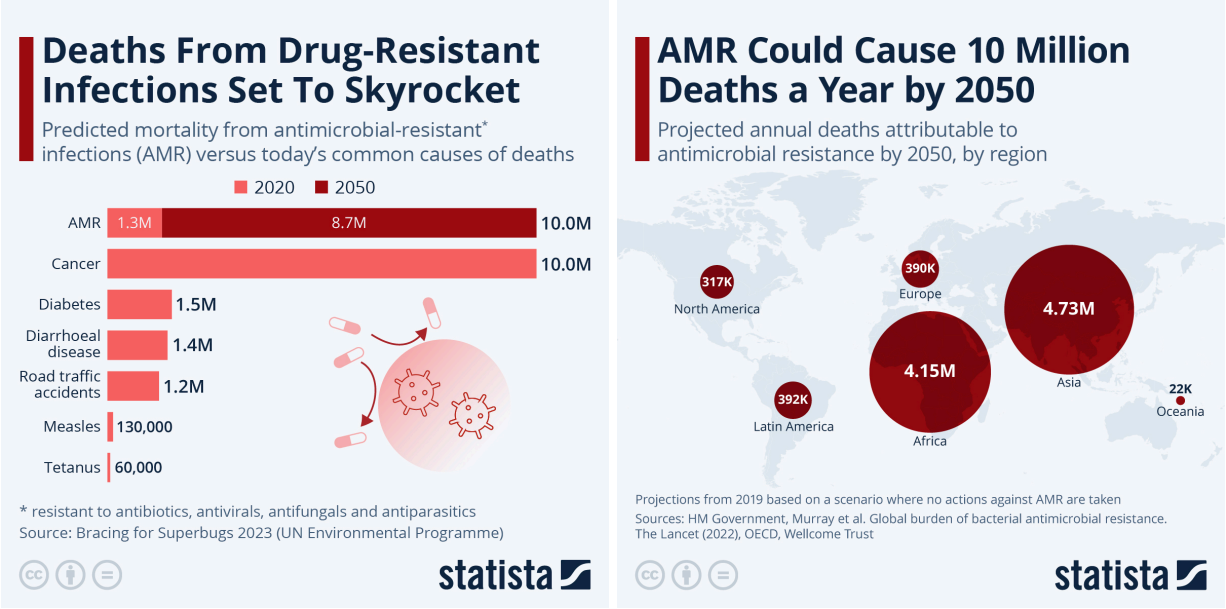

Figure 3: Global distribution and mortality burden associated with antimicrobial resistance based on large-scale epidemiological analyses.[56]

Limitations of Current Antibiotic Development Strategies

Despite widespread recognition of the AMR crisis, the development of new antibiotics has slowed dramatically over the past several decades. Many pharmaceutical companies have reduced investment in antibiotic research because antibiotics are typically used for short treatment durations and therefore generate lower long-term revenue compared with chronic disease medications. As a result, the pipeline for new antibacterial drugs remains limited.[60]

Recent analyses of the antibiotic development pipeline indicate that many candidate drugs currently in development are derivatives of existing antibiotic classes rather than entirely new mechanisms of action. While such modifications can temporarily restore effectiveness against resistant strains, bacteria frequently evolve resistance to these derivatives as well.[48]

Public health strategies such as antibiotic stewardship programs and infection control measures are essential components of combating AMR, but they cannot fully eliminate the need for new antibiotics. Because bacteria will continue to evolve resistance, sustainable solutions must include the discovery and development of antibiotics that target bacterial processes in novel ways.

Beyond scientific challenges, economic factors play a significant role in limiting antibiotic development. Because antibiotics are typically administered over short treatment courses and are often held in reserve to prevent resistance, they generate substantially lower long-term revenue compared to medications used to treat chronic conditions. As a result, many pharmaceutical companies have deprioritized antibiotic research in favor of more profitable therapeutic areas, contributing to a declining pipeline of novel antibacterial agents. This economic imbalance highlights the need for alternative incentive structures, including public

funding initiatives, policy reforms, and public–private partnerships, to support sustained innovation in antibiotic discovery and ensure that new treatments can be developed to address the ongoing threat of antimicrobial resistance.

III. Tunicamycin - A New Frontier in Antibiotic Discovery

Brief Overview of Tunicamycin

Tunicamycin is a naturally occurring antibiotic produced by *Streptomyces* bacteria and belongs to a class of compounds known as nucleoside antibiotics.[32] It was first discovered in 1970 in Japan during a large-scale screening program designed to identify antimicrobial compounds from natural products.[32] In this study, researchers examined the antimicrobial activity of more than 4,000 microbial extracts and identified tunicamycin as a compound with potent antibacterial activity.[32] The discovery of tunicamycin during this type of systematic natural-product screening reflects the broader strategy used during the mid-twentieth century to identify antibiotics produced by soil microorganisms, particularly members of the genus *Streptomyces*, which remain one of the most prolific sources of bioactive secondary metabolites.

Nucleosides are fundamental biological molecules composed of a nitrogenous base attached to a pentose sugar, and they serve as the core building blocks of nucleotides, which in turn form DNA, RNA, and key metabolic intermediates. As illustrated in Figure 4, nucleotides consist of a nucleoside linked to one or more phosphate groups, and these units are assembled into long polymers such as DNA through phosphodiester bonds. Because nucleosides are universally required for cellular life, enzymes that interact with nucleotide substrates are highly conserved and tightly regulated. This conservation makes nucleotide-processing enzymes particularly attractive targets for antibiotic intervention, as molecules that mimic natural nucleosides can interfere with essential biochemical reactions while maintaining strong molecular recognition by enzyme active sites.[26]

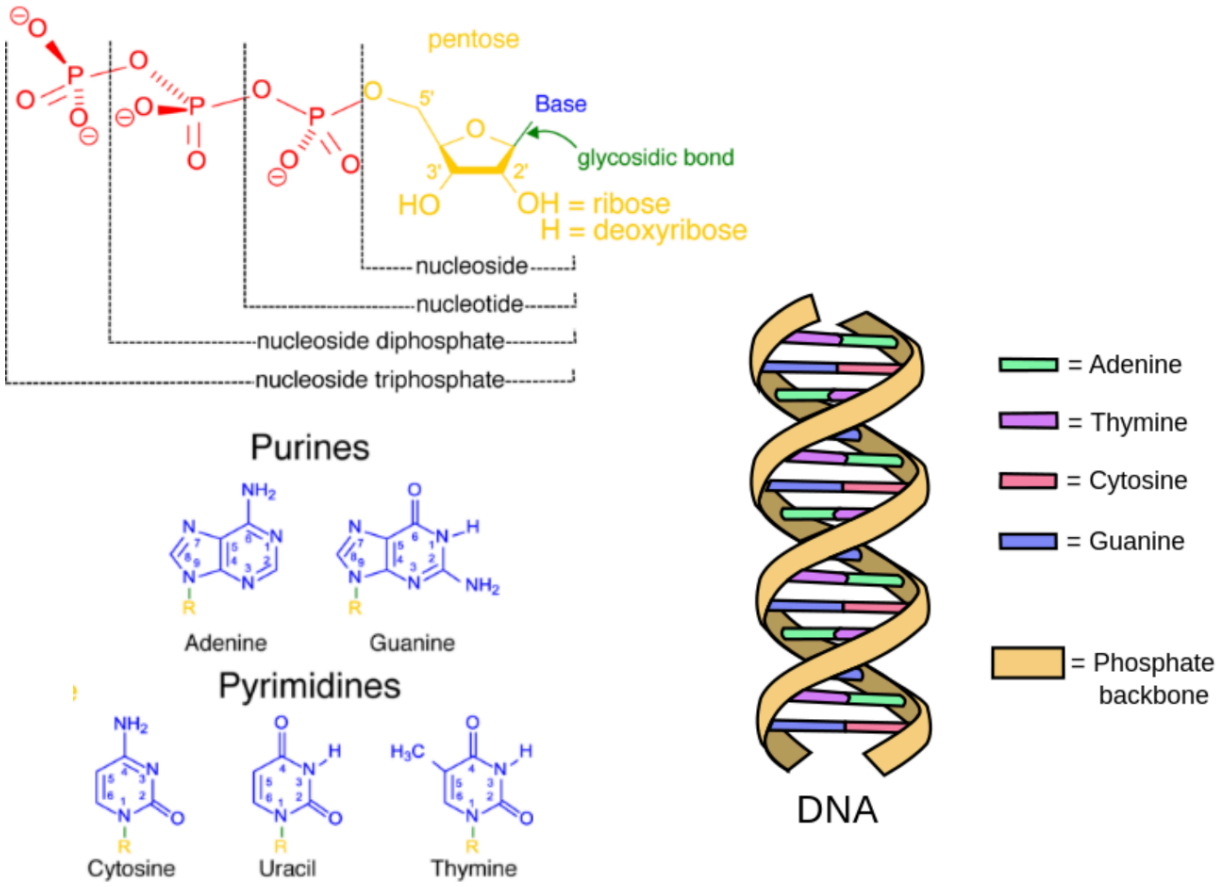

Figure 4: Overview of nucleosides, nucleotides, and DNA structure, illustrating the relationship between phosphate groups, pentose sugars, and nitrogenous bases, as well as base pairing within the DNA double helix. Adapted from OpenStax Biology 2e and related educational resources.

Tunicamycin exploits this vulnerability by structurally resembling nucleotide intermediates involved in bacterial cell wall synthesis, allowing it to disrupt an early and essential step in peptidoglycan biosynthesis. This nucleoside mimicry forms the mechanistic basis of tunicamycin's antibacterial activity and underlies its classification as a nucleoside antibiotic.

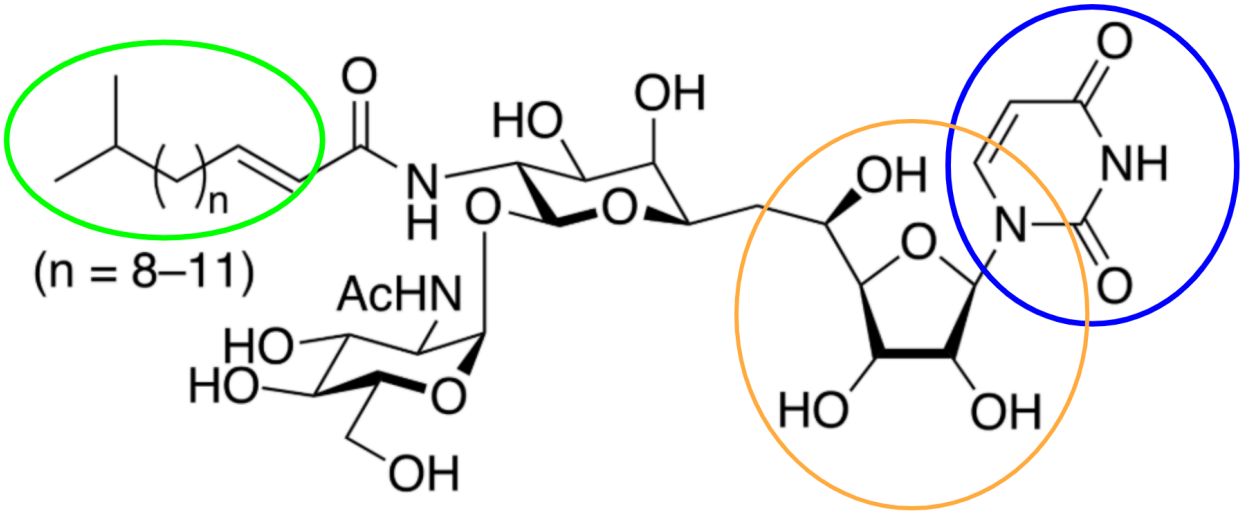

Figure 5: Chemical structure of tunicamycin showing its uridyl nucleoside core (blue circle), N-acetylglucosamine moiety (orange circle), and variable lipid tail (green circle).

Tunicamycin exploits this vulnerability by mimicking the structure of natural nucleoside substrates used in bacterial cell wall synthesis. Figure 5 shows the chemical structure of tunicamycin, which includes a uridyl nucleoside core linked to an N-acetylglucosamine moiety and a hydrophobic lipid tail. This combination allows tunicamycin to interact with membrane-associated enzymes while retaining structural similarity to native nucleotide substrates. The lipid tail varies in length among tunicamycin homologs and contributes to membrane association and biological activity, while the nucleoside portion enables molecular recognition by bacterial enzymes.[15,32]

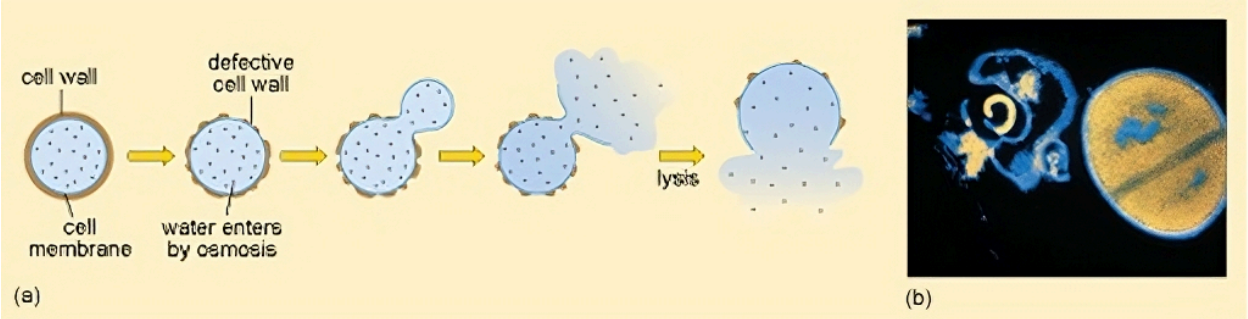

Figure 6: Bacterial cell lysis resulting from disruption of peptidoglycan synthesis, shown schematically and by electron micrograph.

The antibacterial effect of tunicamycin arises from its disruption of peptidoglycan synthesis, a process essential for bacterial survival. Peptidoglycan forms a rigid, mesh-like cell wall that protects bacteria from osmotic pressure and maintains cellular shape. When synthesis of this structure is inhibited, the cell wall weakens, allowing water to enter the cell, leading to swelling and eventual rupture. This sequence of events is illustrated in Figure 6, which shows both a schematic depiction of bacterial lysis and an electron micrograph comparing intact and lysed cells.[26]

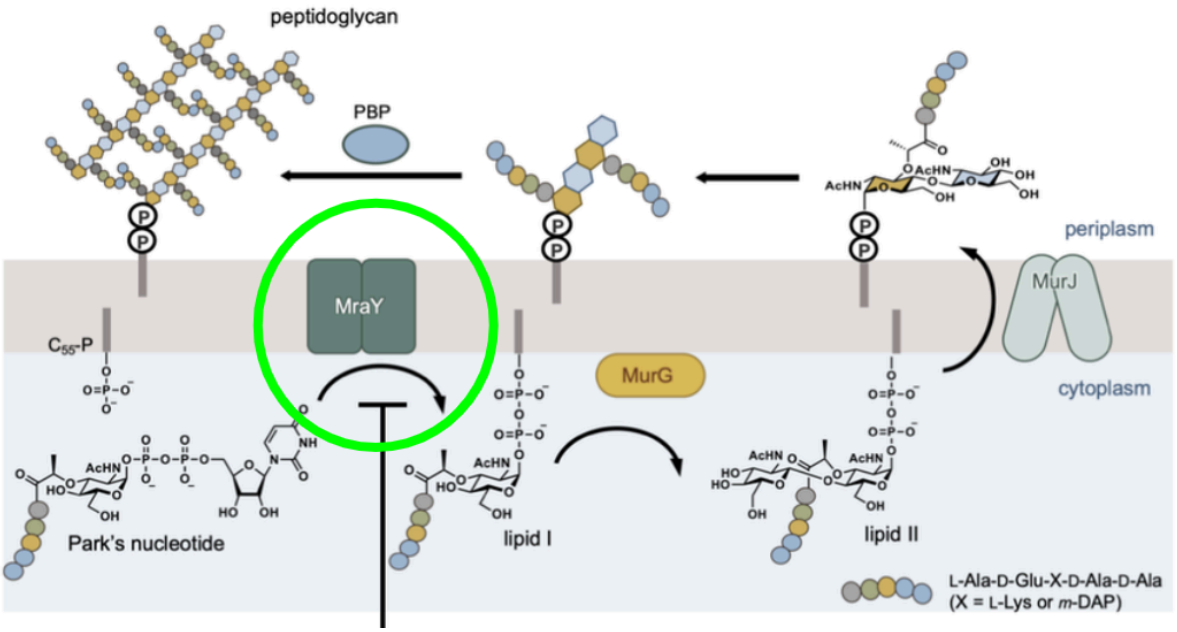

Figure 7: Lipid cycle of bacterial peptidoglycan biosynthesis highlighting the MraY-catalyzed step (green circle).

Figure 7 shows the in-depth process of bacterial cell wall synthesis. During this process, the enzyme MraY transfers the peptidoglycan precursor Park's nucleotide (UDP-MurNAc-pentapeptide) from the cytosol to the membrane-bound lipid carrier bactoprenol phosphate (C55-P), forming the lipid-linked intermediate Lipid I. Lipid I is subsequently converted to Lipid II by MurG and transported across the membrane by the flippase MurJ for incorporation into the growing peptidoglycan cell wall. The green circle highlights the MraY enzyme, the step targeted by several nucleoside antibiotics. Tunicamycin inhibits this reaction by blocking the formation of Lipid I, thereby preventing downstream peptidoglycan assembly.[1,15]

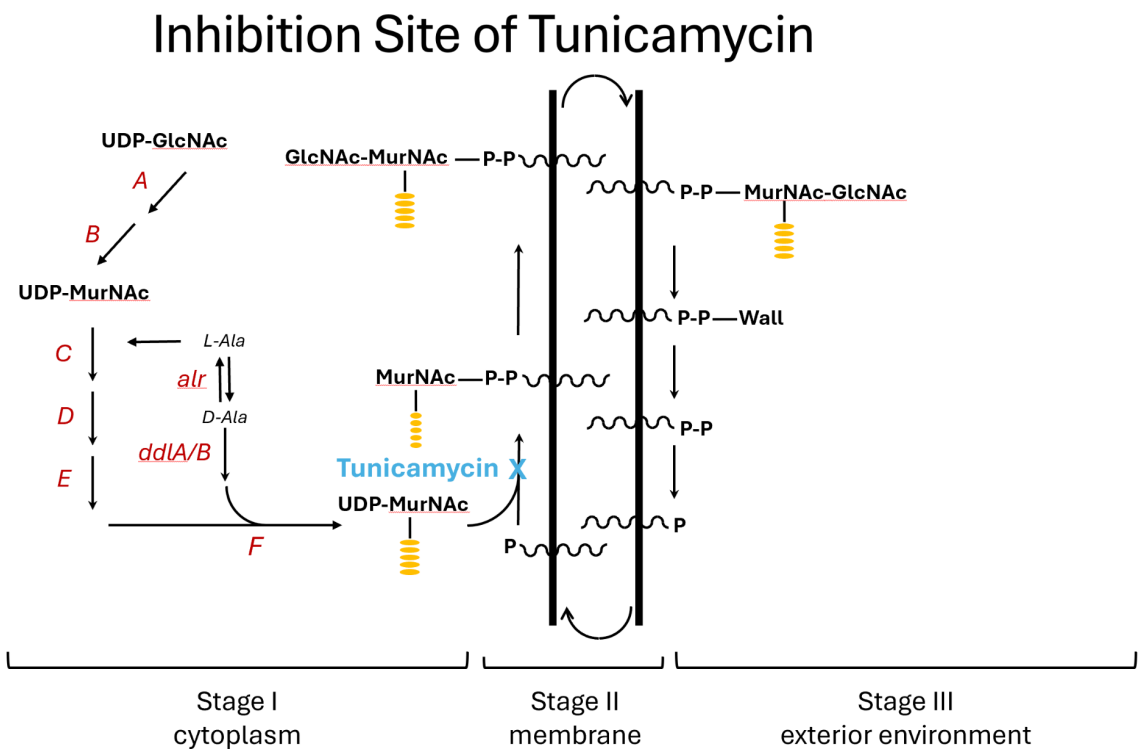

Figure 8: Schematic overview of peptidoglycan (murein) biosynthesis highlighting the site of tunicamycin inhibition at the MraY-catalyzed step.

Figure 8 places this inhibition within the broader context of peptidoglycan metabolism. By preventing the MraY-catalyzed step, tunicamycin interrupts Stage II of cell wall biosynthesis, which ultimately leads to bacterial death. This mechanism is particularly effective in Gram-positive bacteria, which lack an outer membrane and therefore allow tunicamycin direct access to its membrane-associated target.[1]

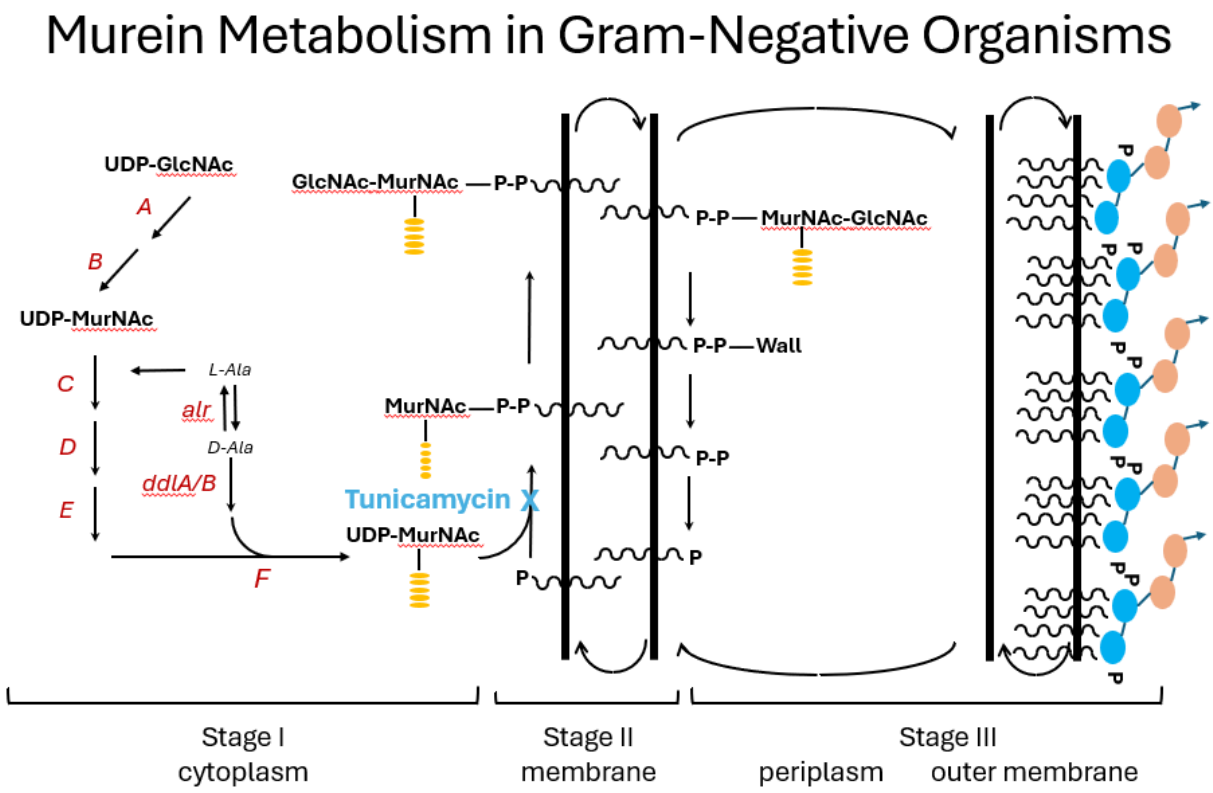

Figure 9: Comparison of peptidoglycan biosynthesis in Gram-negative bacteria, illustrating compartmentalization of synthesis stages and limited accessibility of tunicamycin to its membrane-associated target.

In contrast, Gram-negative bacteria possess an additional outer membrane that acts as a permeability barrier. As illustrated in Figure 9, this outer membrane restricts tunicamycin from reaching MraY in the cytoplasmic membrane, explaining the compound's limited activity against many Gram-negative species.[1] Gram-positive bacteria, which lack this outer membrane, are responsible for many common infections such as skin and soft tissue infections caused by Staphylococcus aureus and respiratory infections caused by *Streptococcus pneumoniae*. In contrast, Gram-negative bacteria are major causes of urinary tract infections, pneumonia,

bloodstream infections, and sepsis, commonly involving pathogens such as *Klebsiella pneumoniae* and *Pseudomonas aeruginosa*. These organisms represent a major clinical challenge. Gram-negative bacteria account for approximately 30% of healthcare-associated infections and a majority of severe hospital-acquired infections, largely due to the protective outer membrane and additional resistance mechanisms.[29] This structural distinction between bacterial groups highlights both the strengths and limitations of tunicamycin as an antibiotic and underscores why structural modification or biosynthetic engineering may be necessary to broaden its therapeutic potential.[29]

Together, Figures 4-9 establish tunicamycin as a nucleoside-mimicking antibiotic that targets a highly conserved and essential step in bacterial cell wall biosynthesis.

However, native tunicamycin interferes with eukaryotic N-linked glycosylation, making it unsuitable for clinical use due to eukaryotic cytotoxicity and limited spectrum.[15] In spite of this, its well-defined mechanism of action and biosynthetic flexibility make it a compelling scaffold for antibiotic development.[25,29] Understanding how tunicamycin is assembled and how its structure can be selectively modified is therefore critical for designing new antimicrobial agents that retain potency while overcoming existing limitations.

Therapeutic Uses of Tunicamycin Analogs

Although native tunicamycin is unsuitable for direct clinical use due to toxicity, its mechanism of action and structural modularity make it a compelling scaffold for antibiotic development. Tunicamycin inhibits MraY, an essential and highly conserved enzyme involved in the earliest membrane-associated step of bacterial cell wall biosynthesis.[1,15] Because this step occurs upstream of many clinically targeted processes, MraY represents an underexploited antibacterial target with limited preexisting resistance mechanisms.

Early investigations demonstrated that tunicamycin exhibits potent antibacterial activity but also interferes with eukaryotic N-linked glycosylation, resulting in significant cytotoxicity.[15] These findings initially limited its therapeutic prospects. However, subsequent studies revealed that this toxicity is not an unavoidable consequence of MraY inhibition but rather arises from specific structural features of the molecule. In particular, interactions between the planar uracil nucleobase and eukaryotic glycosyltransferases contribute disproportionately to eukaryotic cytotoxicity.[29] This discovery allows the engineering of tunicamycin derivatives that lack eukaryotic cytotoxicity while retaining the bactericidal qualities (Figure 10).

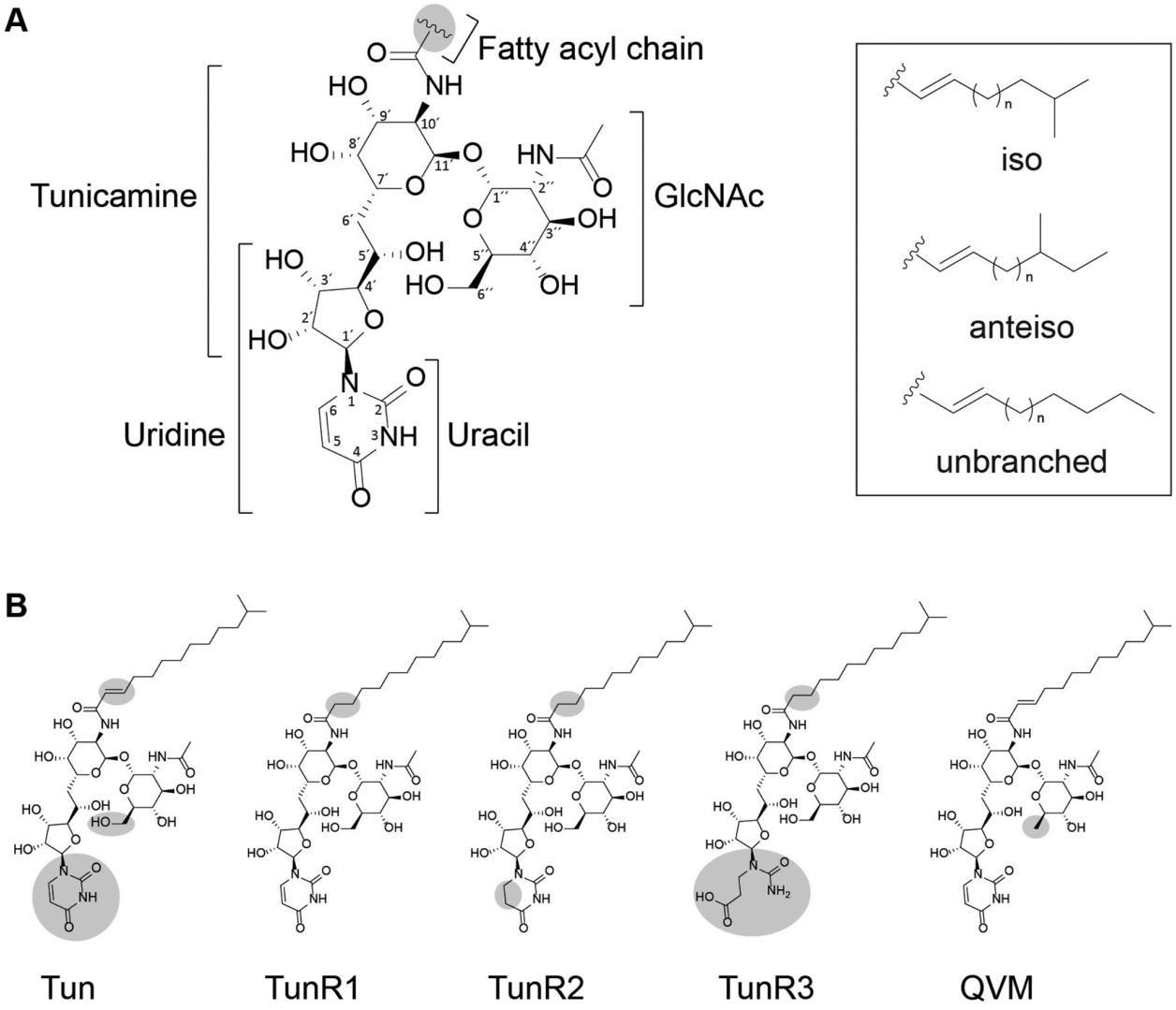

Figure 10: Representative structural modifications of tunicamycin derivatives highlighting changes to the lipid tail associated with reduced cytotoxicity.[4]

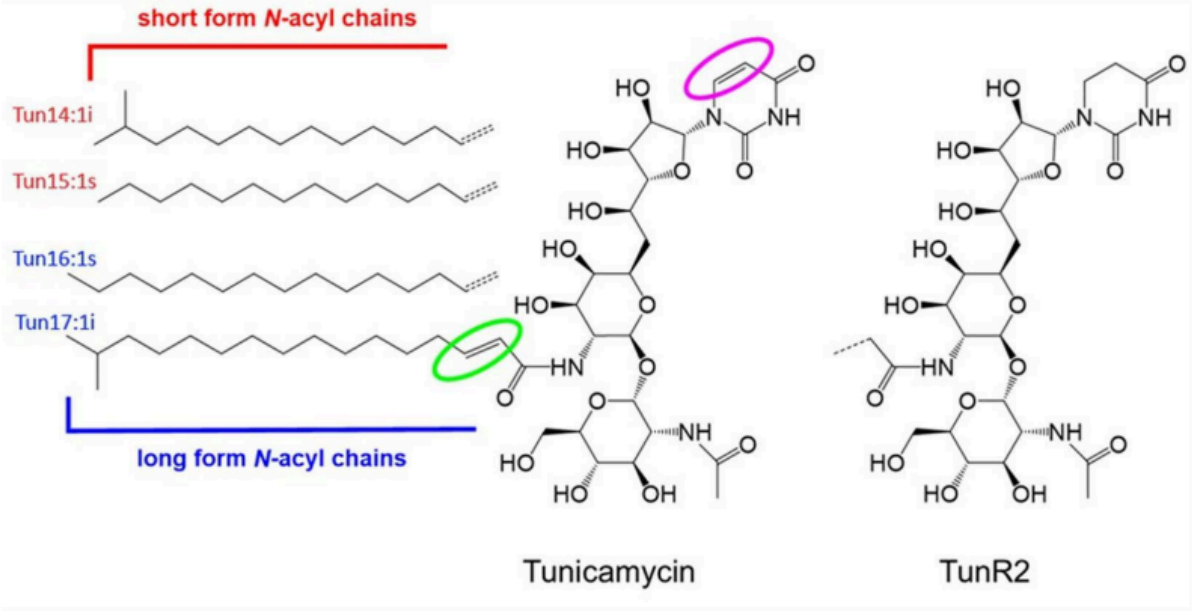

Figure 11: Comparative chemical structures of native tunicamycin and the modified analog TunR2, highlighting differences in lipid chain composition and nucleobase structure.

Native tunicamycin exists as a mixture of congeners that differ in the length and saturation of their N-acyl lipid chains. The parent molecule contains an unsaturated lipid tail and a planar uracil ring, features that facilitate binding to both bacterial and eukaryotic enzymes. Structural modification of these regions has enabled the development of tunicamycin analogs that retain antibacterial potency while significantly reducing cytotoxicity.[25,29] One such derivative, TunR2, incorporates targeted reductions within the lipid chain and modification of the nucleobase, demonstrating that rational redesign of the tunicamycin scaffold can decouple antibacterial efficacy from host toxicity (Figure 11).

These advances have repositioned tunicamycin from a biologically interesting but clinically impractical compound to a viable platform for antibiotic innovation. Modified

tunicamycins have shown activity against clinically relevant pathogens, including *Mycobacterium* species, while exhibiting improved safety profiles in both cellular and animal infection models.[25,29] Importantly, these improved safety and efficacy profiles have been demonstrated using in vivo infection systems, including the zebrafish model illustrated below in Figure 12, which allows direct visualization of pathogen growth and host immune responses during treatment.

In addition, some tunicamycin derivatives have demonstrated synergistic effects when combined with β-lactam antibiotics, an approach increasingly used to combat antimicrobial resistance. Combination antibiotic therapy works by targeting multiple steps in an essential pathway simultaneously, reducing the likelihood that bacteria can survive by mutating a single target. In this case, tunicamycin analogs inhibit the early stage of peptidoglycan biosynthesis by blocking MraY activity, thereby weakening bacterial cell wall precursor formation. β-lactam antibiotics, in contrast, inhibit penicillin-binding proteins that catalyze the final cross-linking steps of peptidoglycan assembly. When these drugs are used together, disruption of early precursor synthesis sensitizes bacteria to downstream inhibition by β-lactams, amplifying antibacterial effects and helping overcome resistance mechanisms that would otherwise limit the efficacy of either drug alone.[29]

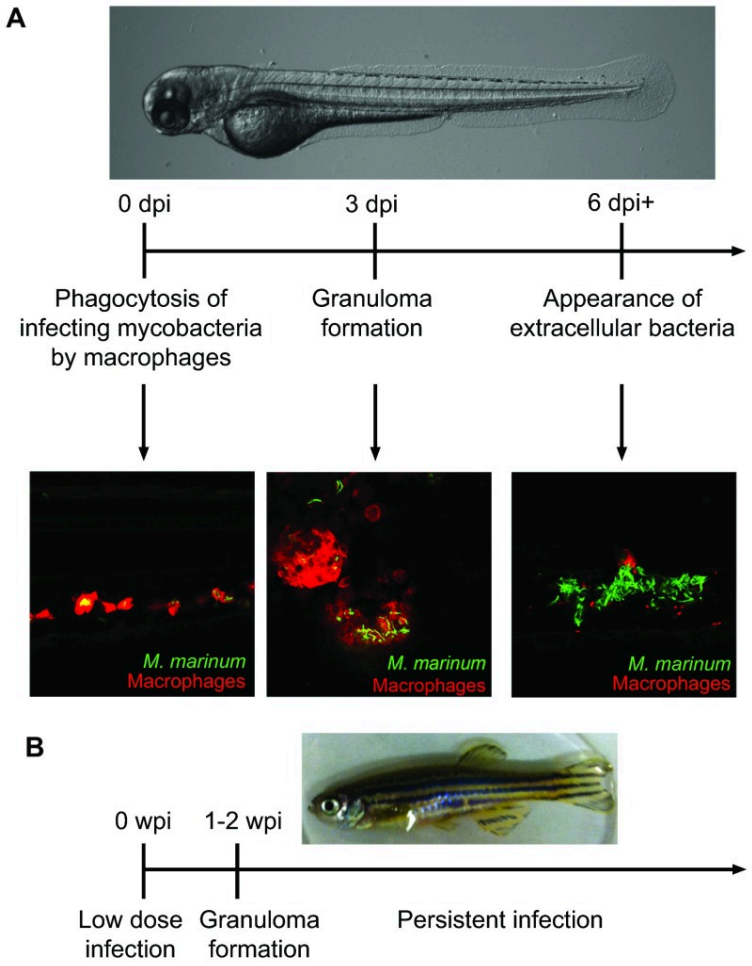

Figure 12: Zebrafish infection model used to evaluate the therapeutic efficacy of the tunicamycin derivative TunR2 against *Mycobacterium marinum*.[9]

In vivo validation of tunicamycin-derived antibiotics has been achieved using the zebrafish (*Danio rerio*) infection model. As illustrated in Figure 12, the optical transparency of larval zebrafish allows direct visualization of fluorescently labeled *Mycobacterium marinum* and host immune cells days past infection (dpi) and also weeks past infection (wpi). Following bacterial uptake by macrophages, infected cells aggregate to form granulomas, a hallmark of

mycobacterial disease progression that closely parallels aspects of human tuberculosis pathology.[9]

Adult zebrafish models further enable assessment of persistent infection, therapeutic uptake, and host survival over time.[9] Drug administration through gill absorption or embryonic exposure allows noninvasive evaluation of antibacterial efficacy in vivo. Application of this model to TunR2 has demonstrated reduced bacterial burden and improved host tolerance relative to native tunicamycin, providing critical proof-of-concept that tunicamycin derivatives can function as effective and safer antimicrobial agents in living systems.[25]

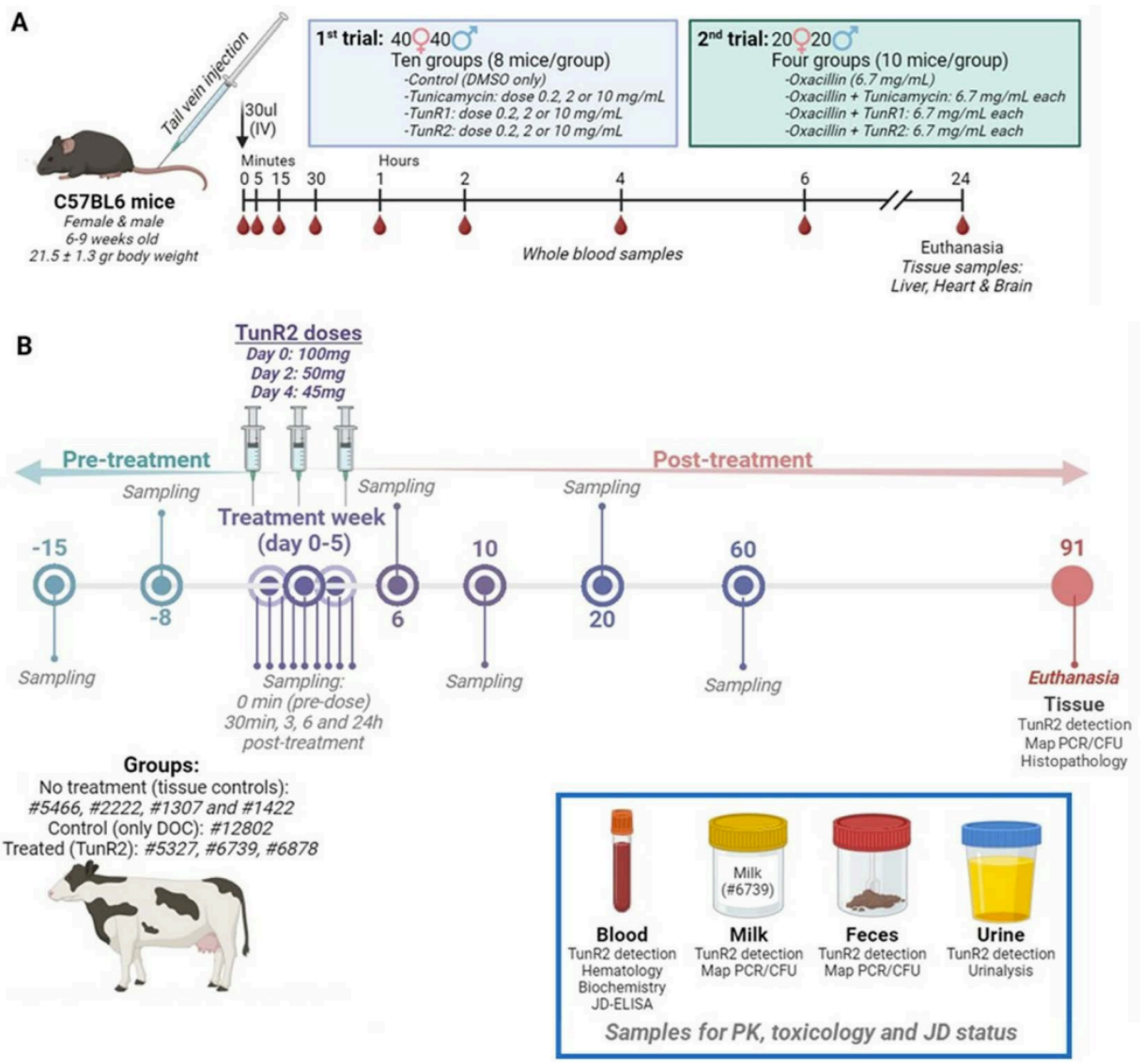

Figure 13: Schematic overview of pharmacokinetic experimental designs for tunicamycin compounds in mice and cattle.[6]

Recent pharmacokinetic studies further support the therapeutic potential of TunR2 in mammalian systems. In a study evaluating TunR2 in C57BL/6 mice and Holstein cattle, TunR2 exhibited a longer half-life and greater systemic persistence compared to native tunicamycin, suggesting an extended duration of antibacterial activity and the potential for less frequent

dosing regimens.[6] As shown in Figure 13, panel A, C57BL/6 mice received intravenous injections of Tun, TunR1, or TunR2 with time-course blood sampling and terminal tissue collection, while in panel B, Holstein cattle received multiple intravenous doses of TunR2 followed by longitudinal sampling of biological fluids to assess systemic distribution.

Additionally, TunR2 demonstrated reduced toxicity while maintaining antimicrobial efficacy, with evidence indicating minimal activation of the eukaryotic unfolded protein response and sustained reduction of mycobacterial burden in vivo.[6] In large animal models, TunR2 was shown to distribute systemically and clear over time without significant accumulation, highlighting its potential safety and applicability in higher-order organisms.[6] These findings extend the earlier zebrafish-based observations into mammalian systems and provide critical support for the continued development of tunicamycin derivatives as viable therapeutic agents, particularly in combination with established antibiotics such as β-lactams.

Together, these findings establish tunicamycin not as a finished therapeutic, but as a powerful foundation for antibiotic development. By exploiting its unique mechanism of action and leveraging biosynthetic and structural flexibility, tunicamycin-derived compounds offer a promising route toward new antimicrobial therapies capable of addressing the growing challenge of antibiotic resistance. Continued investigation into the biosynthetic pathway and enzymatic tailoring of tunicamycin is therefore essential for translating this potential into clinically relevant treatments.

Overview of Bacterial Biosynthetic Pathways

Biosynthetic pathways describe the natural processes by which organisms produce complex molecules through a series of enzyme-catalyzed chemical transformations. In bacteria, antibiotics such as tunicamycin are synthesized intracellularly from simple precursor molecules that are sequentially modified by specialized proteins. These proteins are encoded by genes clustered together within the bacterial genome, collectively forming a biosynthetic gene cluster responsible for antibiotic production. While the identities of many genes required for tunicamycin biosynthesis have been established, the precise biochemical functions of their encoded proteins remain largely uncharacterized.

In most cases, proposed enzyme activities are inferred from sequence homology, in which the DNA or amino acid sequence of an unstudied protein is compared to those of known enzymes to predict function. Although this approach provides valuable hypotheses, it cannot replace direct experimental validation. As a result, key steps within the tunicamycin biosynthetic pathway remain speculative, underscoring the need for experimental evidence of functional characterization of individual pathway enzymes.[38]

Organization of the Tunicamycin Biosynthetic Gene Cluster

Tunicamycin is produced through a highly conserved biosynthetic pathway encoded by a clustered set of genes found in multiple actinomycete species. In bacteria, genes involved in the synthesis of complex natural products are often organized into contiguous gene clusters and are frequently transcribed together as a single operon, enabling coordinated expression of the enzymes required for biosynthesis. This operon organization has been demonstrated for the tunicamycin biosynthetic gene cluster in *Streptomyces*, where transcriptional analysis showed that the *tun* genes are co-transcribed and regulated as a functional biosynthetic unit.[37] The tunicamycin biosynthetic gene cluster therefore encodes all enzymes required to assemble the nucleoside core, attach lipid chains, and perform tailoring modifications that produce the final antibiotic structure.[39,38]

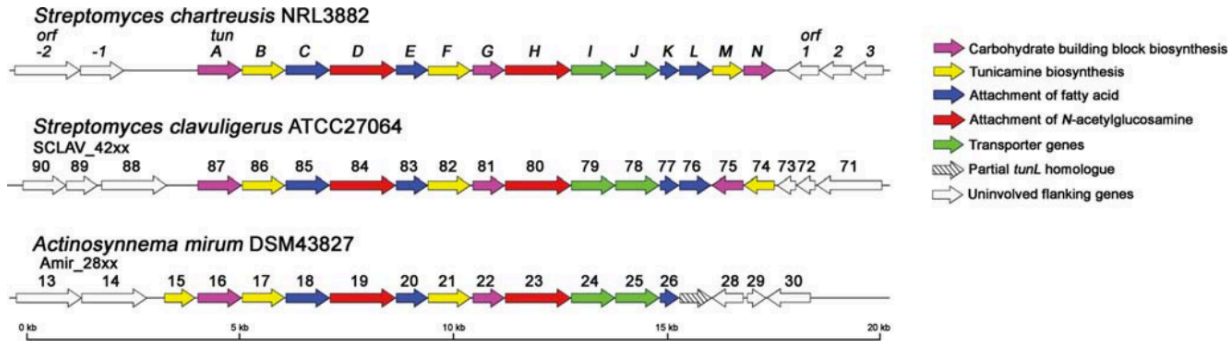

Figure 14: Comparative organization of the tunicamycin biosynthetic gene cluster in *Streptomyces chartreusis*, *Streptomyces clavuligerus*, and *Actinosynnema mirum*, showing conserved gene order and functional groupings involved in tunicamycin biosynthesis.

As illustrated in Figure 14, the overall organization of the tunicamycin gene cluster is conserved across diverse producing organisms, including Streptomyces chartreusis,

Streptomyces clavuligerus, and Actinosynnema mirum. Despite differences in genomic context and species-specific regulation, the preservation of gene order and functional groupings indicates a shared biosynthetic logic. This conservation strongly suggests that the fundamental steps of tunicamycin assembly are universal among producing species and that insights gained from one organism are broadly applicable.[5,38]

The gene cluster can be functionally divided into several modules, each responsible for a distinct stage of biosynthesis. One set of genes encodes enzymes involved in generating carbohydrate precursors, which provide the foundational building blocks for the tunicamine core.[39] Another group directs the formation of the tunicamine nucleoside scaffold, a defining feature of tunicamycin that enables molecular mimicry of native nucleotide substrates.[34] Additional genes encode enzymes responsible for attaching N-acetylglucosamine and lipid chains, modifications that critically influence membrane association, antibacterial potency, and toxicity.[29]

This modular organization highlights an important advantage of natural product biosynthesis: structural diversity can be generated through selective modification of individual steps without disrupting the entire pathway. Small changes in enzyme activity or substrate specificity can produce distinct tunicamycin analogs with altered lipid chain length, saturation, or glycosylation patterns. Such variation underlies the natural diversity observed among tunicamycin homologs and provides opportunities for rational engineering of improved antibiotics.[29,37]

Transporter genes located within the cluster further support the coordinated nature of tunicamycin production. These genes are thought to facilitate export of the antibiotic or protect

the producing organism from self-toxicity by limiting intracellular accumulation.[37] Their presence underscores the evolutionary pressure to balance potent antibacterial activity with cellular self-preservation.

Together, the conserved architecture of the tunicamycin biosynthetic gene cluster demonstrates that tunicamycin production is governed by a tightly regulated and evolutionarily optimized pathway. Understanding the roles of individual enzymes within this pathway is therefore essential for deciphering how tunicamycin structure is assembled. This framework provides the foundation for examining the function of individual biosynthetic enzymes, including the TunG protein, whose precise biochemical role remains incompletely characterized.

Current Models of the Tunicamycin Biosynthetic Pathway

Heterologous expression and genome mining studies have defined a minimal gene cluster sufficient for tunicamycin production; however, the precise biochemical activities of several enzymes within this pathway remain experimentally unvalidated.[37] While the overall sequence of biosynthetic steps is well supported, many proposed enzyme functions are derived primarily from bioinformatic prediction rather than direct biochemical characterization. As a result, current models of tunicamycin biosynthesis represent informed hypotheses that require experimental confirmation.

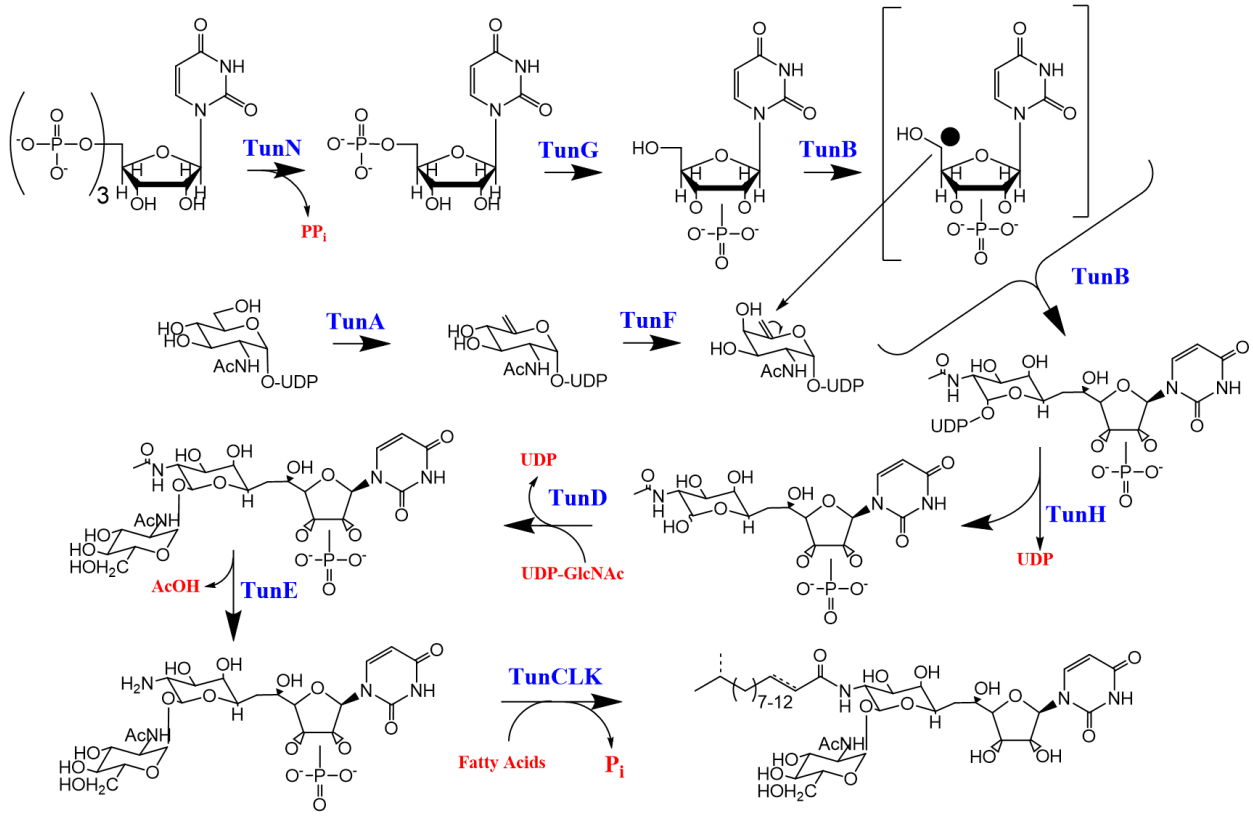

Figure 15: Proposed biosynthetic pathway of tunicamycin in *Streptomyces chartreusis*, illustrating enzymatic steps from nucleotide precursors to lipid-tailed tunicamycin homologs.[38]

Figure 15 presents a proposed biosynthetic pathway for tunicamycin assembly in Streptomyces chartreusis, beginning with uridine-5′-triphosphate and UDP-GlcNAc precursors and proceeding through formation of tunicaminyl-uracil intermediates prior to lipid tail attachment. Enzymes encoded by the tun gene cluster are assigned to individual steps based on sequence homology, genetic context, and analogy to characterized pathways. While many of these assignments are well supported, several enzymatic roles, most notably those attributed to the TunG and TunB proteins, remain hypothetical.[38]

Within this framework, the TunG protein is positioned early in the pathway as a nucleotide-processing enzyme acting on uridine monophosphate–derived intermediates. Because this step precedes glycosylation and lipidation reactions, the biochemical activity of the TunG protein is likely to influence downstream pathway flux and intermediate availability. Consequently, defining the TunG protein's function is critical for understanding both tunicamycin biosynthesis and opportunities for pathway manipulation.

IV. The TunG Protein - A Key Component of the Tunicamycin Biosynthetic Pathway

Bioinformatic Evidence for the TunG Protein's Likely Function

Sequence-based analysis provides strong support for a dephosphorylase role for the TunG protein. Using BLASTP to compare the TunG amino acid sequence against the NCBI non-redundant database (accessed 10-26-2025), the vast majority of high-confidence matches were annotated as dephosphorylases. Approximately 97% of the top 100 sequence alignments display homology to enzymes that catalyze hydrolytic removal of phosphate groups, whereas only ~3% exhibit similarity to mutases or other phosphate-rearranging enzymes.

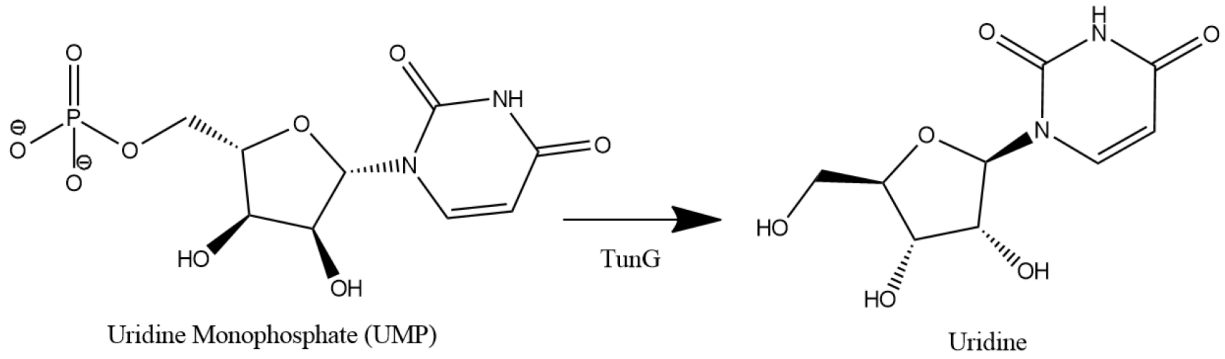

Figure 16: Proposed dephosphorylase activity of the TunG protein acting on uridine 5′-monophosphate within the tunicamycin biosynthetic pathway.[37]

This overwhelming bias strongly suggests that the TunG protein most likely catalyzes dephosphorylation of uridine 5′-monophosphate to generate uridine. As illustrated in Figure 16, such activity would position the TunG protein as a nucleotide-processing enzyme responsible for regulating phosphorylation state early in the biosynthetic pathway. This proposed function is

consistent with biochemical logic, as controlled dephosphorylation of nucleotide intermediates is often required to enable subsequent glycosylation and acylation steps.[37]

Taken together, the dominance of dephosphorylase-associated homology, combined with the scarcity of alternative catalytic signatures, supports dephosphorylation of UMP as the most likely primary function of the TunG enzyme. While bioinformatic predictions cannot replace experimental validation, the available evidence strongly favors this model over competing hypotheses.

Unlikely Mutase Functional Possibility for TunG

Despite the dominant dephosphorylase signature observed for TunG, low-frequency sequence similarity to mutases introduces a remote alternative possibility. In this model, the TunG protein would catalyze intramolecular phosphate transfer within the ribose moiety of UMP, relocating the phosphate group from the 5′ position to the 2′ or 3′ hydroxyl groups without removing it entirely. This speculative mechanism is illustrated in Figure 17.

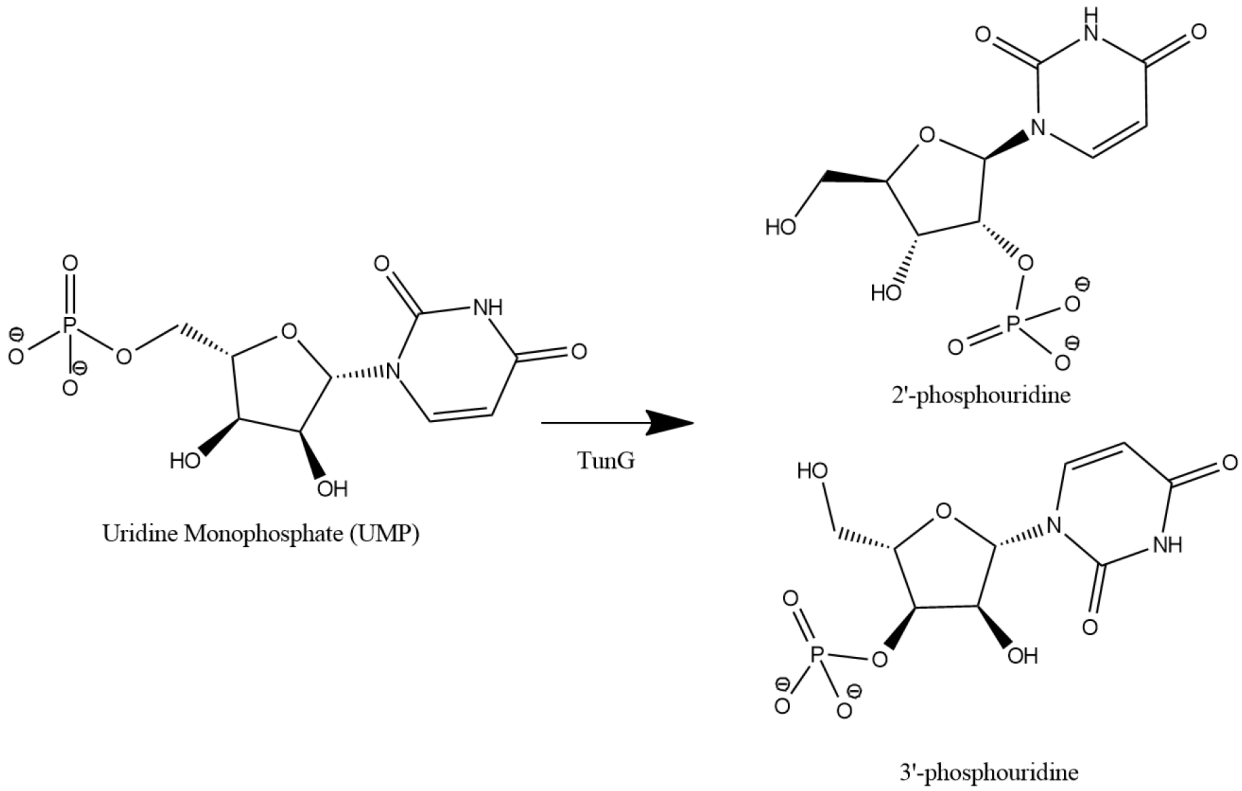

Figure 17: Proposed mutase activity model for the TunG protein involving intramolecular phosphate rearrangement of uridine monophosphate.

However, several factors argue strongly against mutase activity as the primary function of TunG. First, mutase-like homology constitutes only a small minority of sequence matches and

lacks consistent conservation across TunG homologs. Second, no experimental evidence directly supports phosphate rearrangement activity within the tunicamycin pathway. The mutase hypothesis has largely been invoked to rationalize the accumulation of a phosphorylated tunicamycin species ("phospho-TUN") observed in TunL mutational studies.[22]

Given the overwhelming prevalence of dephosphorylase-associated homology and the absence of biochemical validation for mutase activity, this model is considered highly unlikely relative to a dephosphorylase function. If phosphate rearrangement occurs during tunicamycin biosynthesis, it is more plausibly mediated by downstream enzymes rather than TunG itself.

Cyclase Activity as a Least-Likely Functional Model

A third, mechanistically distinct possibility is that TunG functions as a nucleotide cyclase, catalyzing intramolecular condensation of UMP to form cyclic phosphate derivatives such as 2′,3′-cUMP or 3′,5′-cUMP. Cyclic pyrimidine nucleotides have recently been identified as signaling molecules in bacterial systems, analogous to cyclic AMP and cyclic GMP.[40]

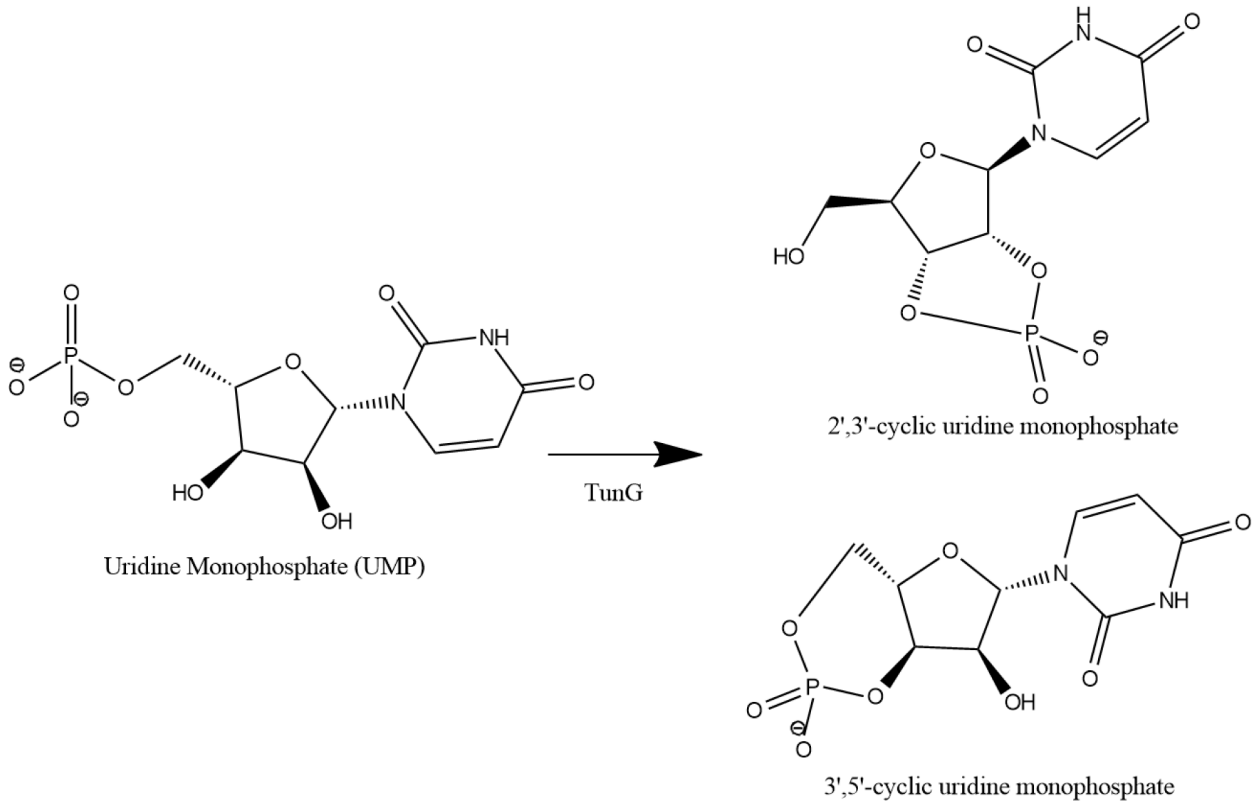

Figure 18: Least-likely cyclase activity model proposed for the TunG protein acting on uridine monophosphate to form cyclic phosphate derivatives.

However, sequence homology between TunG and characterized uridylate cyclases is minimal, and no features characteristic of cyclase active sites are strongly conserved. As illustrated in Figure 18, cyclization would require formation of a phosphodiester linkage between

ribose hydroxyl groups and the phosphate moiety, a reaction mechanistically distinct from both dephosphorylation and mutase activity.

Given the weak bioinformatic support and lack of pathway context suggesting a signaling role for cyclic nucleotides in tunicamycin biosynthesis, cyclase activity is considered the least likely functional role for TunG. While this possibility cannot be formally excluded without experimental testing, it is presented here as a boundary case illustrating the full range of conceivable nucleotide-modifying activities.

Overview of TunG Experiments

Because tunicamycin is synthesized through a defined biosynthetic gene cluster, understanding the function of each enzyme in this pathway is essential for enabling rational engineering of the molecule. Detailed knowledge of the biosynthetic steps would allow targeted modification of the pathway to alter structural features such as the lipid tail, nucleoside core, or other functional groups that influence antibacterial activity and toxicity. Such biosynthetic engineering strategies are increasingly used to generate improved antibiotic derivatives by modifying enzyme activity within natural product pathways. Consequently, identifying the biochemical roles of individual *tun* genes is a critical step toward developing tunicamycin-based therapeutics with improved safety and broader antibacterial activity.

Despite extensive bioinformatic and pathway-level modeling of tunicamycin biosynthesis, the biochemical function of the TunG protein remains unverified experimentally. This knowledge gap provides the central motivation for the present work. The objective of this study is to characterize the enzymatic activity of the product of the *tunG* gene and to define its role early in the tunicamycin biosynthetic pathway through direct biochemical analysis.

To achieve this, the *tunG* gene was cloned with the addition of six tandem histidine residues at the C terminus to facilitate purification. This construct was created in a T7 promoter-driven expression vector and heterologously expressed in *Escherichia coli* (*E. coli*). Protein production was carried out using a BL21(DE3) expression strain, which contains a chromosomally integrated T7 RNA polymerase gene under inducible control of isopropyl β-D-1-thiogalactopyranoside (IPTG).[16] This system enables tight regulation of transcription and high-level expression of recombinant proteins. To minimize leaky expression and improve

soluble protein yield, a co-expression plasmid encoding T7 lysozyme (lysS) was employed to suppress basal T7 RNA polymerase activity prior to induction. The coding sequence for the *tunG* gene was codon optimized for expression in *E. coli* using an algorithmic sequence optimization strategy designed to enhance translational efficiency and protein yield.[40]

The expression construct, pET22b(+)-*tunG*-6×His, was was designed at Drew and created through a vendor (GenScript) using a sequence-optimized design strategy developed to enhance recombinant protein expression efficiency.[40] Chemically competent *E. coli* cells were prepared and transformed with this plasmid, and successful transformants were selected, inoculated, and cultured for protein expression. Following IPTG induction, cells were harvested and lysed to release intracellular contents, and the soluble protein fraction was isolated for purification.

Purification of the TunG protein was achieved using nickel–nitrilotriacetic acid (Ni-NTA) affinity chromatography, exploiting the engineered C-terminal hexahistidine tag on the recombinant protein. Under these conditions, the His tag coordinates with immobilized nickel ions, allowing selective retention of the TunG protein while nonspecific proteins are washed away. Eluted fractions were collected and analyzed by sodium dodecyl sulfate-polyacrylamide gel electrophoresis (SDS-PAGE) to confirm protein size, purity, and successful isolation of the TunG protein. Fractions containing the purified protein were subsequently dialyzed to remove imidazole and equilibrate samples into appropriate reaction buffers.

Purified TunG protein samples were then subjected to in vitro enzymatic assays designed to distinguish between dephosphorylase, mutase, and cyclase activities. Reaction mixtures contained defined nucleotide substrates, including uridine monophosphate (UMP), thymidine

monophosphate (TMP), and adenosine monophosphate (AMP), along with varying pH values, temperatures, and alternative divalent metal cofactors such as Mg^{2+}, Mn^{2+}, and Co^{2+}. Aliquots were withdrawn at defined time points and analyzed by high-performance liquid chromatography (HPLC) to quantify substrate depletion and product formation. Depending on the substrate used, reactions were monitored for interconversion between nucleotide, nucleoside, and nucleobase species, such as UMP, uridine, and uracil.

By integrating controlled recombinant expression, affinity purification, and time-resolved enzymatic assays with chromatographic analysis, this approach enables direct interrogation of the biochemical activity of the TunG protein. Experimental validation of the TunG protein's function provides a critical test of existing biosynthetic models and represents an essential step toward reconstructing and engineering the tunicamycin pathway in heterologous hosts. Ultimately, defining the activity of the TunG protein may facilitate rational manipulation of tunicamycin biosynthesis to generate novel analogues with improved therapeutic potential.

V. Methods

Preparation of Competent E. coli Cells and Heat-Shock Transformation

To enable uptake of foreign DNA, *E. coli* cells were rendered competent, meaning their cell membranes were temporarily permeabilized to allow entry of circular DNA molecules called plasmids. Plasmids are small, self-replicating DNA molecules separate from the bacterial chromosome that can carry genes of interest, such as antibiotic resistance markers or cloned inserts like the *tunG* gene. Once inside the cell, plasmids replicate independently and express their encoded genes, providing an efficient method for recombinant protein production.

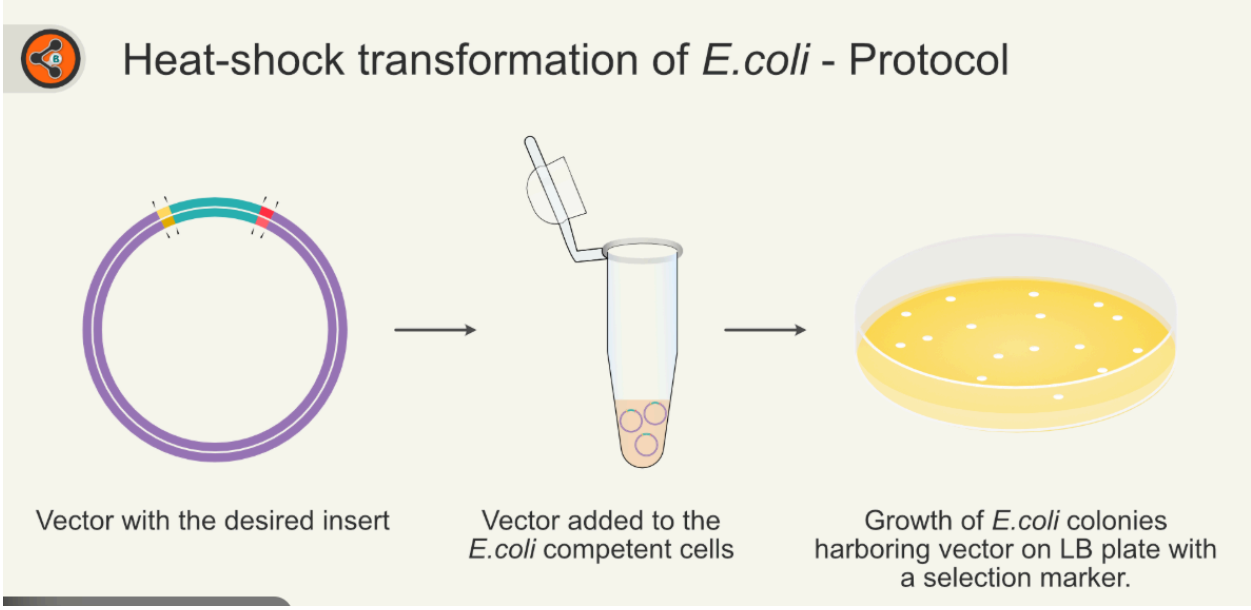

Figure 19: Overview of heat-shock transformation in *E. coli*, illustrating plasmid uptake following brief exposure to elevated temperature.[18]

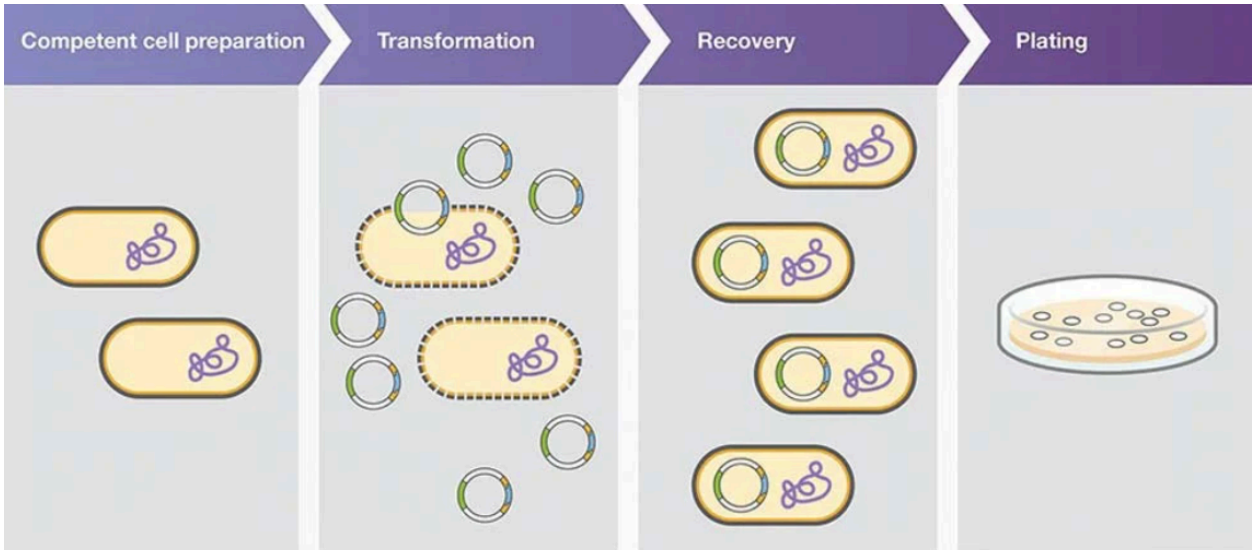

Figure 20: Major stages of chemical transformation in *E. coli*, including competent cell preparation, plasmid uptake, recovery, and antibiotic selection.[14]

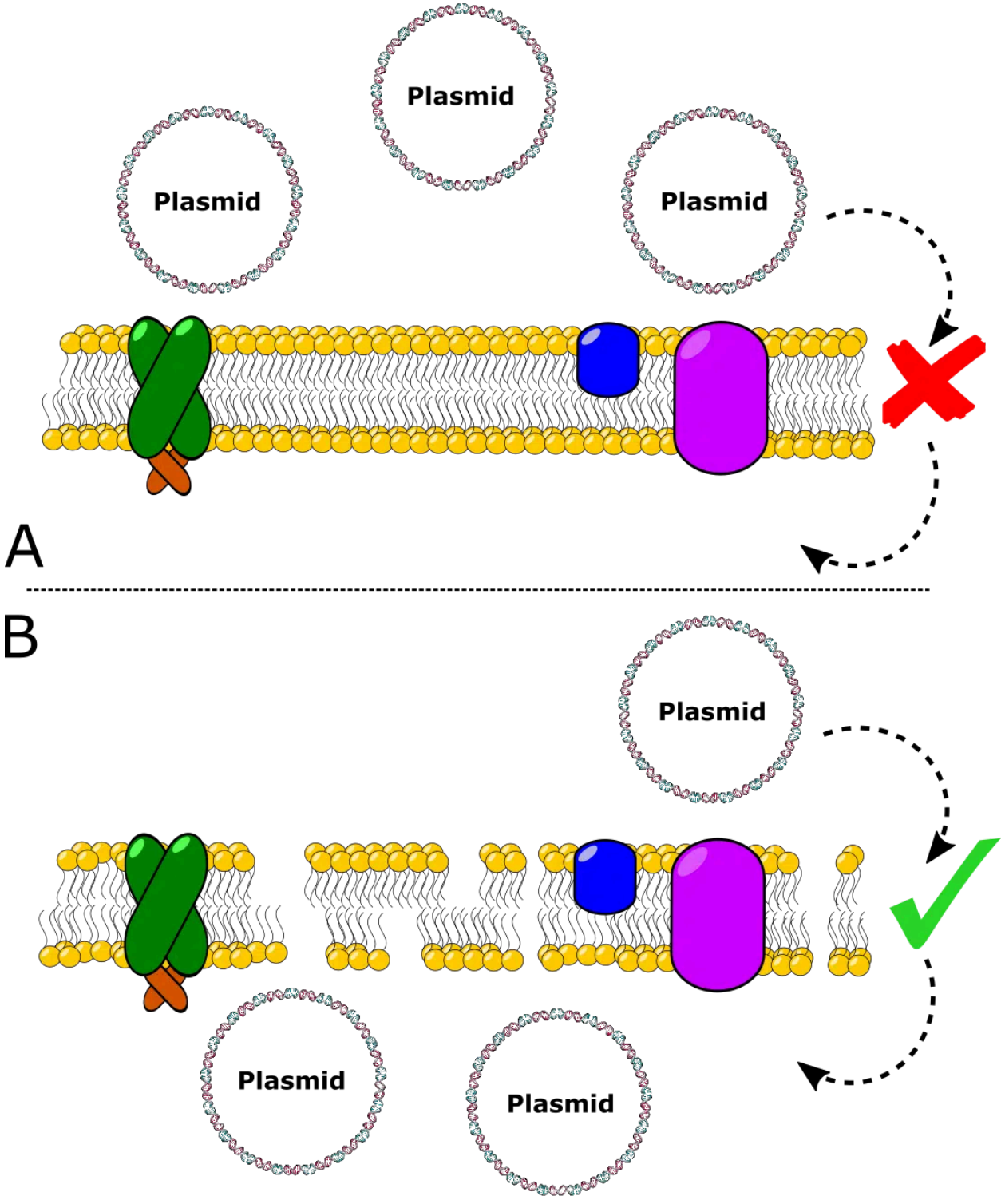

Figure 21: Molecular model of membrane permeability changes during heat-shock transformation.[20]

Competent *E. coli* cells were prepared following a standard calcium chloride method. Starter cultures were grown overnight, diluted into fresh LB medium, and incubated at 37 °C with shaking until mid-log phase ($OD_{600} \approx 0.4–0.6$). Cells were chilled on ice to stabilize membranes, harvested by centrifugation at 4 °C, and resuspended in ice-cold 0.1 M $CaCl_2$. This treatment increases membrane permeability by neutralizing surface charges. After a second wash, aliquots were stored at −80 °C until use.

Aliquots (100 µL) of competent cells were thawed on ice and mixed with 2–3 µL of plasmid DNA (100 ng/µL stock). The mixture was incubated on ice for 12–15 min, heat-shocked at 42 °C for 120 s, and immediately returned to ice for 2 min. LB broth (800 µL) was added, and the culture was incubated at 37 °C with shaking (200 rpm) for 40 min to allow expression of antibiotic resistance genes. Portions of 1 µL, 10 µL, and 100 µL from the transformation mixture were plated on LB agar containing ampicillin (AMP) and chloramphenicol (CAM). Plates were incubated overnight at 37 °C.

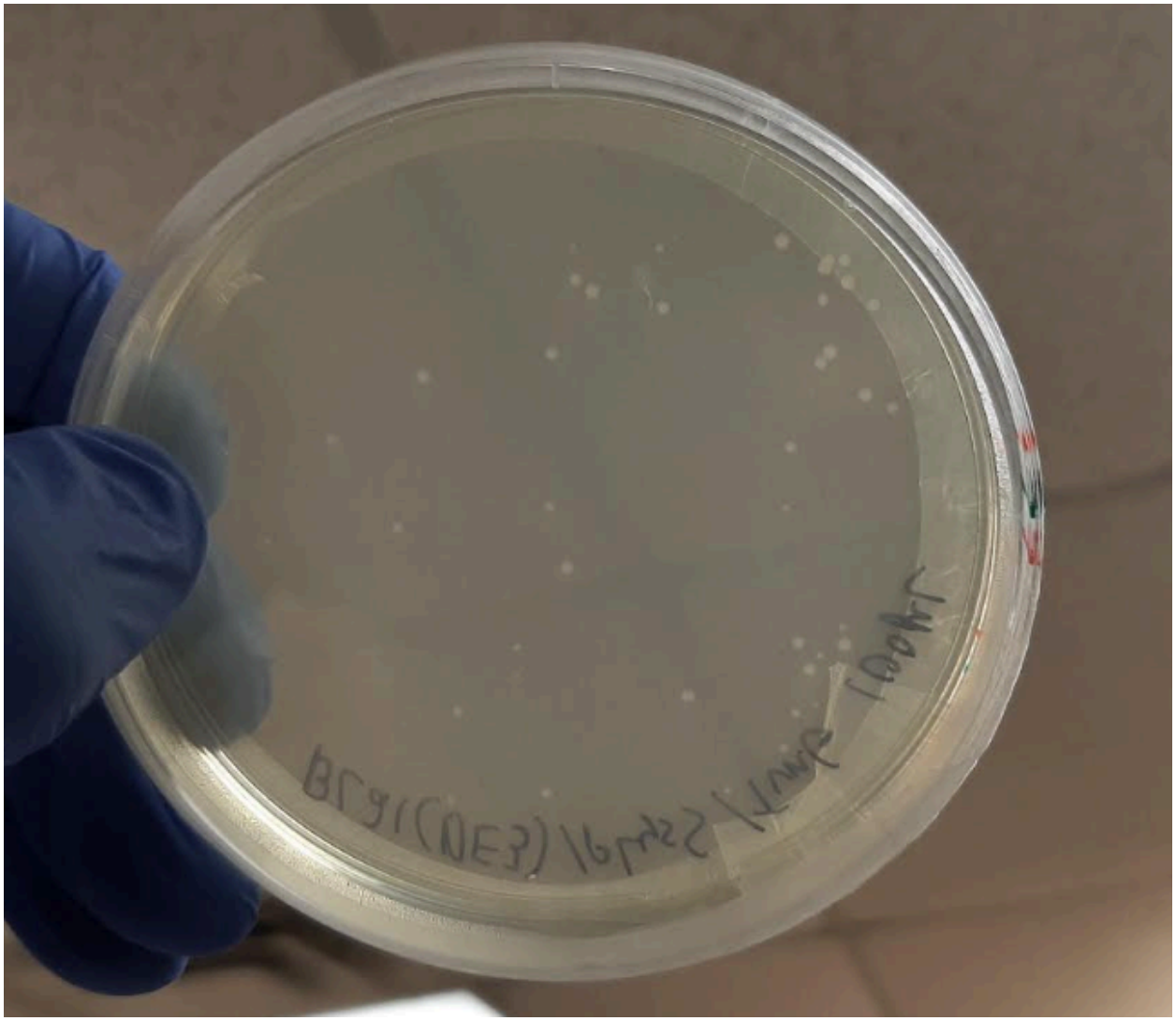

Figure 22: Growth of transformed *E. coli* colonies on LB agar containing ampicillin and chloramphenicol following heat-shock transformation.

Following incubation, colonies that grew on selective plates indicated successful uptake of the plasmids conferring resistance to AMP and CAM. The pLysS plasmid provided chloramphenicol resistance, while the pET vector carrying the *tunG* gene conferred ampicillin

resistance. To ensure that all colonies indeed contained the target plasmids, one colony plate (100 µL transformation plate) was restreaked on a fresh AMP + CAM LB agar plate (Figure 23).

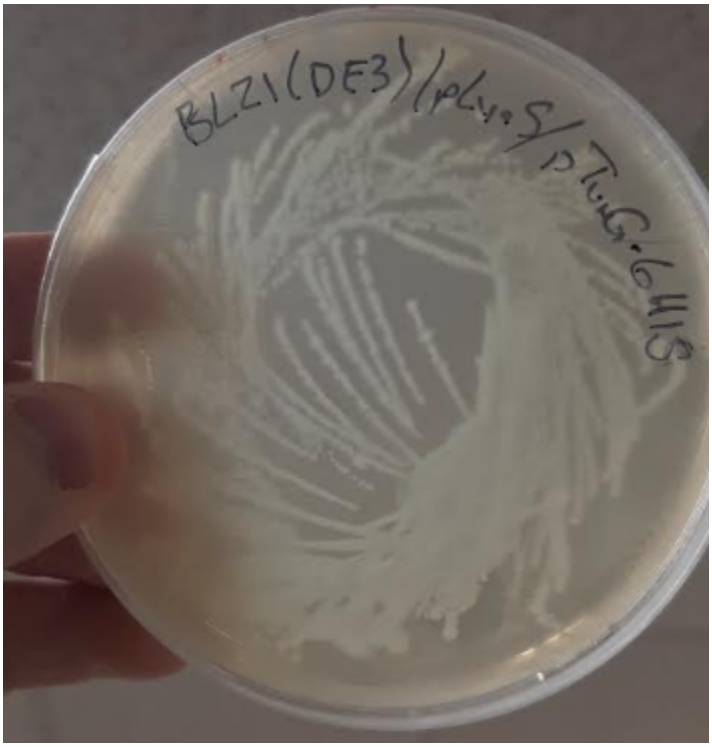

Figure 23: Restreaking of transformed *E. coli* colonies on selective media to confirm plasmid retention.

Restreaking is a standard verification step to eliminate colonies that may have appeared resistant because they were physically shielded by neighboring transformants. By isolating individual colonies, restreaking confirmed that each selected *E. coli* colony contained the intended plasmids prior to downstream protein expression experiments.

T7 Promoter System

Recombinant expression of the *tunG* gene was carried out using the T7 RNA polymerase expression system, which allows high-level transcription of cloned genes under the control of a T7 promoter. In this system, the host strain of *E. coli* BL21(DE3) carries a chromosomally integrated copy of the T7 RNA polymerase gene regulated by the lacUV5 promoter.

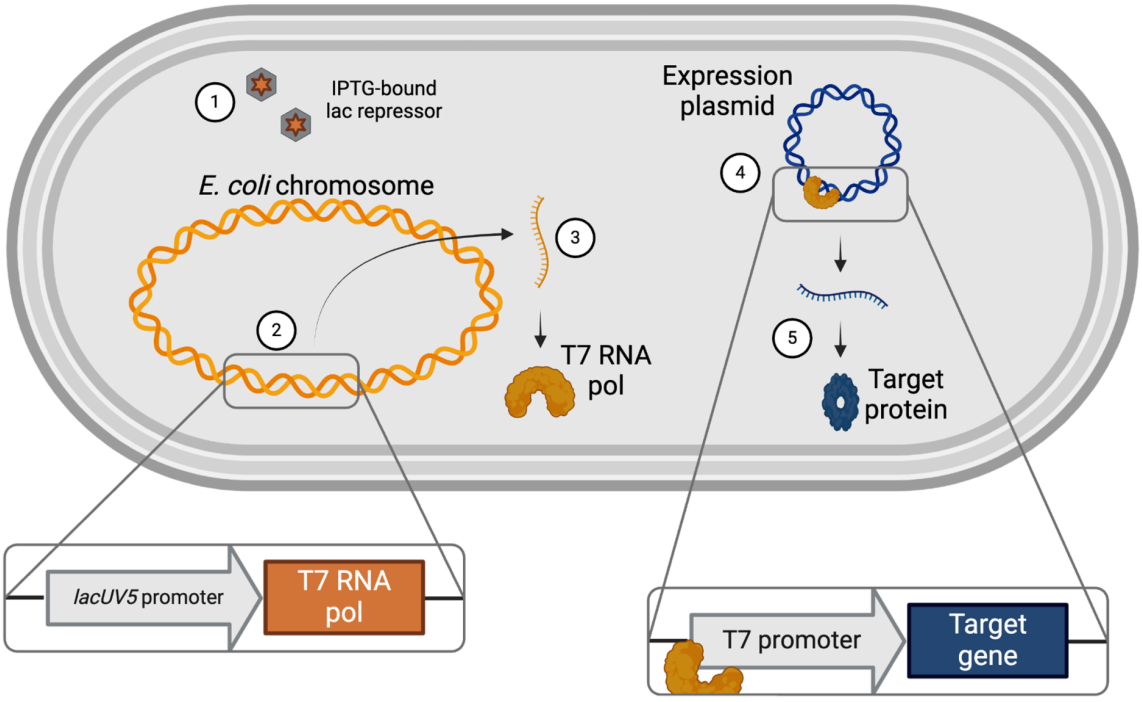

Figure 24: Schematic of the T7 RNA polymerase expression system used for recombinant protein production in *E. coli* BL21(DE3).[16]

Upon addition of isopropyl β-D-1-thiogalactopyranoside (IPTG), the lac repressor is derepressed, enabling transcription of the T7 RNA polymerase gene. The resulting enzyme recognizes only the T7 promoter sequence on the expression plasmid, initiating strong transcription of the target gene, in this case, the TunG protein (Figure 25). Because T7 RNA

polymerase is extremely efficient, even minimal uninduced activity can lead to unwanted background expression or protein toxicity.

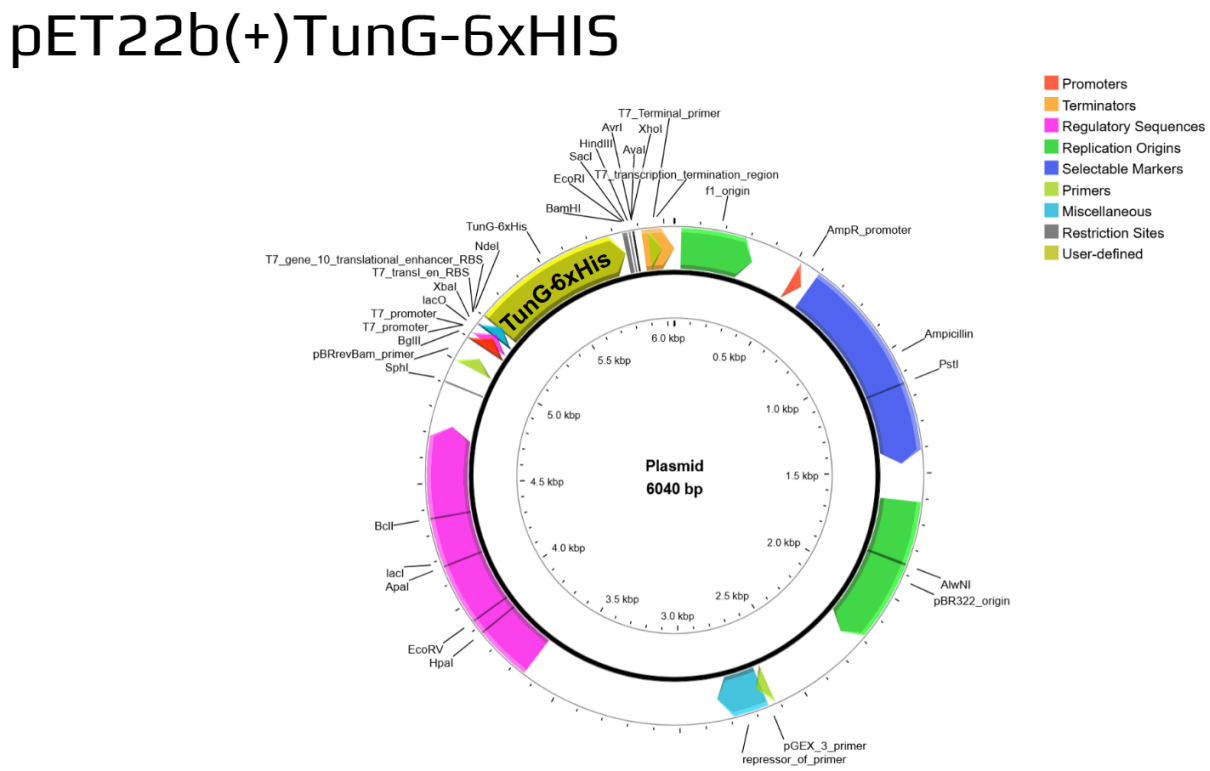

Figure 25: Map of the pET22b(+)-*tunG-6*×His expression plasmid used for production of the TunG protein.

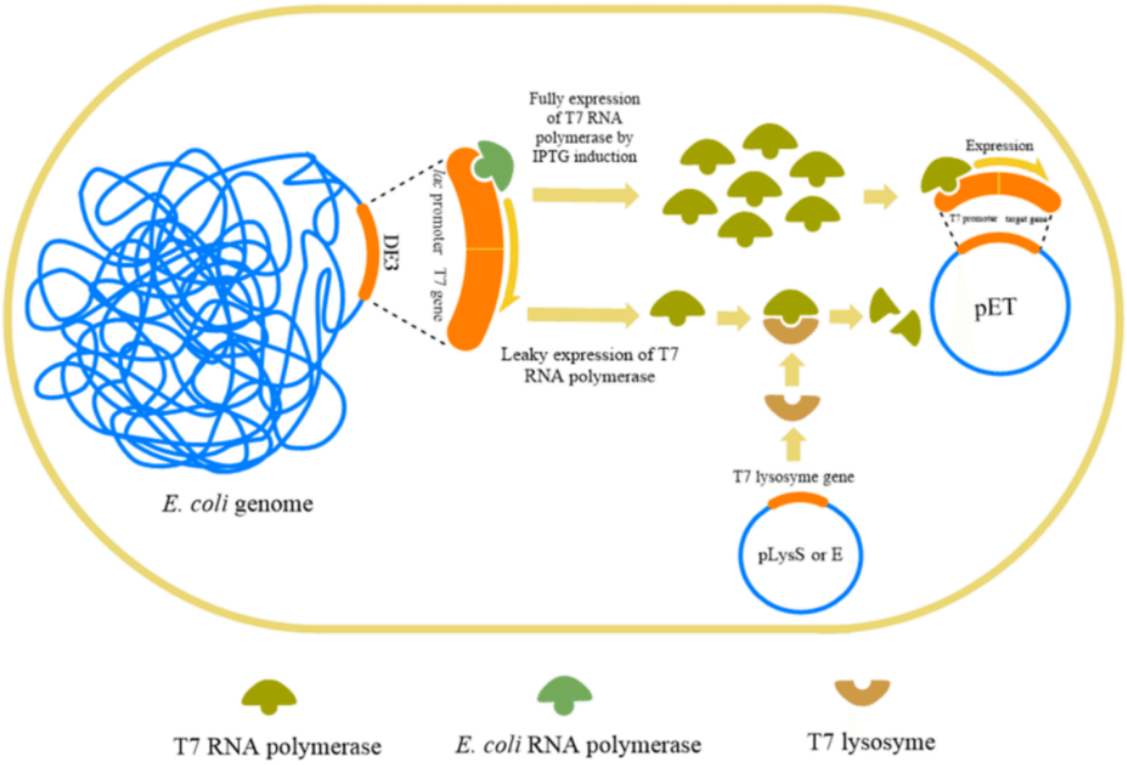

Figure 26: Regulation of T7 RNA polymerase activity by T7 lysozyme in the pLysS system.[16]

To minimize this basal transcription, a T7 lysozyme (lysS) plasmid was co-expressed. Lysozyme is an enzyme that hydrolyzes the β-(1,4)-glycosidic bonds between N-acetylmuramic acid and N-acetylglucosamine in the peptidoglycan layer of bacterial cell walls, leading to cell wall weakening and eventual lysis. In nature, lysozyme serves as part of the bacterial defense and remodeling system, helping to degrade or reshape the peptidoglycan matrix. Lysozyme binds and transiently inhibits T7 RNA polymerase until full induction occurs, thus improving control of protein expression (Figure 27).[16] In this experiment, lysozyme plays a dual role. Within the pLysS plasmid, T7 lysozyme is expressed at low levels to partially inhibit T7 RNA polymerase, thereby reducing “leaky” transcription of the target gene before induction with IPTG. This

regulation improves control over recombinant protein expression and prevents premature production of the TunG protein. Additionally, the presence of lysozyme facilitates later stages of protein purification by making bacterial cells easier to lyse during mechanical disruption. The weakened peptidoglycan layer enhances the efficiency of cell lysis methods such as bead beating, allowing for higher recovery of soluble TunG protein from the cytoplasmic fraction.[21] This tightly regulated two-tier system provides rapid, high-yield expression of recombinant proteins while maintaining low background levels prior to induction while also making cell lysis to extract synthesized protein products easier.[11]

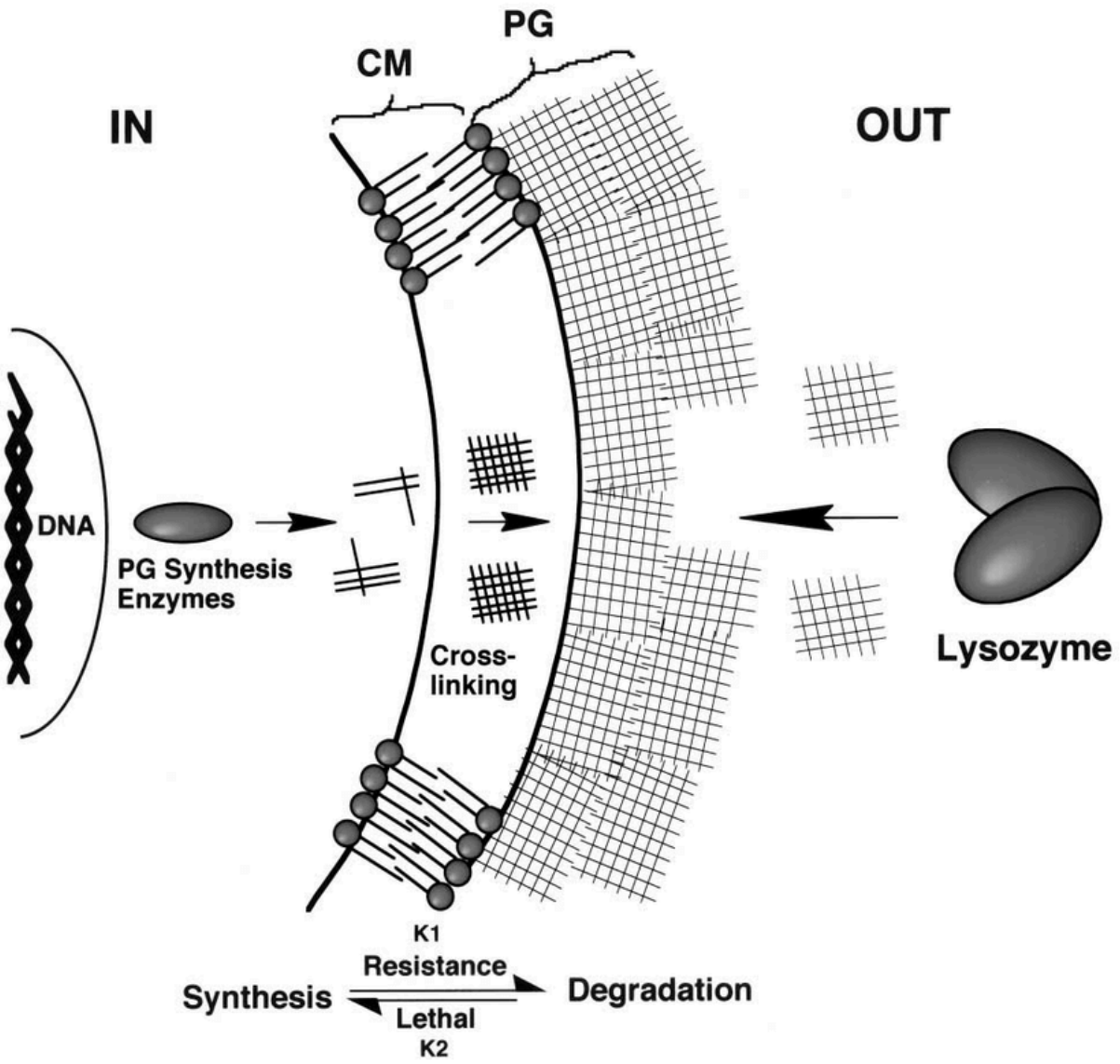

Figure 27: Overview of peptidoglycan synthesis and degradation in bacterial cell walls.[17]

For experimental controls, two expression conditions were used throughout this study: pET− strains, which contained the pLysS plasmid but lacked the pET expression vector and therefore did not produce the TunG protein, and pET+ strains, which carried both the pLysS plasmid and the pET22b(+)-*tunG*-6×His expression plasmid. These designations were used

consistently to distinguish samples lacking recombinant protein expression from those expressing the TunG protein during downstream purification and enzymatic analyses.

Centrifugation, Cell Growth, and Lysis

Centrifugation is a key step in protein and DNA purification workflows. It separates cellular components or molecular complexes based on their size and density by spinning samples at high speeds to generate strong centrifugal forces. In this experiment, microcentrifugation was used to isolate bacterial cell pellets after growth and to remove insoluble debris during protein purification and dialysis preparation. This process ensured that the soluble fraction contained the purified TunG enzyme for downstream analysis.

Centrifugation separates components of a liquid sample by subjecting them to high centrifugal force generated by rapid rotation around a central rotor. Under these conditions, all particles experience an outward force; however, the rate at which individual components move depends on their mass, size, and density relative to the surrounding medium. In biological samples, this results in separation into two operational fractions: a pellet containing denser or aggregated material (such as whole cells, membranes, or insoluble proteins) and a supernatant containing soluble molecules that do not sediment under the applied conditions. As shown in Figure 28, the pellet forms at the bottom of the tube while the supernatant remains above it and can be carefully removed or retained depending on the target fraction. Centrifugation was performed at 4 °C to minimize enzyme denaturation and preserve the stability of sensitive biomolecules.

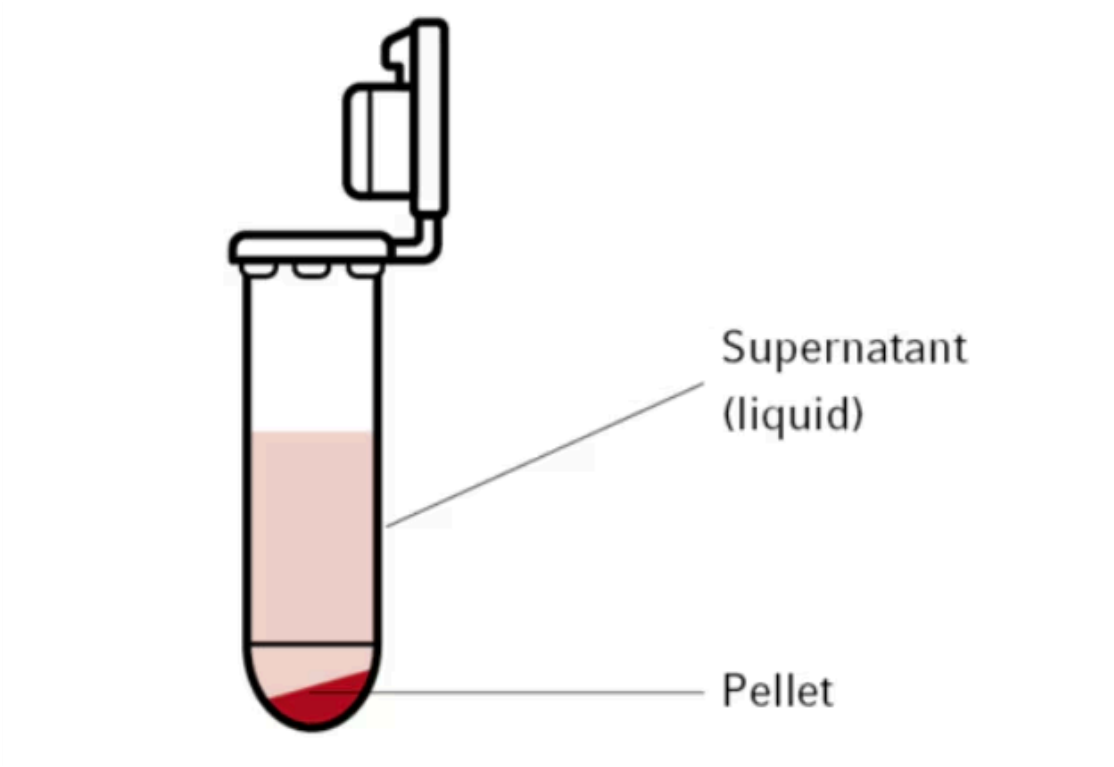

Figure 28: Formation of pellet and supernatant following centrifugation of a biological sample.[22]

The overall operation of a centrifuge is illustrated in Figure 29, which shows how molecules of different sizes separate along a density gradient. During high-speed rotation, larger or denser molecules sediment faster, forming a pellet at the bottom, while smaller or less dense molecules remain in suspension. By controlling rotational speed and time, specific fractions (such as soluble protein) can be isolated with precision.

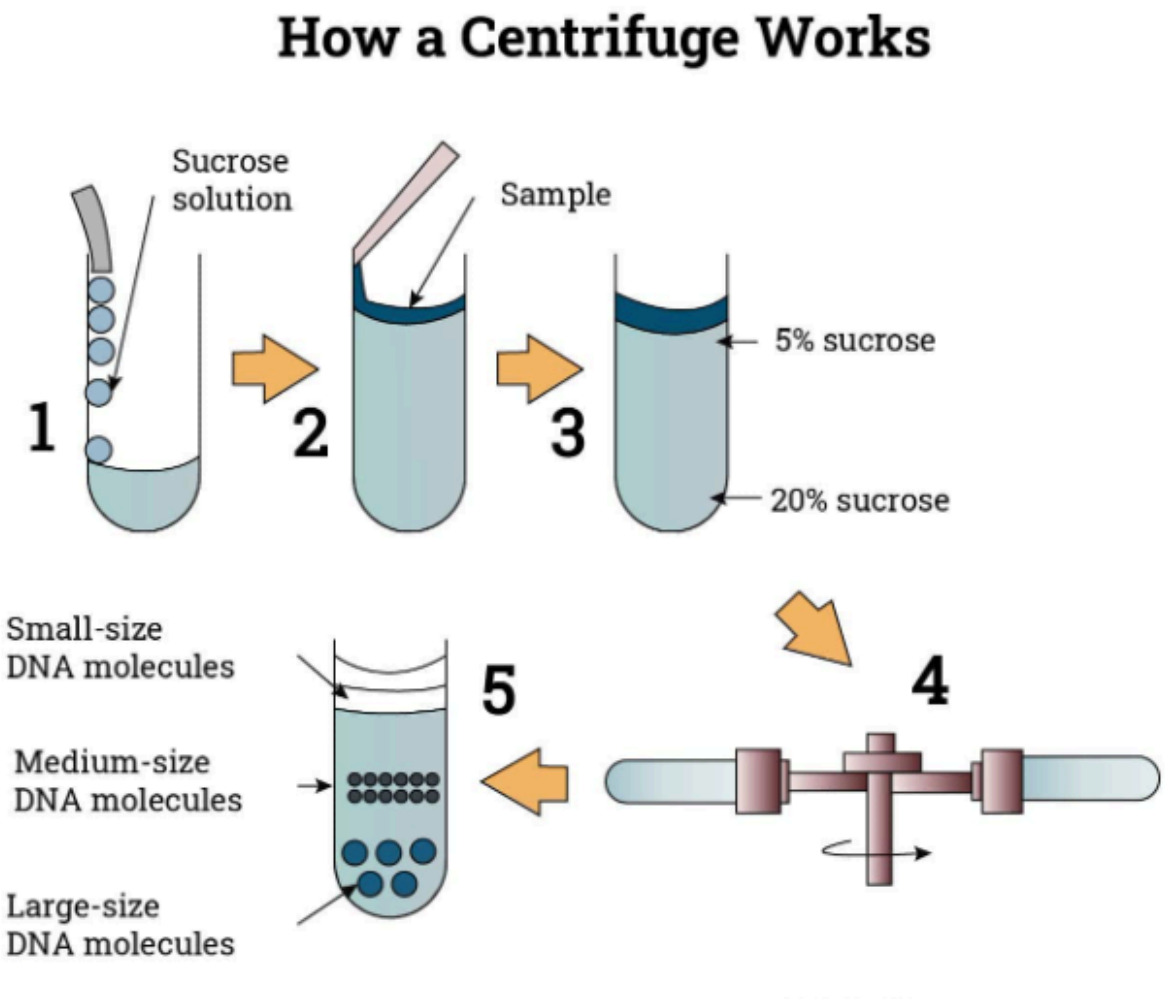

Figure 29: Principle of centrifugal separation based on particle size and density.[23]

Figure 30 highlights the major parts of a standard laboratory centrifuge, including the rotor, chamber, and armored casing, which together maintain balance and ensure safe high-speed operation. Tubes must always be balanced. Each tube has a counterweight of equal mass positioned directly opposite in the rotor. This balance prevents mechanical stress and vibration that could damage the instrument or distort the separation process.

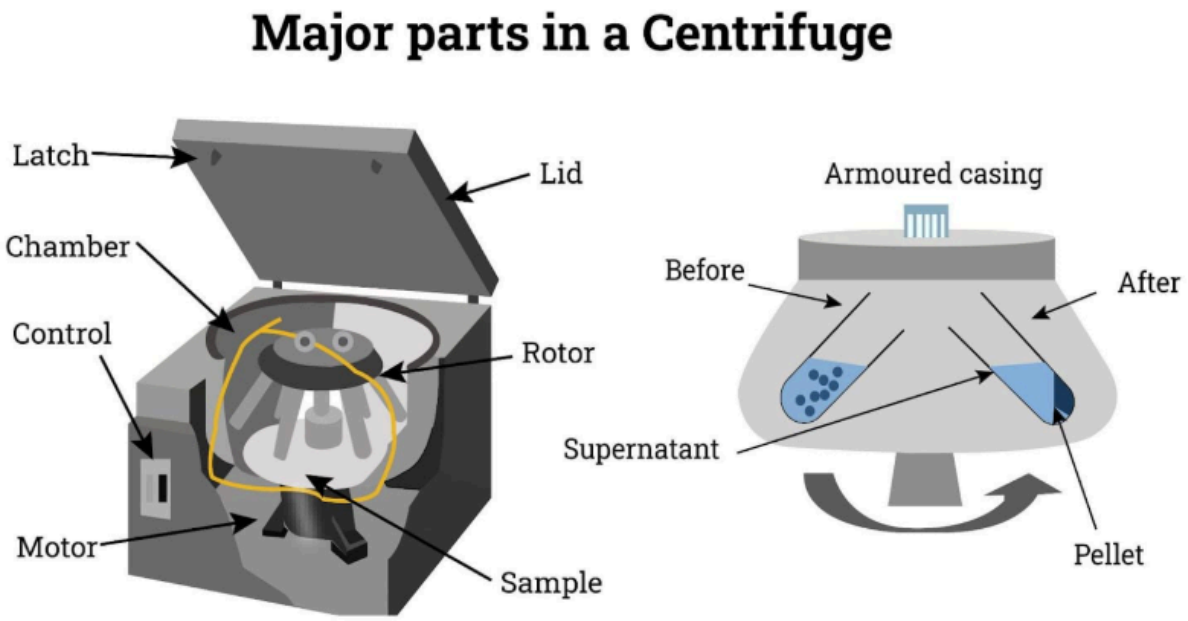

Figure 30: Major components of a benchtop laboratory centrifuge.[23]

In this research, microcentrifugation was used after bacterial growth and protein expression to collect the cell pellet containing expressed TunG protein. Cells were centrifuged at 4 °C to prevent thermal denaturation, and the supernatant was discarded. The resulting pellet was then resuspended in a lysis buffer for protein extraction. Later steps of centrifugation were also used to clarify lysates before loading samples onto the nickel affinity column and again before dialysis, ensuring only soluble, purified protein was used in subsequent procedures.

Following IPTG induction, *E. coli* cultures expressing *TunG* were harvested by centrifugation at 8000 x g for 10 minutes, and the supernatant was carefully discarded. The resulting cell pellet was resuspended in 2 mL of 50 mM MOPS lysis buffer, pH 7.0, to maintain physiological stability during lysis. Mechanical disruption was performed by bead beating, in which approximately 400 mg of 0.4 mm glass beads were added to the suspension and vortexed

vigorously for 10 minutes to rupture the bacterial cell walls to release intracellular contents and shear DNA. After lysis, the mixture was separated from the beads by pipetting the liquid fraction into a new microcentrifuge tube, which was then centrifuged at 14,000 rpm for 2 minutes to pellet insoluble debris. The supernatant (soluble protein fraction) was transferred to a fresh tube, while the pellet (insoluble fraction) was resuspended in 50 mM MOPS, pH 7.0, buffer. Both fractions were retained for analysis. These lysate samples were subsequently analyzed by SDS-PAGE to assess *TunG* expression and solubility, allowing comparison of soluble versus insoluble protein distribution across samples.

Figure 31: Workflow for harvesting and lysing *E. coli* cells expressing the TunG protein by bead beating.

SDS Protein Gel Electrophoresis

Gel electrophoresis is a laboratory technique used to separate molecules such as DNA, RNA, or proteins based on their size and charge. The process involves placing samples into wells within a gel matrix, typically agarose for nucleic acids or polyacrylamide for proteins, and applying an electric current across the gel. Because molecules carry an electrical charge, they migrate through the gel toward the electrode of opposite charge: negatively charged molecules move toward the positive electrode, and vice versa. The gel acts as a molecular sieve, allowing smaller molecules to travel more quickly and farther than larger ones. In protein electrophoresis, sodium dodecyl sulfate (SDS) is often used to denature proteins and impart a uniform negative charge, ensuring that separation occurs primarily by molecular weight rather than shape or charge. After the run, the separated molecules are visualized using specific stains, such as Coomassie Brilliant Blue for proteins or ethidium bromide for DNA, revealing distinct bands that can be analyzed to determine purity, size, or expression level of the sample.

After induction and expression, *E. coli* cells were harvested by centrifugation and lysed by bead beating in a lysis buffer consisting of 50 mM MOPS, pH 7.0. The soluble fraction was collected after centrifugation at 8000 x g for 10 min and analyzed for the presence of the recombinant TunG protein using sodium dodecyl sulfate–polyacrylamide gel electrophoresis (SDS-PAGE).[20]

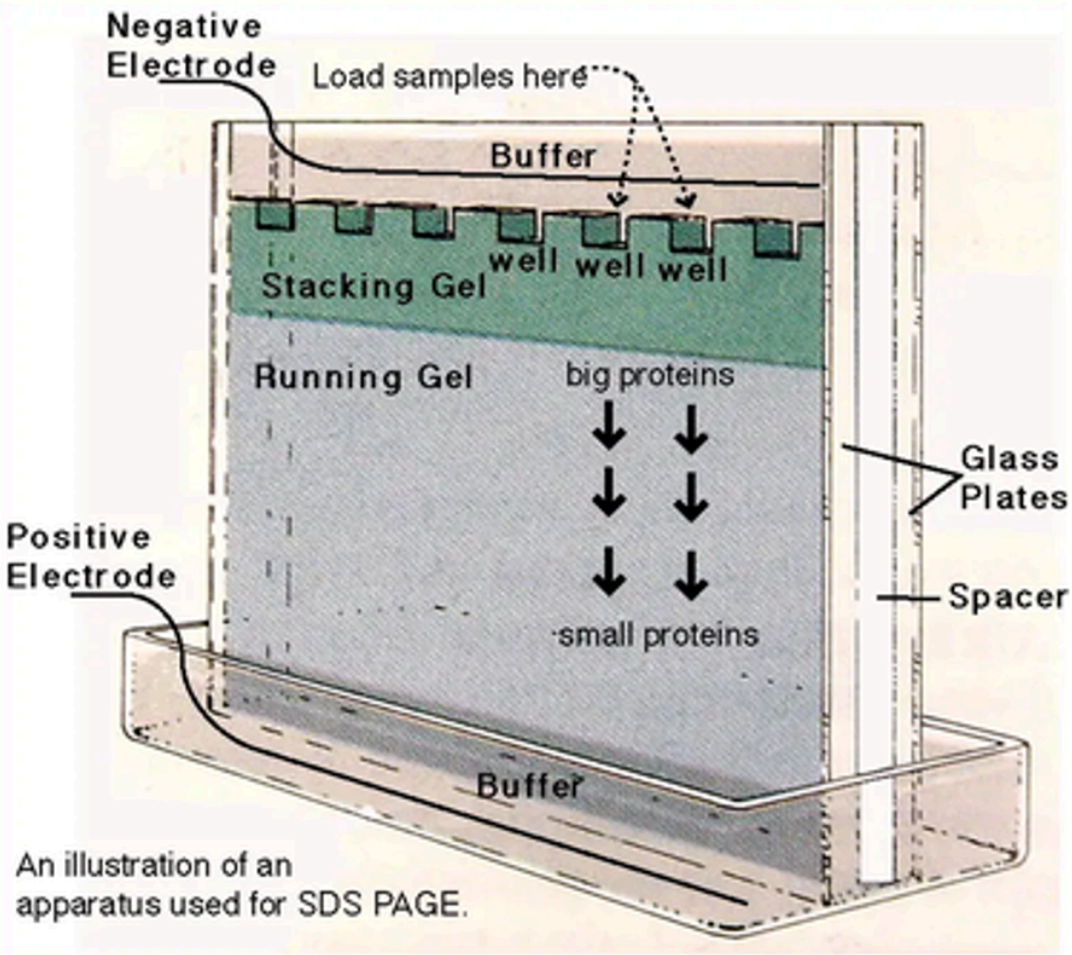

Figure 32: Diagram of the SDS–PAGE apparatus used for protein separation by molecular weight.[24]

Samples were mixed with 4X Laemmli sample buffer (Bio-Rad) containing β-mercaptoethanol, heated at 95 °C for 5 minutes to denature proteins, and loaded onto a 12% resolving gel with a 5% stacking gel. Electrophoresis was performed at a constant voltage of 100 V until the dye front reached the bottom of the gel (~2 hours).

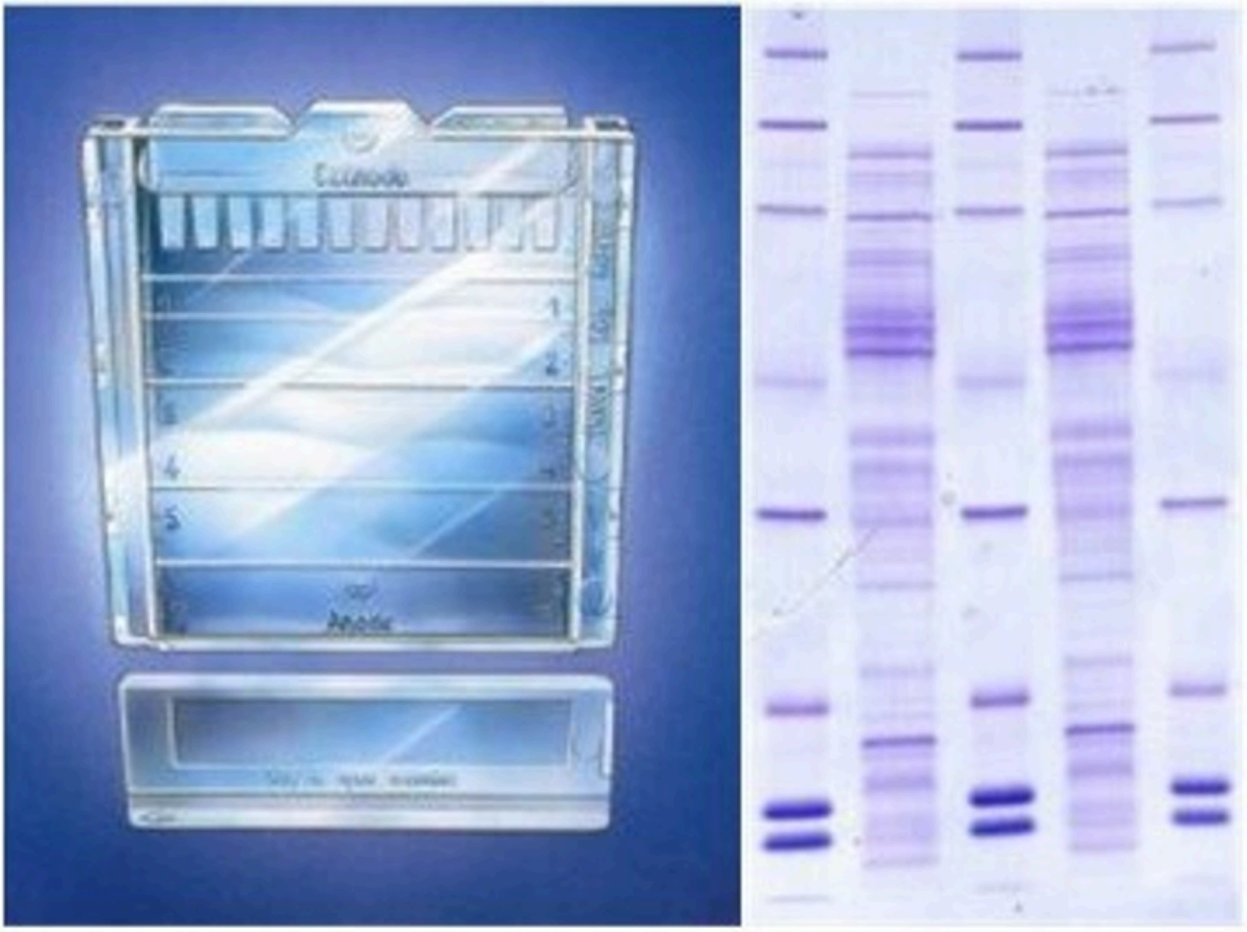

Figure 33: Polyacrylamide gel electrophoresis setup and representative stained gel.[24]

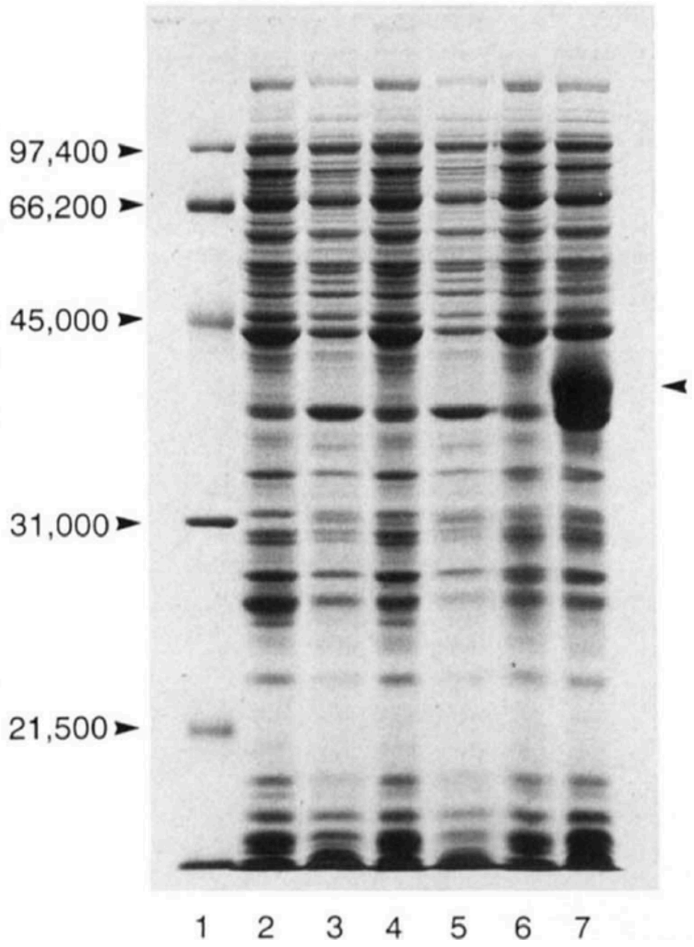

Figure 34: Example of inducible protein overexpression in *E. coli* BL21(DE3) using a T7 promoter system.[25]

Figure 34 serves as a reference for evaluating the expression pattern observed in the present study. Similar to the *firA*$^{+}$ construct shown here, induction of the *tunG* gene with IPTG was expected to yield a distinct band at the predicted molecular weight for the TunG protein (23 kDa), demonstrating successful transcriptional activation by T7 RNA polymerase. The contrast between uninduced and induced lanes underscores the effectiveness of the T7/pLysS system in tightly regulating recombinant protein expression.

Following electrophoresis, gels were stained with Coomassie Brilliant Blue G-250 and destained with 40% methanol, 10% acetic acid 50% deionized water solution until protein bands were clearly visible. The molecular weight of the expressed TunG protein was estimated by comparison with a prestained protein ladder (Invitrogen by Thermo Fisher Scientific).

Protein Purification and Dialysis

Nickel affinity chromatography is a selective purification technique used to isolate recombinant proteins that contain a polyhistidine tag (His-tag). The His-tag, typically composed of six consecutive histidine residues, has a strong affinity for divalent nickel ions (Ni^{2+}), which are immobilized on a solid support such as agarose beads.[28] This property allows the His-tagged protein to bind specifically to the nickel resin, while untagged proteins and other cellular components are washed away.

As illustrated in Figure 35, each agarose bead is functionalized with a chelating ligand, such as nitrilotriacetic acid (NTA), which coordinates a central Ni^{2+} ion. The nickel ion forms coordination bonds with the nitrogen atoms of the histidine imidazole side chains on the target protein.[28] When a cell lysate containing the recombinant protein is passed through the column, the His-tagged TunG protein binds tightly to the nickel-charged matrix, whereas non-specific proteins lacking histidine residues are washed away with buffer.[28]

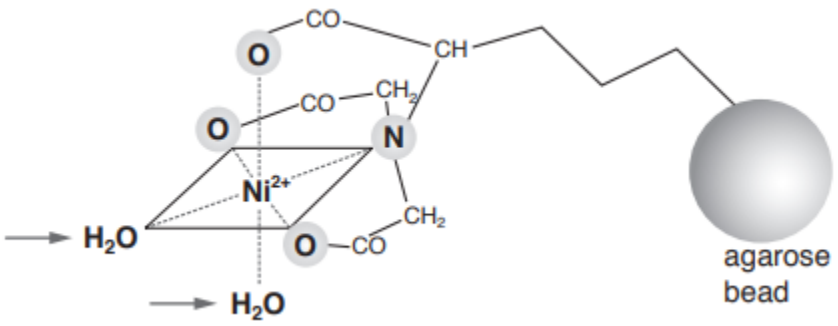

Figure 35: Coordination of Ni^{2+} ions in Ni–NTA agarose beads used for affinity purification of His-tagged proteins.[31]

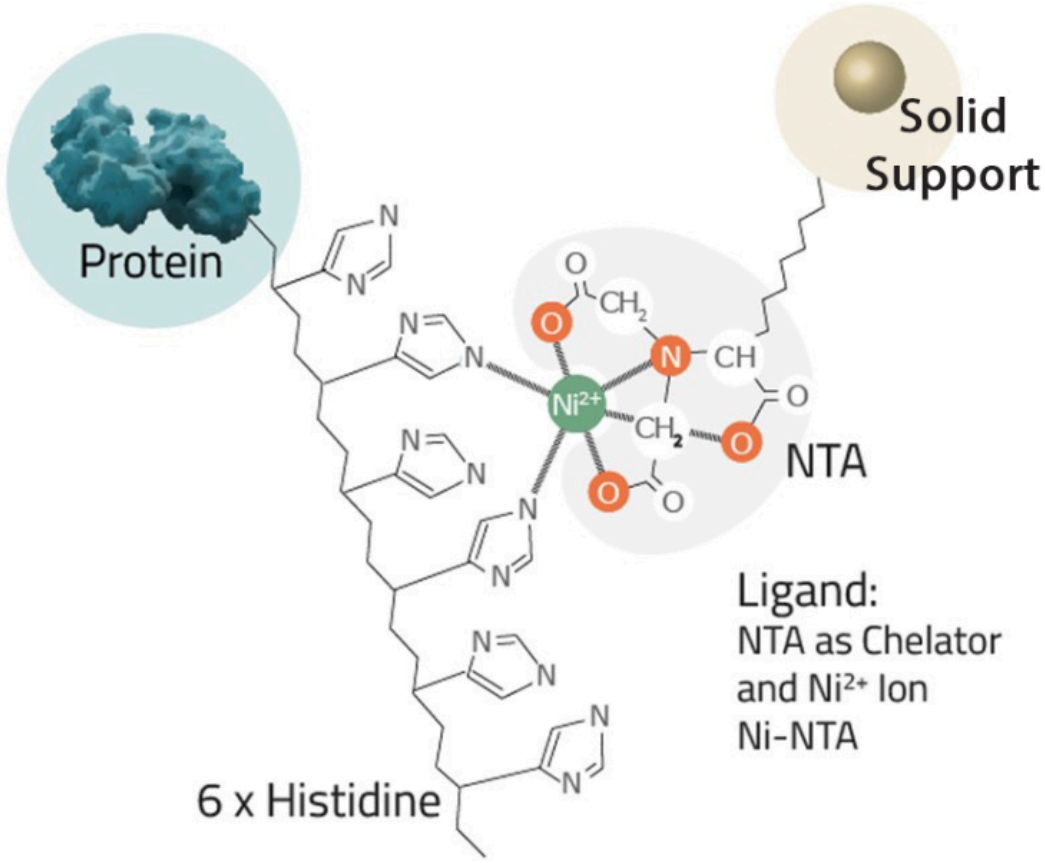

Figure 36: Molecular interaction between a His-tagged protein and Ni–NTA resin.[24]

After binding, the column is washed with a buffer containing a low concentration of imidazole (typically 10–30 mM) to remove weakly bound contaminants. The target protein is then eluted using a higher concentration of imidazole (200–300 mM), which competes with histidine for nickel binding sites, releasing the purified His-tagged protein from the resin.[28] All steps are performed at 4 °C to maintain protein stability and prevent denaturation. The result is then confirmed by using gel electrophoresis.

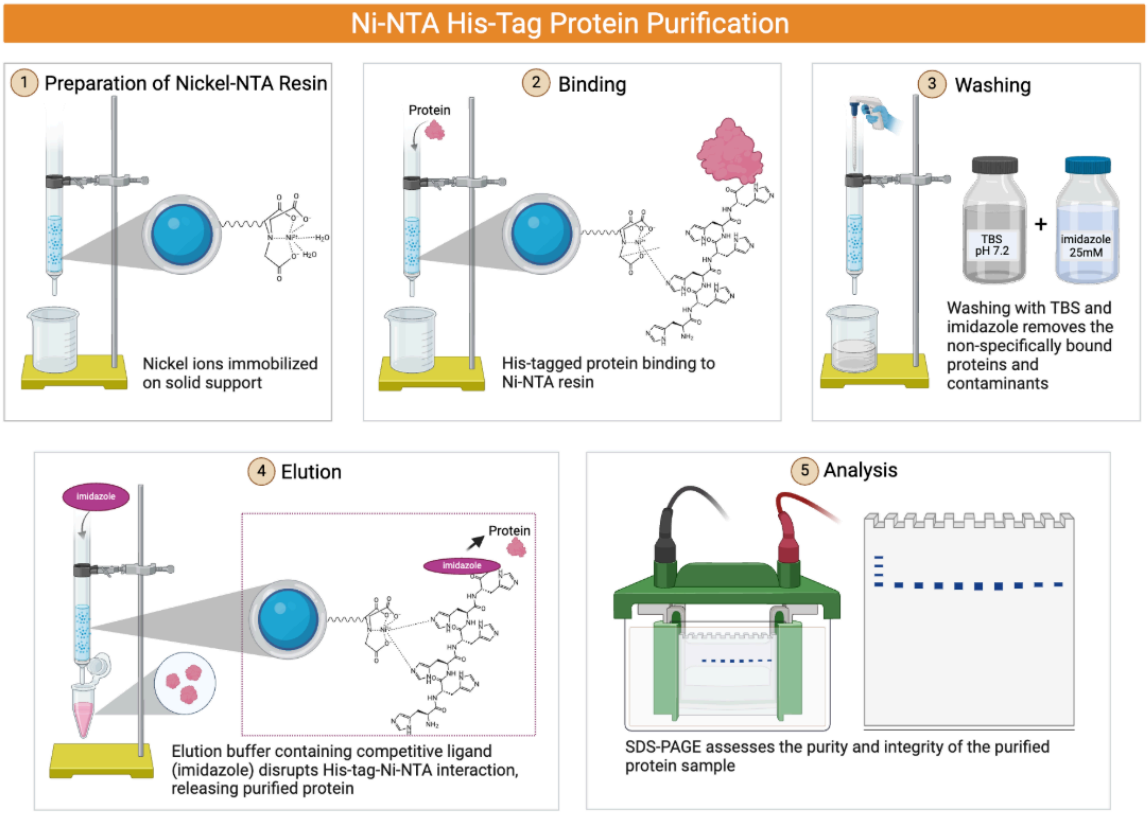

Figure 37: Workflow of Ni-NTA affinity purification of His-tagged proteins.

In this research, nickel affinity spin columns were used to purify the recombinant TunG enzyme expressed in *E. coli*.[28] The lysate containing soluble protein was applied to the Ni–NTA column, followed by washing and elution according to manufacturer guidelines. The resulting eluate contained purified TunG protein, which was subsequently dialyzed to remove imidazole and equilibrate the protein in a storage buffer for downstream enzymatic analysis.

Following cell lysis and centrifugation, the soluble protein fraction containing recombinant TunG protein was purified using a nickel-affinity spin column (Figure 38). The column contained a Ni-NTA agarose resin designed to selectively bind histidine-tagged proteins

under native conditions. Prior to loading the lysate, the resin was equilibrated with Equilibration Buffer (pH 7.4) consisting of 300 mM NaCl, 10 mM imidazole, and 50 mM MOPS. The clarified lysate was then carefully applied to the column and allowed to bind under gravity flow.

Figure 38: Nickel affinity spin column used for purification of the TunG protein.

Unbound proteins and cellular debris were removed with Wash Buffer (50 mM MOPS, 300 mM NaCl, 30 mM imidazole). Elution was achieved by adding Elution Buffer (50 mM MOPS, 300 mM NaCl, 250 mM imidazole) in 2 mL fractions, which selectively displaced the His-tagged TunG protein from the nickel resin. Eluates were collected into microcentrifuge tubes and kept on ice. Eluate fractions were subsequently pooled for dialysis.

Dialysis is a purification technique used to separate small molecules (such as salts, imidazole, and buffer components) from larger macromolecules like proteins. The process relies

on a semipermeable membrane, typically made of cellulose or regenerated cellulose, that allows small solutes and solvents to diffuse freely while retaining larger biomolecules based on their molecular weight.

When a protein solution is placed inside dialysis tubing and submerged in a large volume of buffer, a concentration gradient forms between the inside and outside of the tubing. Small molecules such as salts, urea, or imidazole diffuse out through the membrane pores into the surrounding buffer, while proteins remain trapped inside due to their larger size. Over time, and especially with multiple buffer changes, this diffusion process effectively exchanges the solution inside the tubing with the desired buffer, removing impurities and equilibrating the protein sample.

In this research, dialysis was performed following nickel affinity chromatography to remove imidazole and exchange the TunG protein into a storage buffer. Samples were kept on ice and centrifuged at 4 °C before dialysis to remove insoluble particles and maintain protein stability. Performing dialysis at low temperature prevents denaturation and aggregation of the purified enzyme, ensuring the TunG protein remains active and properly folded for subsequent analyses.

Figure 39: Preparation of microdialysis tubing using a perforated microcentrifuge tube cap.[30]

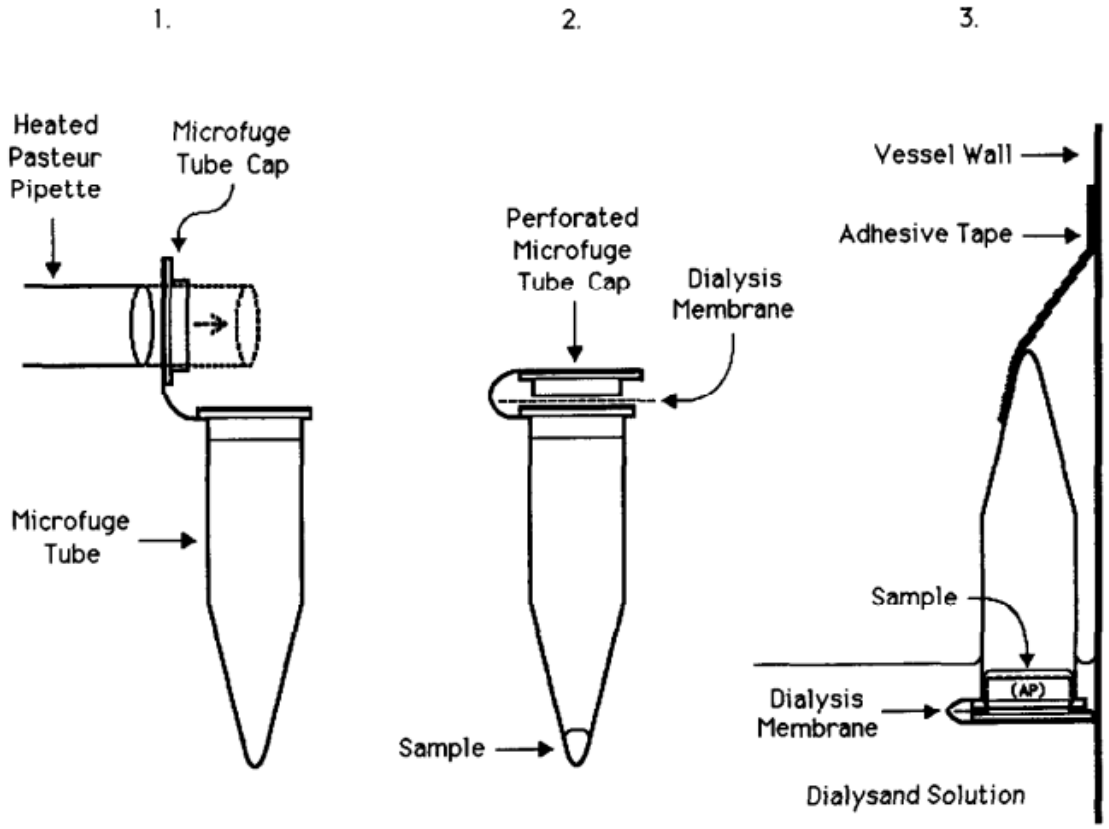

Figure 40: Microdialysis setup for buffer exchange and removal of small molecules from protein samples.[27]

Dialysis was performed to remove excess imidazole and exchange the protein into a physiologically compatible buffer. The purified eluate was dialyzed overnight at 4 °C using Spectra/Por molecular porous membrane tubing (MWCO 12-14 kDa; 10 mm flat width, 6.4 mm diameter). This molecular weight cutoff was selected to retain the TunG protein (22.7 kDa) while allowing efficient diffusion of smaller molecules such as imidazole, salts, and buffer components. Approximately 3 mL of eluate was sealed within the tubing and submerged in a 10 mM MOPS, pH 7.4 dialysis buffer. Dialysis was carried out for 16–18 hours with one buffer

change to ensure complete removal of small molecules and imidazole. The dialyzed protein was then recovered and stored on ice for subsequent SDS–PAGE analysis to verify purity.

Figure 41: Centrifugation of protein samples at low temperature prior to dialysis.[30]

High Performance Liquid Chromatography (HPLC)

High-Performance Liquid Chromatography (HPLC) is an analytical technique used to separate, identify, and quantify the components of a chemical mixture. The method relies on the differential interaction of compounds between two phases: a mobile phase, which is a liquid solvent that carries the sample through the system, and a stationary phase, which is a solid material packed inside the column. Molecules within the sample interact with these two phases to varying degrees, resulting in different retention times as they pass through the column.

As shown in Figure 42, the process begins when a liquid sample is injected into the system and carried by the mobile phase via a solvent delivery pump. The sample mixture enters the column, where its components interact with the stationary phase. Compounds that have stronger interactions with the stationary phase move more slowly, while those that interact weakly elute faster. A detector positioned at the end of the column measures the concentration of each compound as it exits, converting the signal into an electrical output that forms a chromatogram: a graph of signal intensity versus retention time.

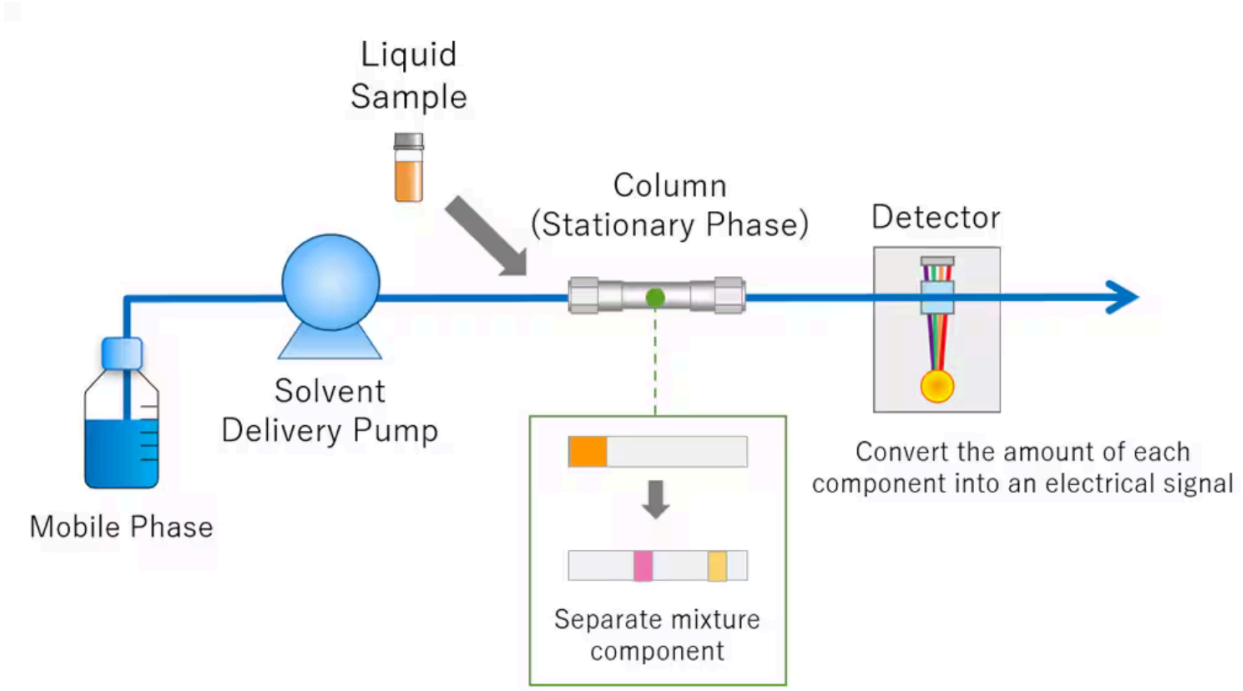

Figure 42: Schematic of a high-performance liquid chromatography (HPLC) system.[36]

Figure 43 illustrates how each compound in a mixture separates based on its unique rate of movement through the column. As each compound elutes, the detector records a distinct peak, with the area under each peak corresponding to the relative quantity of that compound. By comparing retention times and peak areas with known standards, HPLC provides both qualitative (identity) and quantitative (concentration) information about the sample.

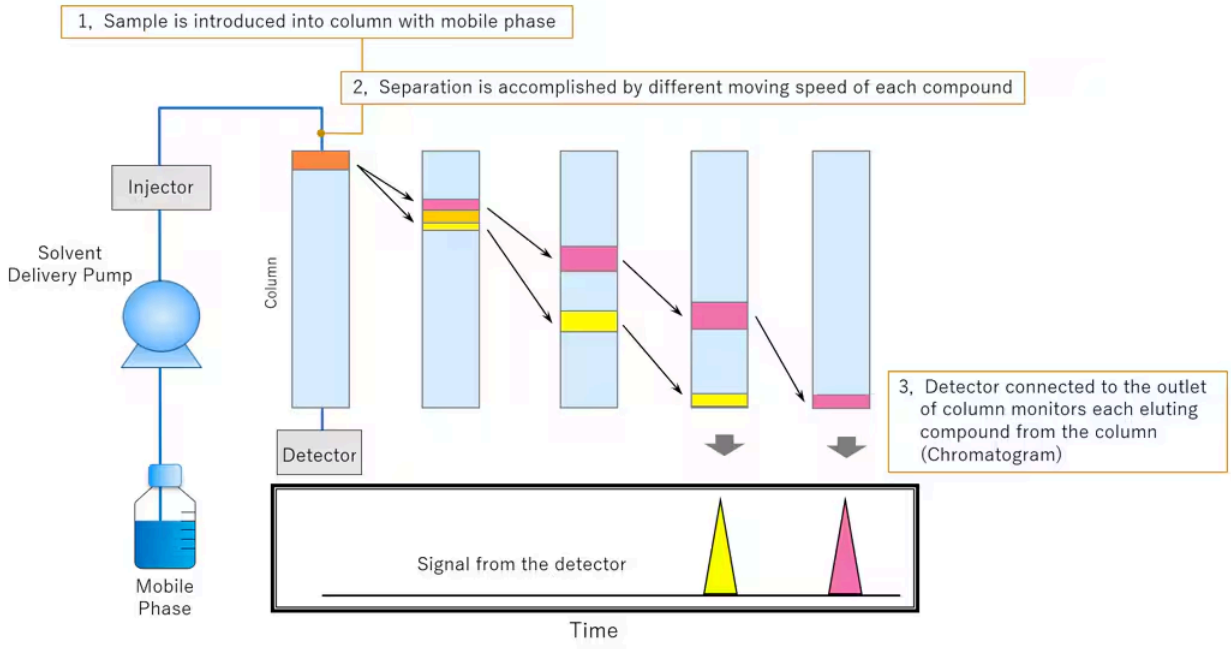

Figure 43: Principle of chromatographic separation and detection in HPLC.[36]

In this research, SDS-PAGE was used to assess the purity and concentration of the TunG protein following nickel affinity purification and dialysis. HPLC, by contrast, was applied to analyze the enzymatic activity of the TunG protein on its imputed substrate, uridine monophosphate (UMP) and other nucleotide monophosphate compounds. The technique allowed separation and identification of nucleotide species produced by the reaction, enabling detection of substrate utilization and potential product formation. By comparing chromatographic profiles of control reactions (without enzyme) to those containing purified TunG protein, HPLC provided evidence of biochemical activity and insight into the enzyme's possible catalytic role in the tunicamycin biosynthetic pathway.

The HPLC system was equipped with a reverse-phase analytical column and a diode array detector (DAD) that measured absorbance across the 200–800 nm wavelength range. This setup enabled the inspection of each eluting peak's absorbance spectrum, allowing for accurate confirmation of compound identity and verification of peak assignments corresponding to uridine-based nucleotides.

Two mobile phases were used throughout the experiment. Buffer A consisted of 20 mM triethylammonium acetate (TEAA) adjusted to pH 6.0, while Buffer B was composed of 0.1% formic acid in acetonitrile (CH_3CN). The HPLC was run at a constant flow rate of 1.0 mL per minute. The gradient began with 100% Buffer A until 10 minutes into the run, at which point it was gradually adjusted to 92% A and 8% B at 18 minutes, before returning to 100% Buffer A at 20 minutes. Between runs, the system was equilibrated with 100% Buffer A to ensure consistent separation and retention times.

To establish baseline retention times and facilitate compound identification, standard solutions of UMP, UDP, and UTP were prepared and analyzed under identical chromatographic conditions. These retention times provided the basis for identifying peaks corresponding to nucleotide species in subsequent experimental samples.

For reaction samples, to ensure what compound the peaks corresponded to, spike tests were performed, in which a sample was run multiple times without any substance added and with other substances "spiked" in to observe which peak increases in size. The peak that increases in size corresponds to the retention time of the substance that was spiked into the sample.

Two primary reaction mixtures were prepared for HPLC analysis: a control reaction and a complete reaction containing the purified TunG enzyme. The control reaction consisted of 780

μL of deionized water, 1000 μL of 50 mM MOPS buffer (pH 7.4), 200 μL of 10 mM $MgCl_2$, and 20 μL of 50 mM substrate solution, with no enzyme added. The complete reaction contained 580 μL of deionized water, 1000 μL of 50 mM MOPS buffer (pH 7.4), 200 μL of 10 mM $MgCl_2$, 20 μL of 50 mM of substrate, and 200 μL of the TunG enzyme solution. Both reactions were incubated under identical conditions. Samples were taken at regular intervals before being centrifuged briefly to remove any insoluble material. The clarified supernatants were then injected into the HPLC system for analysis, allowing for the separation and detection of nucleotide species to determine substrate utilization and product formation in subsequent analyses.

To assess enzyme stability over time, additional reactions were prepared in which all components except the nucleotide substrate were combined and incubated at room temperature for 20-40 hours prior to substrate addition. After this pre-incubation period, the substrate UMP was added to initiate the reaction. These samples were processed in parallel with standard reactions to evaluate whether prolonged incubation affected the catalytic activity of the TunG protein.

VI. Results

Expression and purification of the TunG protein

SDS-PAGE was used to evaluate expression, solubility, and purification of the TunG protein across multiple experimental runs. Protein samples from Run F (pET+) and Run H under both pET− and pET+ conditions were analyzed following induction, cell lysis, nickel affinity purification, and elution.

In Run F (pET+), a distinct protein band was observed at approximately 22.7 kDa, corresponding to the expected molecular weight of the TunG protein (Figure 44). This band was visible in post-induction and soluble (supernatant) fractions and was retained through nickel affinity purification, appearing prominently in early elution fractions. Additional protein bands at other molecular weights were also observed in the elution fractions.

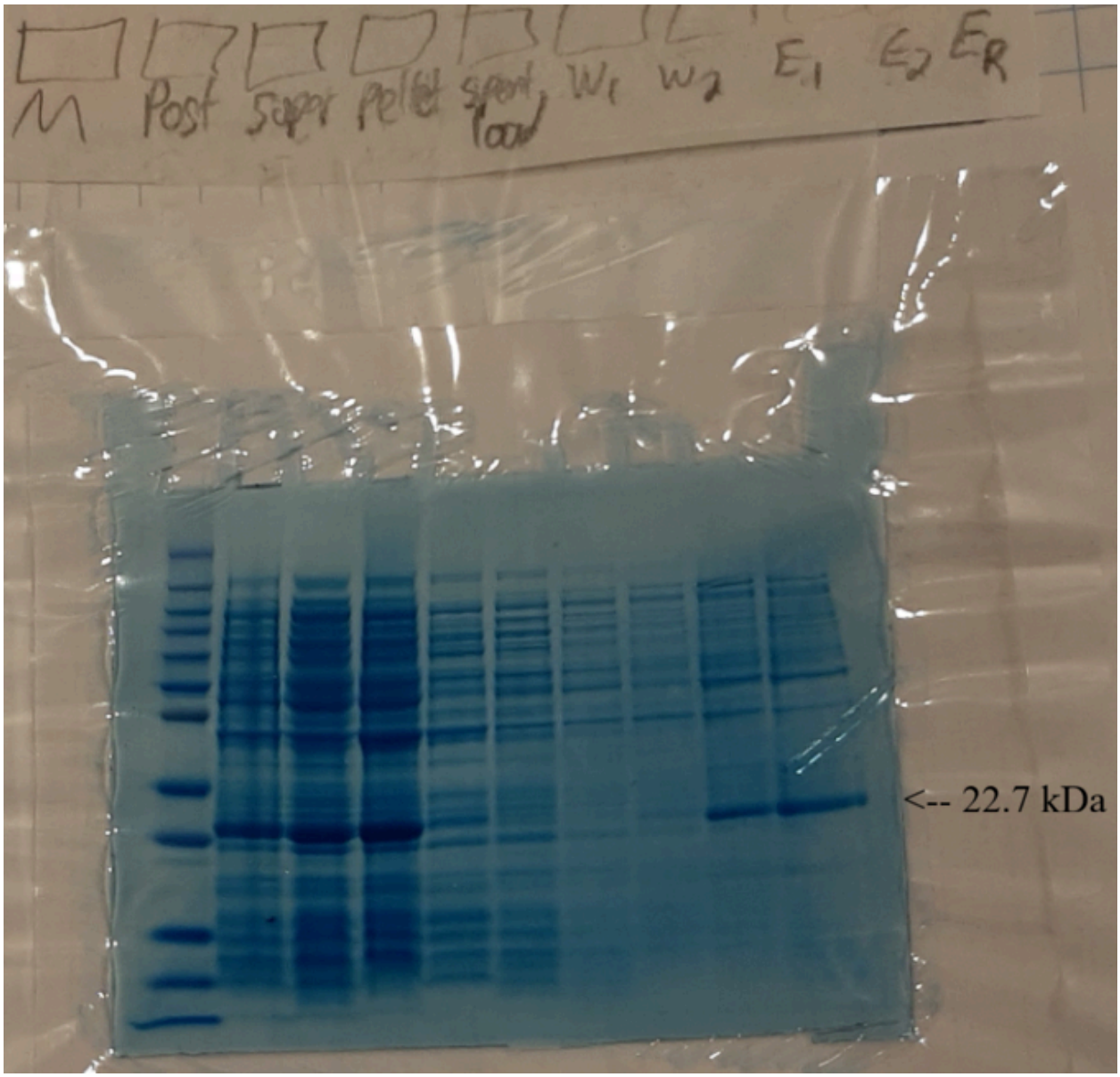

Figure 44: SDS–PAGE analysis of recombinant TunG protein expression and purification from *E. coli* BL21(DE3) pET+ cells (Run F+). Lanes include molecular weight marker (M), post-induction lysate, soluble supernatant, insoluble pellet, spent load, wash fractions (W_1 and W_2), elution fractions (E_1, E_2, and E_R), and remaining elution volume (ER). A band at approximately 23 kDa is observed in post-induction, supernatant, pellet, and elution fractions.

For Run H, SDS–PAGE gels were analyzed for both cells lacking the pET expression plasmid (H−) and cells containing the pET-*tunG*-6×His plasmid (H+; Figure 45). In both conditions, a protein band was observed near 22.7 kDa. However, the band corresponding to this molecular weight appeared more intense in the pET+ condition relative to the pET− condition across comparable fractions. Both H− and H+ gels showed multiple additional protein bands across a range of molecular weights, including within elution fractions.

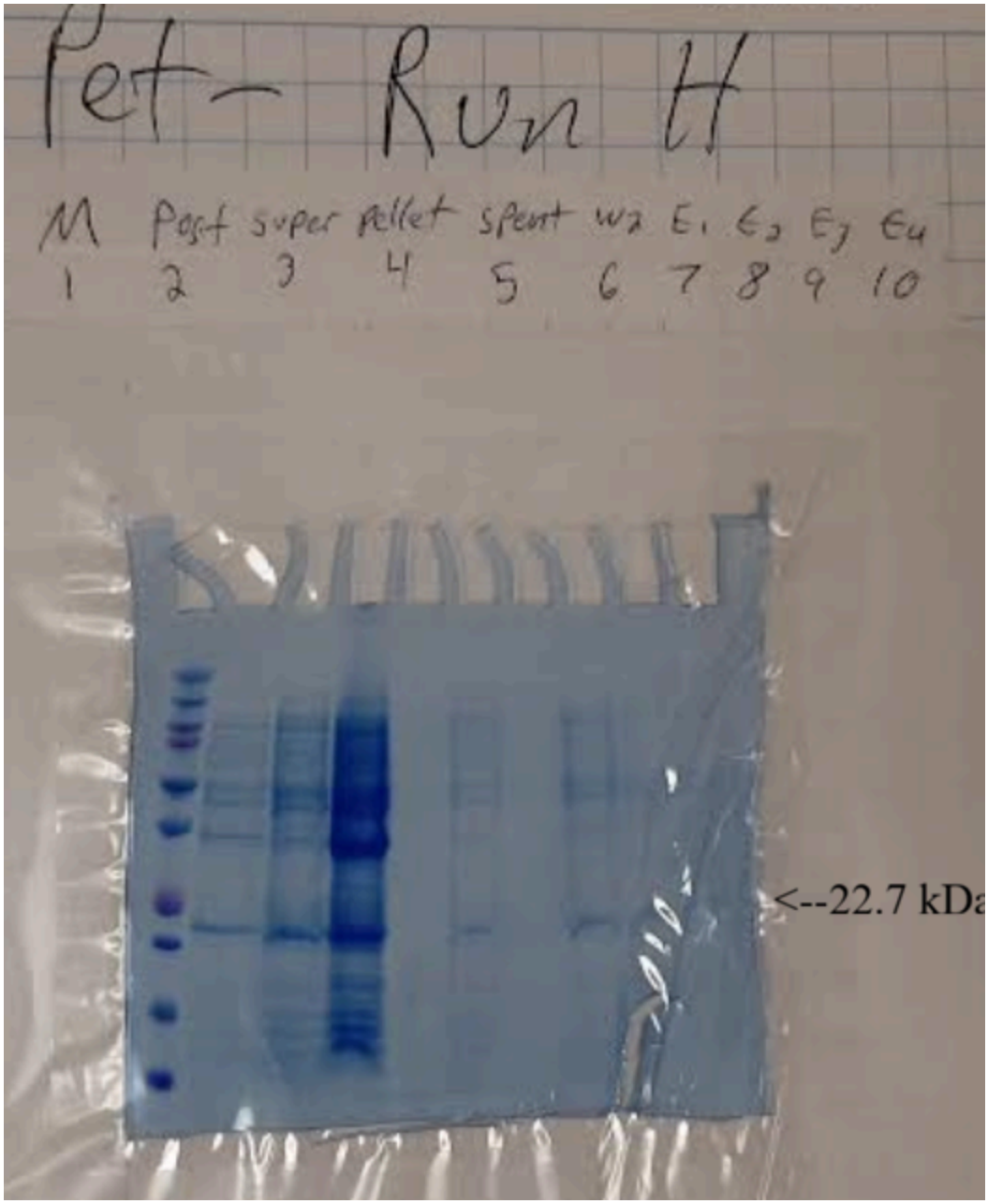
Pet- Run H
M Post super pellet spent w2 E1 E2 E3 E4
1 2 3 4 5 6 7 8 9 10
<--22.7 kDa

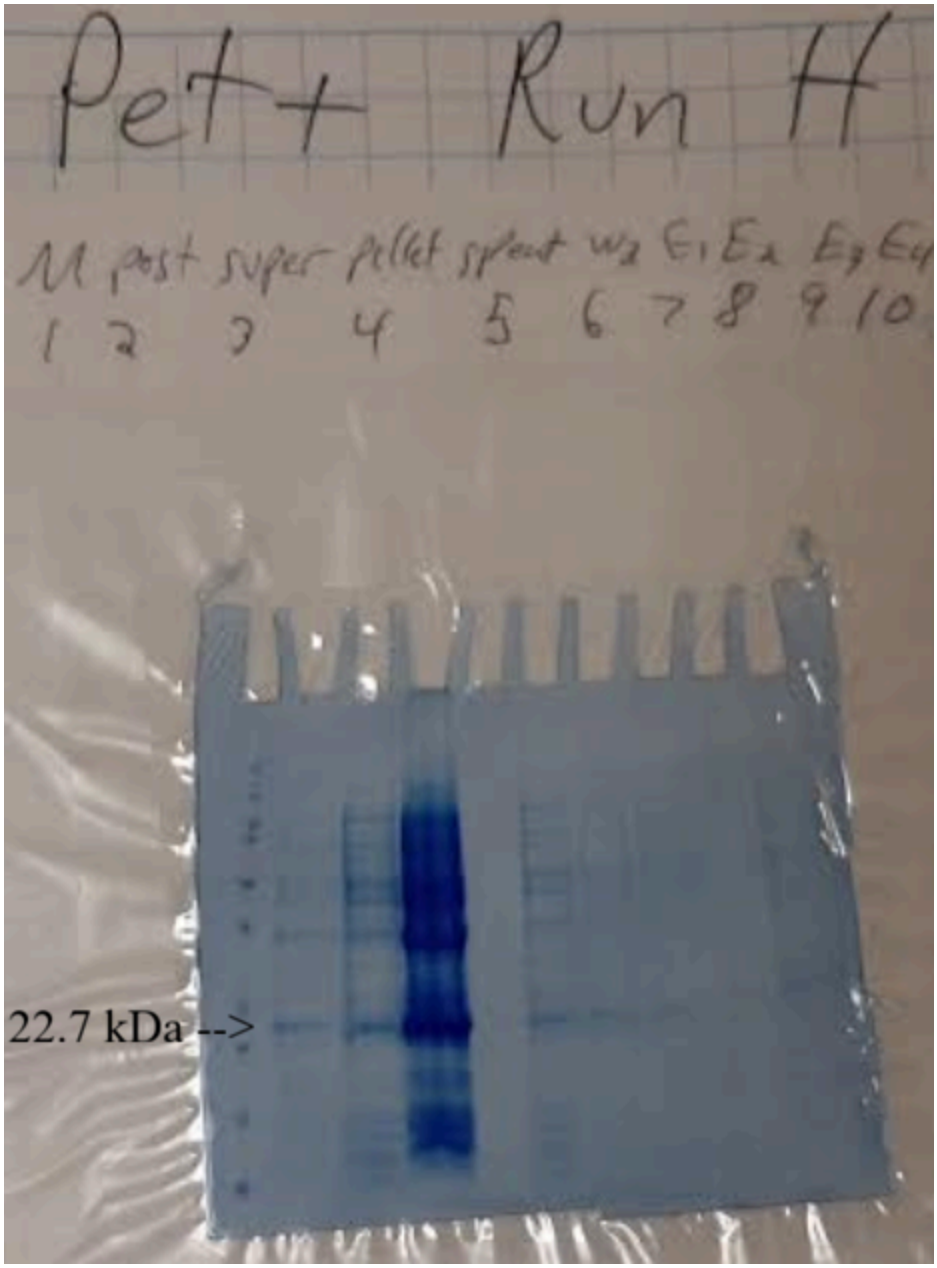

Figure 45: SDS–PAGE analysis of Run H comparing pET− and pET+ conditions.

Coomassie-stained SDS–PAGE gels showing fractions collected during Run H for cells lacking the pET-TunG plasmid (H−, top) and cells containing the pET-*tunG*-6×His plasmid (H+, bottom). Lanes include molecular weight marker (M), post-induction lysate, supernatant, pellet, column flow-through

(spent), wash fractions (W), and elution fractions (E). The expected molecular weight of the TunG protein (22.7 kDa) is indicated.

Chromatographic Identification of Nucleotide Standards

To establish reference retention times for nucleotide, nucleoside, and free base species analyzed in this study, individual standards were examined by HPLC under identical chromatographic conditions. Uracil-based compounds (uridine monophosphate, uridine, and uracil) produced distinct and reproducible peaks with unique retention times (Figure 46). Adenine-based compounds (adenosine monophosphate, adenosine, and adenine) likewise resolved into discrete peaks that were readily distinguishable from one another (Figure 47). Thymine-based compounds (thymidine monophosphate, thymidine, and thymine) exhibited similarly distinct retention profiles (Figure 48). Collectively, these standards established a reference set of retention times for phosphorylated nucleotides, nucleosides, and free bases across all three nucleobase families examined.

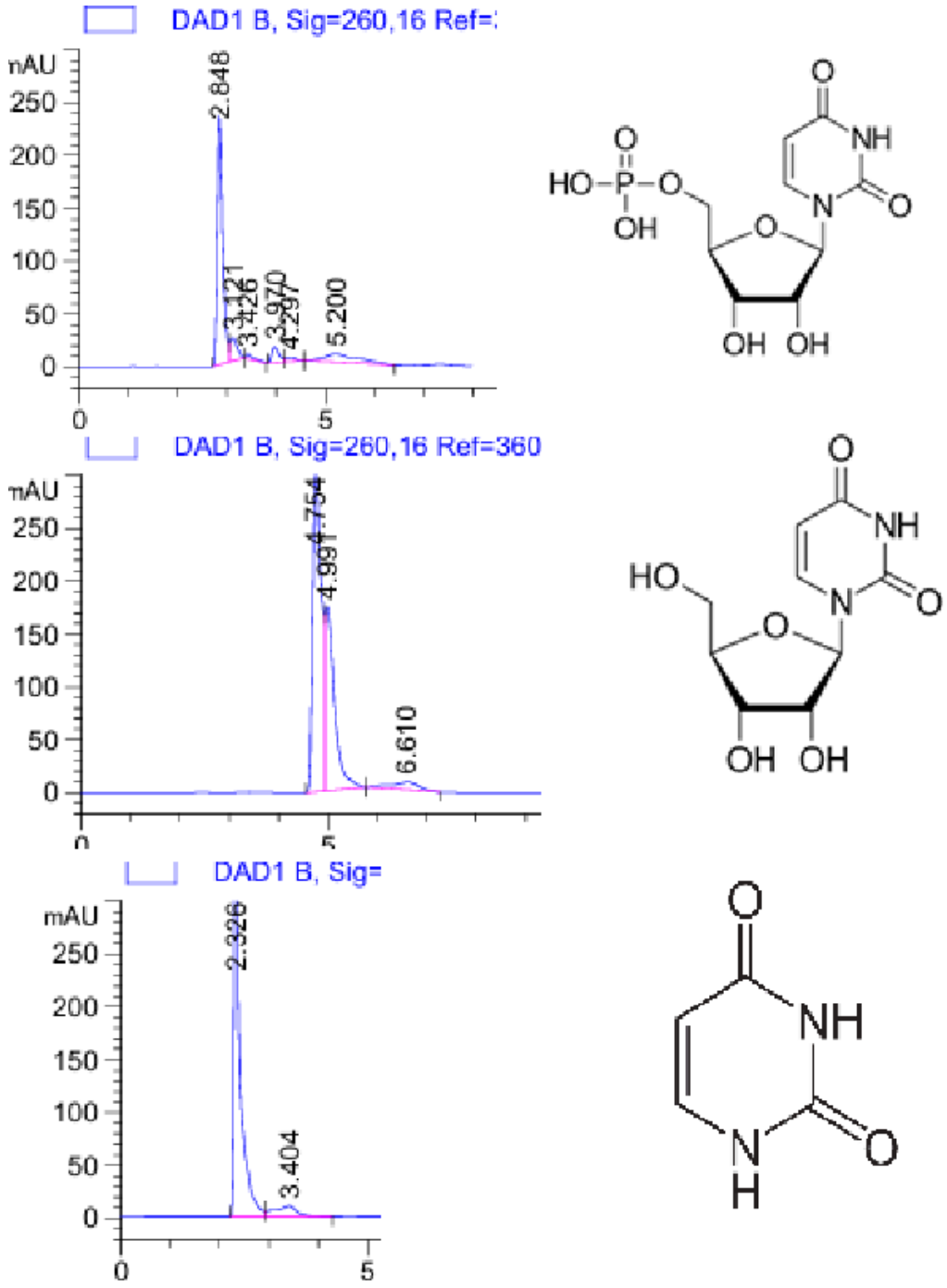

Figure 46: HPLC chromatograms of uracil-based nucleotide and nucleoside standards. Representative chromatograms show from top to bottom uridine monophosphate (UMP), uridine, and uracil analyzed under identical chromatographic conditions.

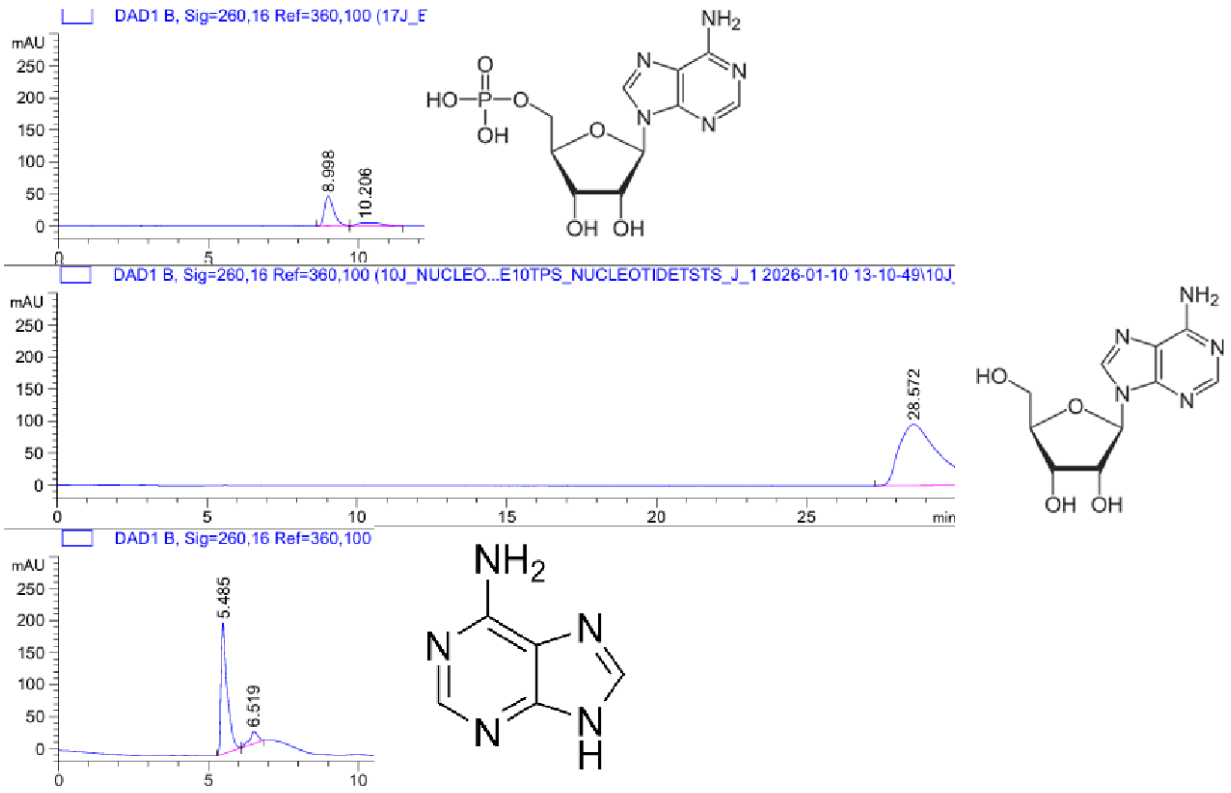

Figure 47: HPLC chromatograms of adenine-based nucleotide and nucleoside standards. Representative chromatograms show from top to bottom adenosine monophosphate (AMP), adenosine, and adenine analyzed under identical chromatographic conditions.

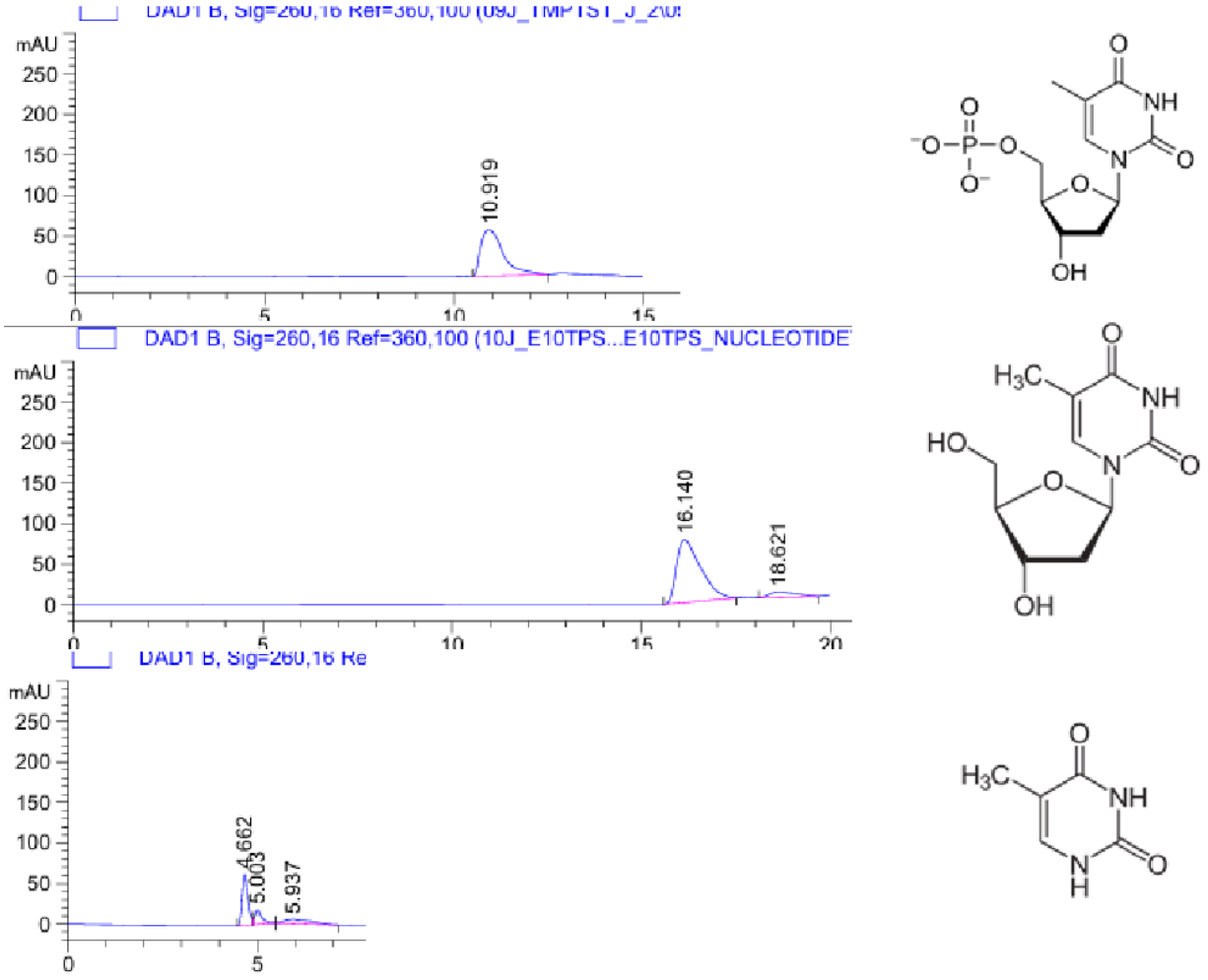

Figure 48: HPLC chromatograms of thymine-based nucleotide and nucleoside standards. Representative chromatograms show from top to bottom thymidine monophosphate (TMP), thymidine, and thymine analyzed under identical chromatographic conditions.

Spike tests were then performed using reaction samples to confirm compound identities within experimental chromatograms. A representative reaction time-point sample was analyzed without addition of standards ("Normal") and then reanalyzed following spiking with individual reference compounds (Figure 48). Upon addition of uracil, uridine, or uridine monophosphate, a

selective increase in peak area was observed at the corresponding retention time relative to the untreated sample. No new peaks were introduced outside the expected retention windows for the added standards. This approach confirmed the assignment of uracil-based species present within reaction mixtures and validated the retention time mapping established using purified standards.

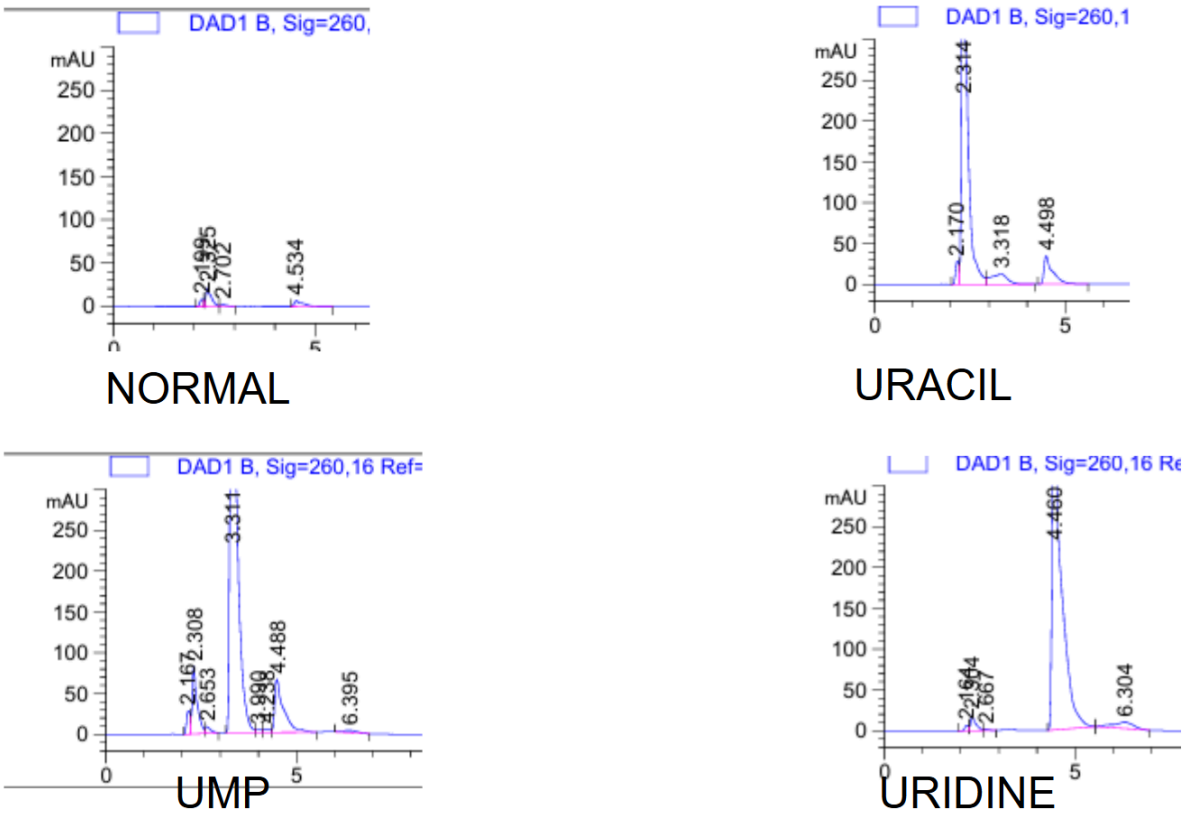

Figure 49: HPLC spike tests used to assign nucleotide identities within a reaction time-point sample.

Together, the standard chromatograms and spike tests provided a consistent framework for identifying nucleotide species in subsequent reaction analyses. These assignments were used throughout the remainder of the study to compare control and enzyme-containing reactions and to track changes in substrate and product profiles over time.

Comparison of Control and TunG-Containing Reaction Profiles

Time-course HPLC analysis was used to compare nucleotide profiles between control reactions and reactions containing the TunG protein. For all chromatograms, peak areas were calculated automatically by the HPLC software using integrated absorbance signals, reported as milli-absorbance units multiplied by time (mAU·s). Peak areas corresponding to uridine monophosphate (UMP), uridine, and uracil were extracted at each time point and plotted as a function of incubation time.

For Run F+, comparison of the control reaction and the complete reaction containing purified TunG protein revealed time-dependent changes in peak areas (Figure 50). In the control reaction, the UMP peak area decreased gradually over the course of the experiment, while the uridine peak area increased over time. The uracil peak remained low throughout the incubation period. In the TunG-containing reaction, UMP peak area also decreased with time, accompanied by the appearance and subsequent increase of uridine and uracil peak areas. These trends were observed consistently across all sampled time points.

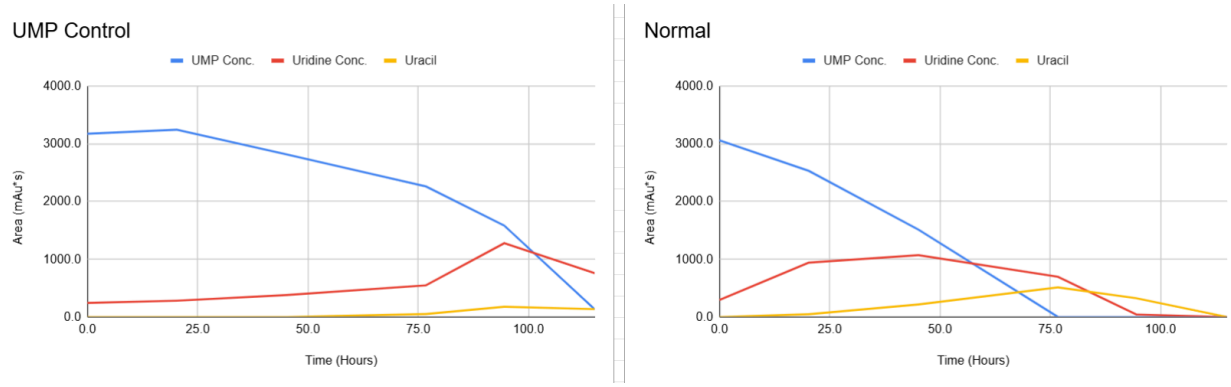

Figure 50: Time-course HPLC comparison of a UMP control reaction and a TunG-containing reaction (Run F+). Peak areas for UMP, uridine, and uracil are shown as a function of incubation time.

To further compare reactions derived from different expression conditions, HPLC profiles were analyzed for control, H−, and H+ samples from Run H (Figure 51). In the control reaction, the UMP peak area remained relatively stable over time, with smaller changes observed for uridine and uracil. In the H− reaction, UMP peak area decreased over time, while uridine and uracil peak areas increased, reaching maxima at intermediate time points before declining. In the H+ reaction, similar time-dependent changes were observed, with decreasing UMP peak area and increasing uridine and uracil peak areas across the incubation period.

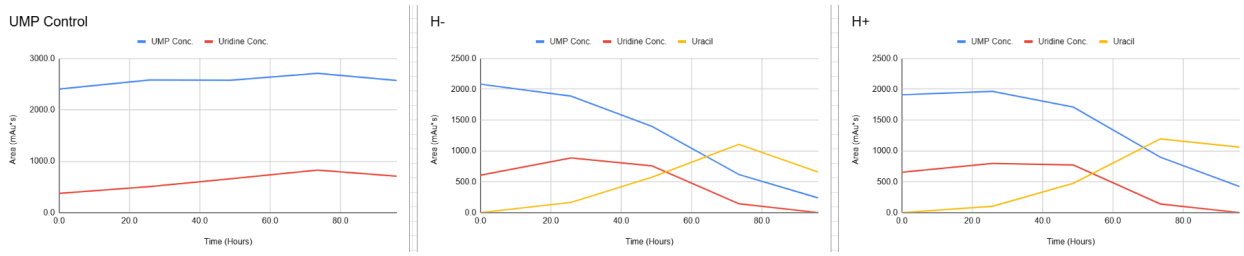

Figure 51: Time-course HPLC comparison of UMP reactions under control, H−, and H+ conditions. Peak areas for UMP, uridine, and uracil are plotted over time for each condition.

Across all conditions shown in Figures 50 and 51, peak areas were determined using identical integration parameters and chromatographic methods, enabling direct comparison of time-course profiles between control, H−, and H+ reactions. These data establish the temporal behavior of nucleotide species under the tested reaction conditions and provide a basis for subsequent comparison of reaction outcomes under varying experimental parameters.

Effect of Reaction Conditions on Chromatographic Profiles

The effect of reaction conditions on nucleotide conversion was evaluated using time-course HPLC analysis under varying enzyme, temperature, pH, and metal cofactor conditions.

Variation in enzyme concentration affected the magnitude of chromatographic changes observed over time. Reactions containing lower amounts of enzyme (1/2 and 1/4 enzyme conditions) displayed slower changes in UMP, uridine, and uracil peak areas compared to reactions containing the full enzyme concentration (Figure 52).

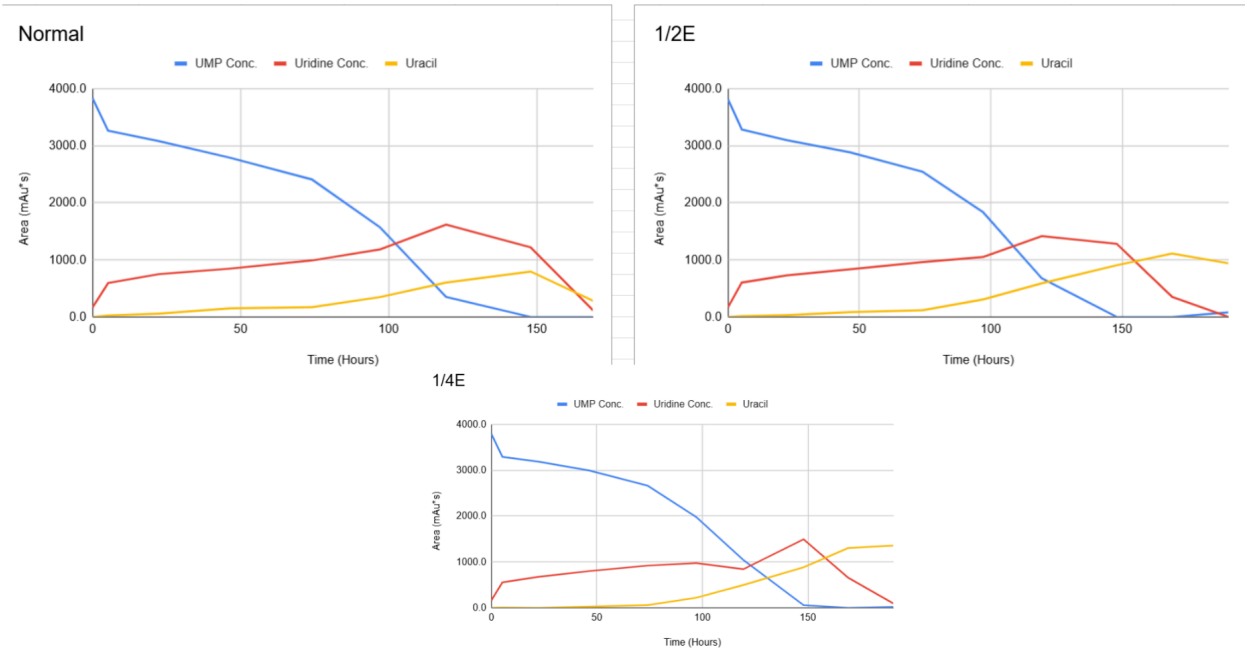

Figure 52: Effect of enzyme concentration on UMP reaction time courses (full enzyme, 1/2 enzyme, and 1/4 enzyme).

Incubation temperature also influenced chromatographic profiles. Reactions performed at 28 °C, 34 °C, and 37 °C showed distinct time-dependent changes in nucleotide peak areas, with

higher temperatures generally associated with more rapid changes in UMP and product peak areas (Figure 53).

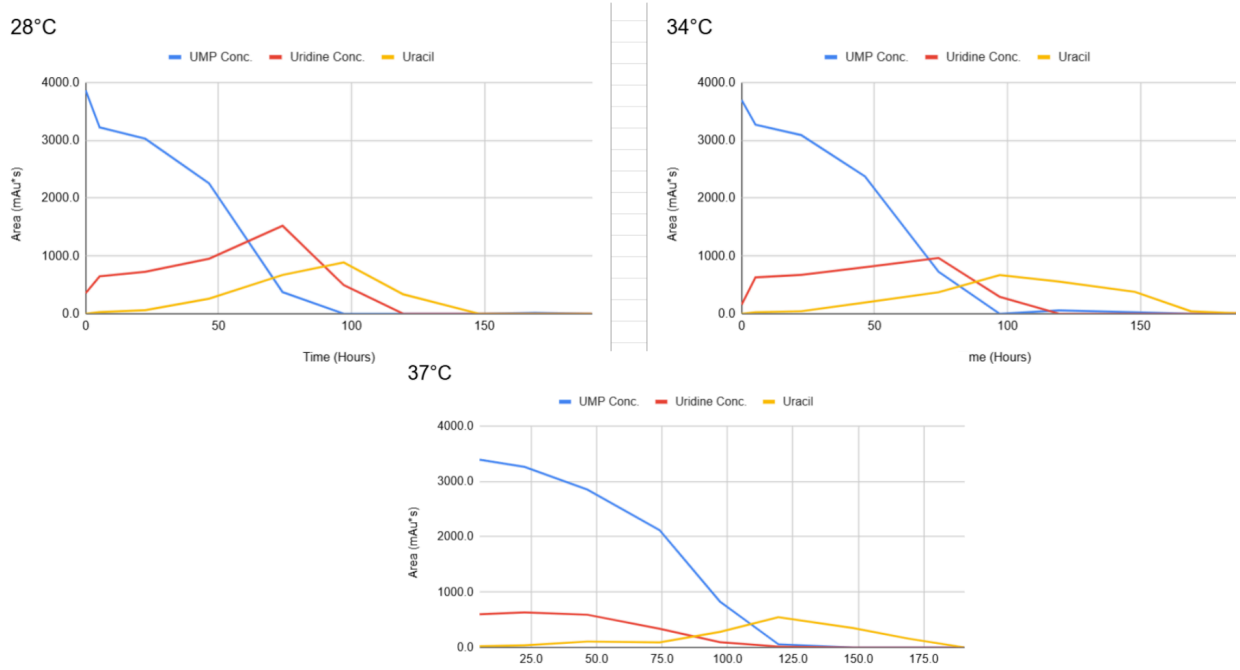

Figure 53: Effect of incubation temperature on UMP reaction time courses (28 °C, 34 °C, and 37 °C).

The effect of pH on reaction profiles was assessed by comparing reactions conducted at pH 6.0, pH 7.0, and pH 8.0. Across these conditions, UMP, uridine, and uracil peak areas changed over time, with differences observed in the relative rates and extents of these changes (Figure 54).

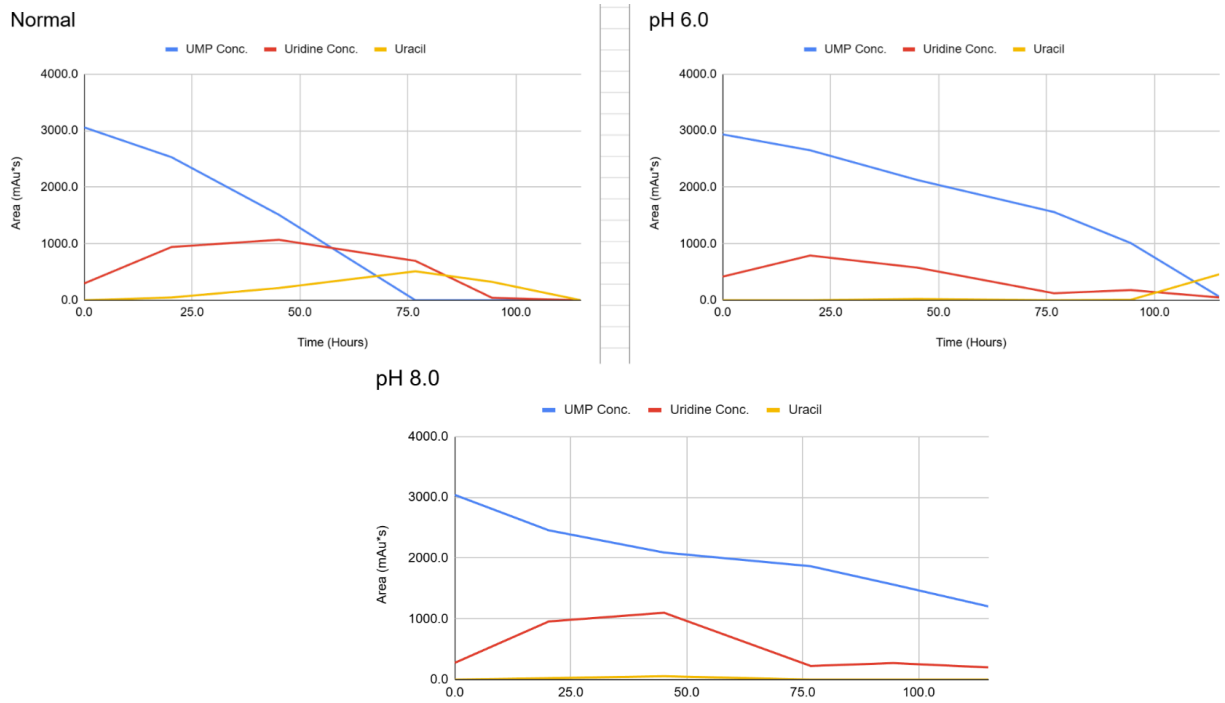

Figure 54: Effect of pH on UMP reaction time courses (pH 6.0, 7.0, and 8.0).

Metal cofactors also influenced chromatographic outcomes. Reactions conducted in the presence of Mg^{2+}, Mn^{2+}, or Co^{2+} displayed distinct time-course profiles for UMP, uridine, and uracil peak areas (Figure 55). Comparison of reactions performed with $MgCl_2$ versus $MgSO_4$ as the magnesium source showed similar chromatographic trends over time, indicating comparable reaction profiles between the two magnesium salts (Figure 56).

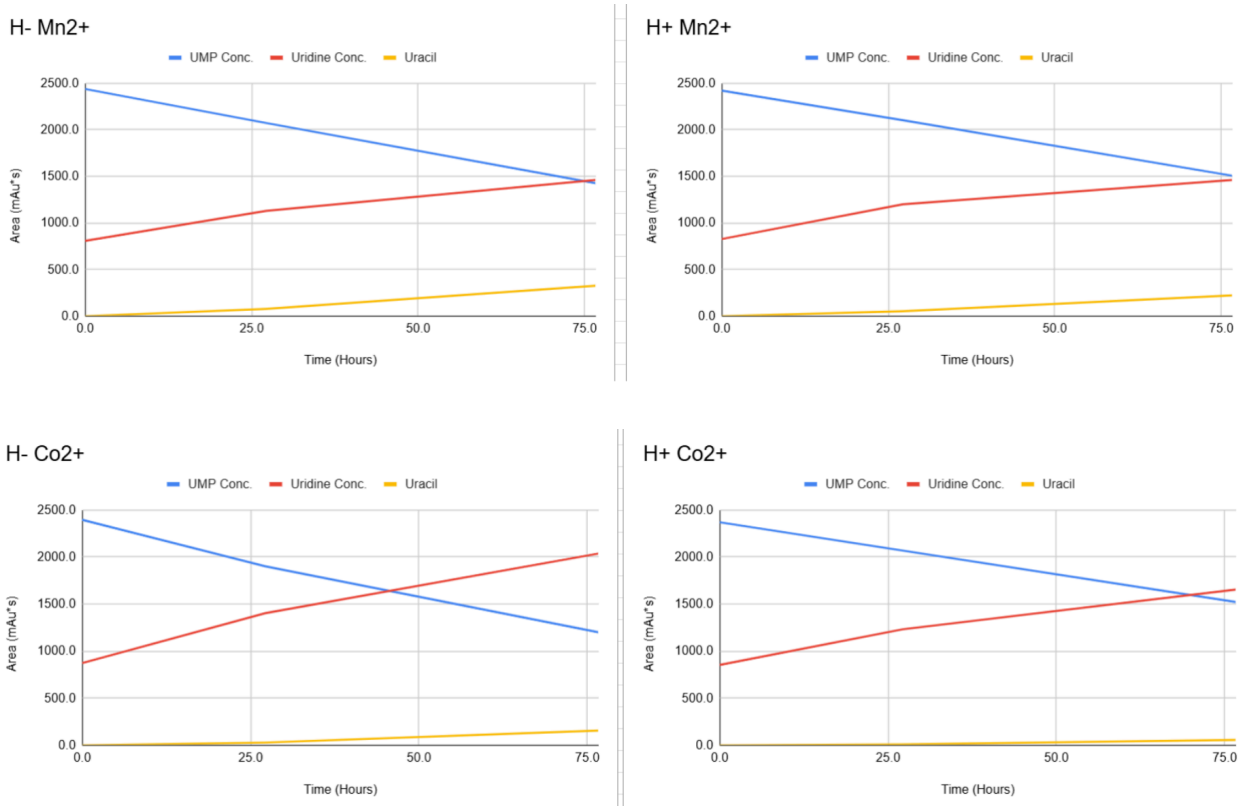

Figure 55: Effect of divalent metal cofactors (Mn^{2+} and Co^{2+}) on UMP reaction time courses.

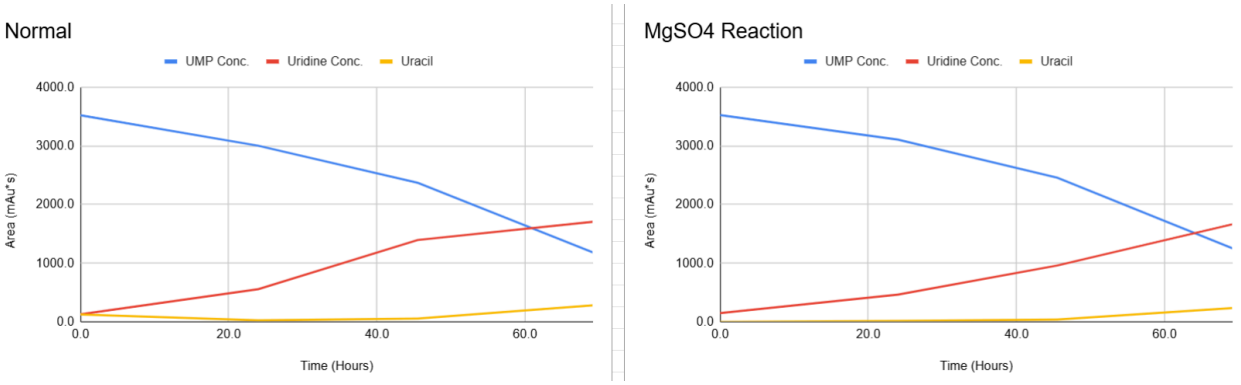

Figure 56: Comparison of $MgCl_2$ and $MgSO_4$ as magnesium sources in UMP reactions.

Additional reactions using alternative nucleotide substrates further demonstrated condition-dependent chromatographic changes. AMP reactions showed time-dependent decreases in AMP peak area with corresponding changes in adenosine and adenine peak areas relative to controls (Figure 57). Similarly, TMP reactions displayed changes in TMP and thymidine peak areas over time when enzyme was present compared to control reactions (Figure 58).

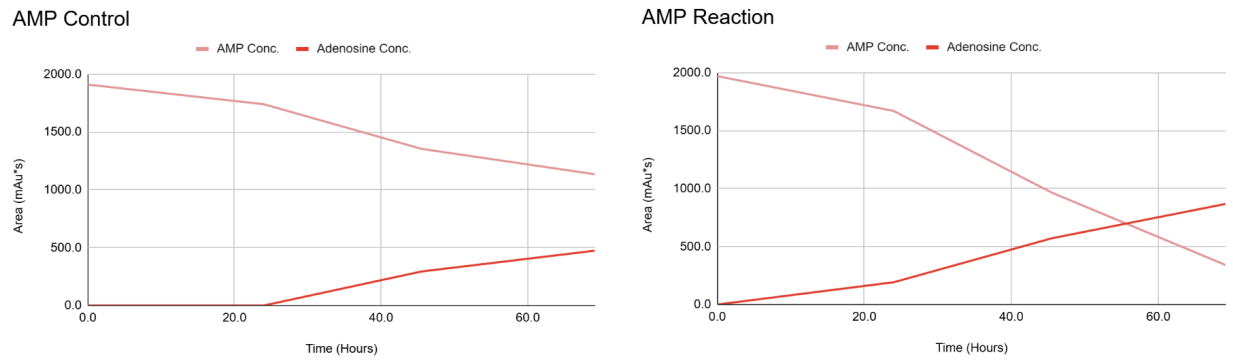

Figure 57: Time-course HPLC analysis of AMP control and AMP reaction samples.

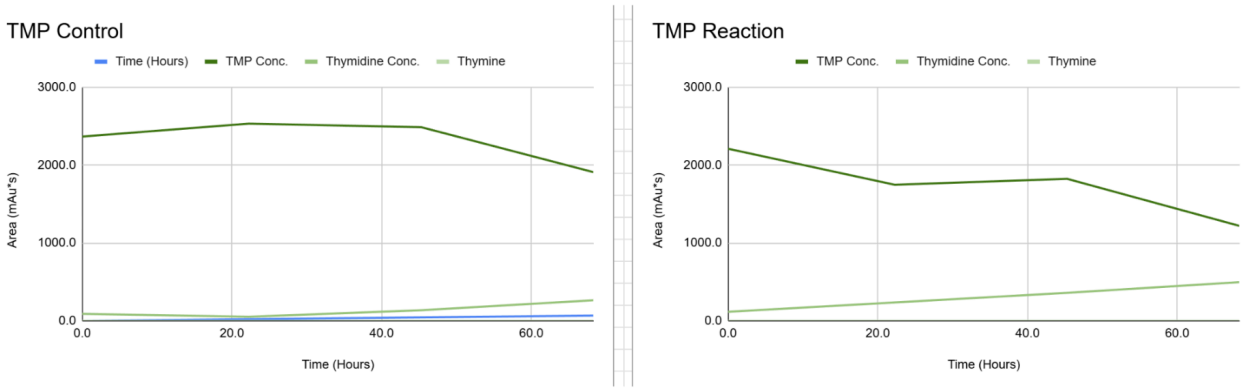

Figure 58: Time-course HPLC analysis of TMP control and TMP reaction samples.

Stability of the TunG Protein

Protein stability was assessed by incubating TunG in reaction buffer without substrate prior to initiating the reaction by substrate spiking. In the first experiment, UMP was added after 46.5 hours of protein incubation at room temperature, resulting in rapid UMP depletion and normal accumulation of uridine and uracil (Figure 59). A second experiment using a shorter pre-incubation period of 22.4 hours produced a comparable reaction profile (Figure 60).

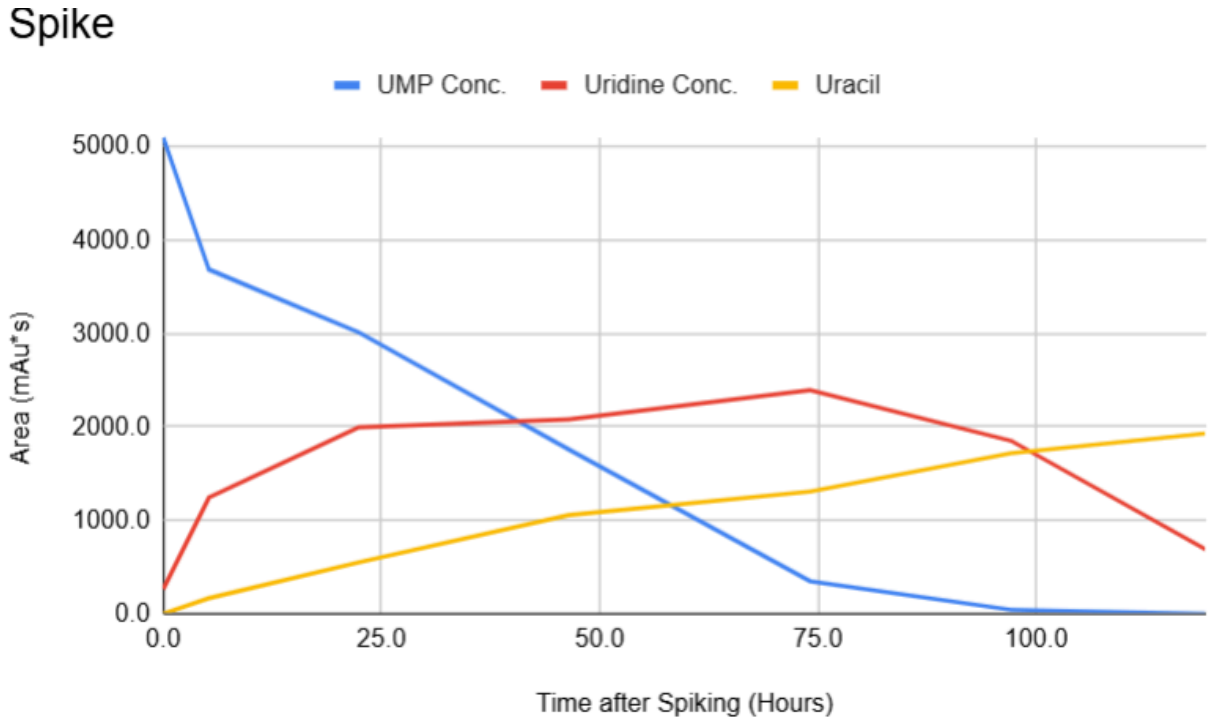

Figure 59: TunG stability assay following substrate spiking after 46.5 hours of protein incubation without substrate.

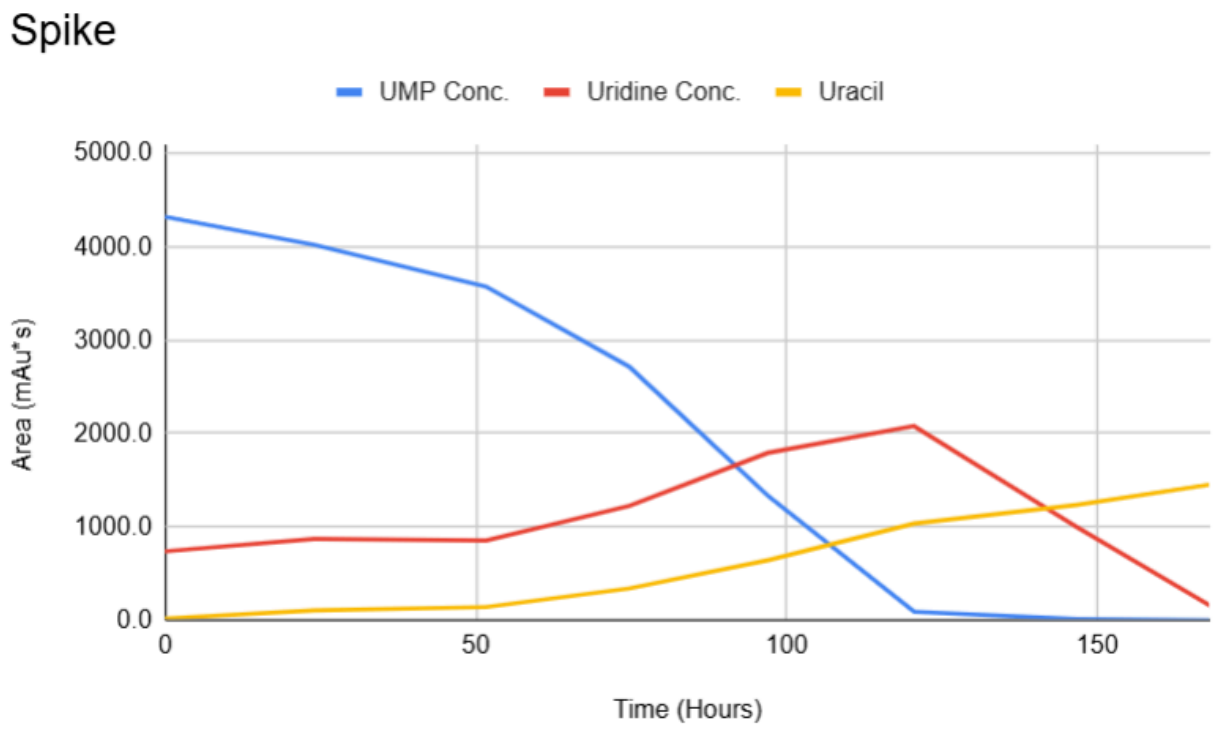

Figure 60: TunG stability assay following substrate spiking after 22.4 hours of protein incubation without substrate.

In both cases, there was an immediate onset of substrate turnover following spiking.

Reaction Profiles for Diphosphate and Triphosphate Uridine Substrates

To evaluate TunG activity toward higher-order uridine nucleotides, time-course reactions were performed using uridine diphosphate (UDP), uridine triphosphate (UTP), and uridine 5′-diphospho-N-acetylglucosamine (UDP-GlcNAc) as substrates.

Across all three substrates, substantial amounts of starting material remained detectable even after extended incubation periods of up to 600 hours. In UDP reactions, the parent nucleotide persisted throughout the time course, with only limited accumulation of downstream uridine or uracil products (Figure 61). Similarly, UTP reactions showed minimal depletion of the triphosphate substrate and little to no showcase of efficient conversion to lower-phosphate or nucleoside species (Figure 62).

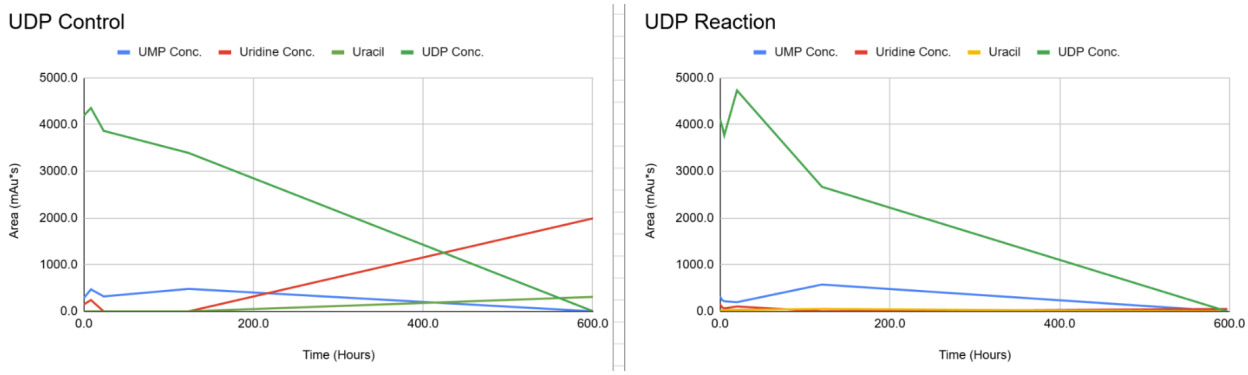

Figure 61: This figure shows the UDP reaction time course. HPLC time-course analysis of UDP incubated with TunG shows persistence of UDP signal with minimal formation of downstream uridine or uracil products over extended incubation.

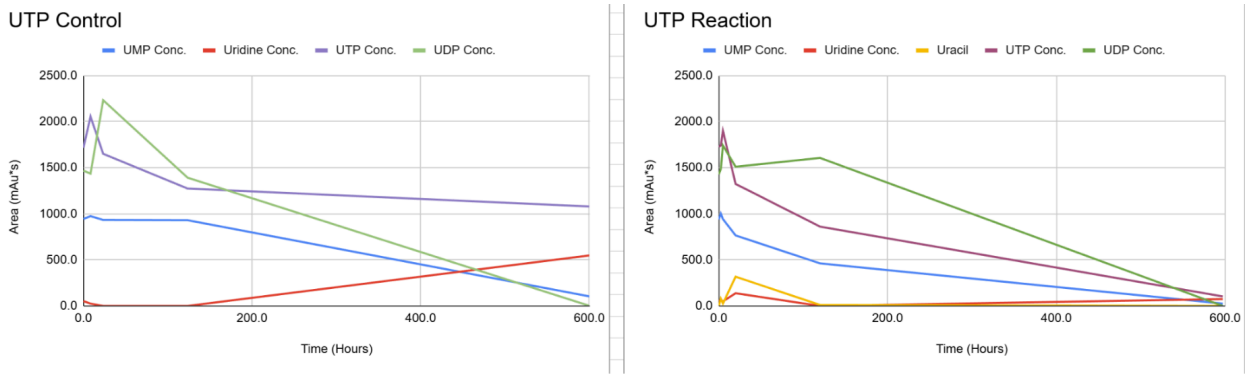

Figure 62: This figure shows the UTP reaction time course. Chromatographic profiles of UTP reactions demonstrate sustained UTP signal with little depletion or conversion to lower-phosphate or nucleoside species during long-term incubation with TunG.

Reactions containing UDP-GlcNAc also retained significant levels of intact substrate after 600 hours at room temperature (Figure 63). Only minor changes in chromatographic profiles were observed over time.

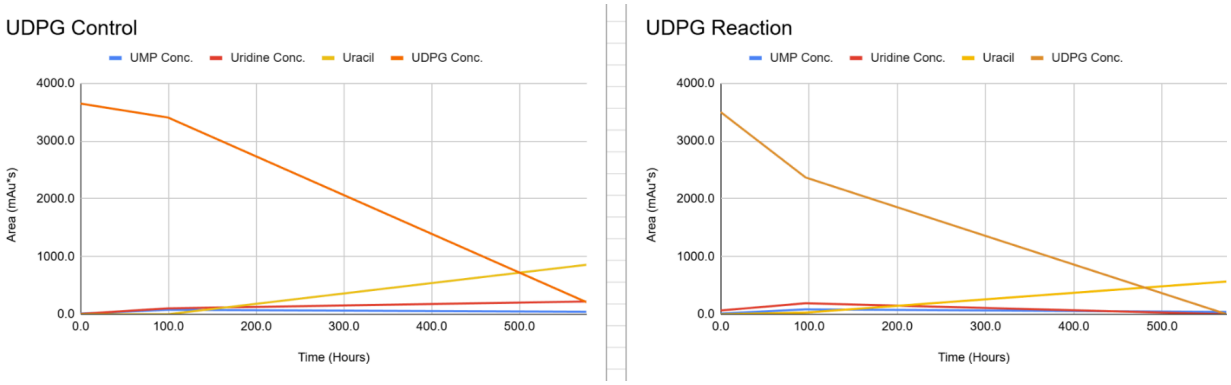

Figure 63: This figure shows the UDP-GlcNAc reaction time course. HPLC analysis of UDP-GlcNAc reactions reveals substantial retention of intact substrate after prolonged incubation at room temperature, with minimal product accumulation.

VII. Discussion

Summary of Key Findings

The goal of this study was to characterize the biochemical function of the TunG protein, a putative enzyme in the tunicamycin biosynthetic pathway. Recombinant expression and purification of the TunG protein were achieved using a T7-based expression system, and enzymatic activity was evaluated through time-course HPLC analysis of nucleotide substrates under a range of reaction conditions.

Although consistent nucleotide turnover was observed in multiple assays, several lines of evidence suggest that the catalytic activity detected in these experiments does not originate primarily from the TunG protein itself. Instead, the results are most consistent with activity from endogenous *E. coli* nucleotidases that co-purified with the TunG protein during nickel affinity chromatography. Likely candidates include YfbR (~22 kDa), SurE (~26 kDa), and YjjG (~29 kDa), all of which are known nucleotide-processing enzymes present in *E. coli*.[41]

SDS-PAGE analysis of purified samples revealed multiple protein bands in addition to the expected TunG band (~22–23 kDa), including bands corresponding to molecular weight ranges consistent with these endogenous nucleotidases. In particular, the overlap in molecular weight between TunG and YfbR complicates their separation, while additional bands at higher molecular weights are consistent with the presence of SurE and YjjG. Together, these observations support the conclusion that the enzymatic activity detected in this study arises from co-purified host enzymes rather than intrinsic catalytic activity of the TunG protein.

Evidence for Co-Purification of Endogenous E. coli Nucleotidases

SDS–PAGE analysis of purified protein fractions revealed that the TunG protein was not isolated to homogeneity. In addition to a band corresponding to the expected molecular weight of TunG (~22.7 kDa), multiple additional protein bands were consistently present in the elution fractions (Figure 44). These bands persisted despite dialysis and indicate that endogenous *E. coli* proteins co-purified with TunG.

This observation is significant because *E. coli* is known to encode several cytosolic nucleotidases capable of dephosphorylating nucleotide substrates. Proudfoot et al. systematically characterized three such enzymes, SurE, YfbR, and YjjG, and demonstrated that they exhibit overlapping yet distinct substrate specificities and metal cofactor preferences.[41] Any of these enzymes could plausibly account for the nucleotide transformations observed in this study.

Influence of Reaction Conditions on Observed Activity

Systematic variation of reaction conditions provided additional insight into the nature of the observed enzymatic activity. Reactions performed at 28 °C consistently exhibited faster conversion of UMP to downstream products than those conducted at 37 °C, where uridine never surpassed UMP in concentration (Figure 53). Similarly, reactions at pH 7.0 showed substantially greater turnover than those conducted at pH 6.0 or pH 8.0, conditions under which UMP remained the dominant species throughout the time course (Figure 54).

These trends are consistent with the behavior of native *E. coli* metabolic enzymes, which typically exhibit maximal activity near physiological temperature and neutral pH. In contrast, enzymes involved in specialized secondary metabolism, such as antibiotic biosynthesis, often display narrower or shifted optima. The strong dependence on near-physiological conditions therefore further supports the conclusion that the dominant activity observed in these assays reflects endogenous *E. coli* enzymes rather than the TunG protein.

Changes in enzyme concentration also produced effects that were inconsistent with simple single-enzyme kinetics. While reducing the volume of enzyme aliquot slowed reactions overall, the magnitude of the change was smaller than expected if the TunG protein were the sole catalytic species (Figure 52). This behavior again suggests that activity may be limited by the abundance or stability of a contaminating enzyme rather than by the concentration of the TunG protein itself.

Comparison of Observed Activity with Known E. coli Nucleotidases

The activity observed in this study shows strong preference for ribonucleoside monophosphates (UMP and AMP), slower turnover of TMP, and minimal activity toward diphosphate and triphosphate substrates (Figures 50, 57, and 58). This pattern is inconsistent with YfbR, which is strictly specific for deoxyribonucleoside 5′-monophosphates and therefore would not be expected to efficiently process UMP or AMP.[41]

YjjG, by contrast, exhibits narrow specificity for 5′-UMP, 5′-dUMP, and 5′-dTMP, and does not act on AMP.[41] Because AMP reacted at a rate comparable to UMP in these experiments, YjjG alone cannot explain the observed activity.

SurE displays broad phosphatase activity and can dephosphorylate a wide range of ribo- and deoxyribonucleoside monophosphates, with highest affinity for 3′-AMP.[41] The comparable rates observed for UMP and AMP in this study are most consistent with SurE-like behavior, although the exact specificity does not match perfectly.

Taken together, the substrate profile suggests that the observed activity likely reflects a mixture of endogenous nucleotidases, rather than a single enzyme species.

Metal Cofactor Preferences

Metal ion dependence provides additional evidence supporting contamination by *E. coli* nucleotidases. Proudfoot et al. reported the following cofactor preferences:[41]

SurE: $Mn^{2+} > Co^{2+} > Ni^{2+} > Mg^{2+}$

YfbR: $Co^{2+} > Mn^{2+} > Cu^{2+}$

YjjG: $Mg^{2+} > Mn^{2+} > Co^{2+}$

In the H-aliquots analyzed in this study, cobalt supported the fastest reaction rates, manganese was intermediate, and magnesium was consistently the slowest (Figures 51 and 55). This pattern closely resembles the cofactor preference of YfbR, with possible contribution from SurE, and is inconsistent with YjjG, which prefers magnesium.

This metal ion dependence strongly supports the conclusion that the observed activity originates primarily from endogenous *E. coli* nucleotidases rather than from the TunG protein.

Uridine to Uracil Conversion and Possible Contributing Enzymes

In several reaction conditions, accumulation of uracil was observed following the appearance of uridine, indicating that at least one enzymatic activity capable of cleaving the ribose-uracil glycosidic bond was present in the reaction mixtures. The TunG protein is not predicted, based on sequence analysis or pathway context, to catalyze nucleoside hydrolysis. Instead, this observation suggests secondary processing by endogenous *E. coli* enzymes that co-purified with the recombinant protein.

Multiple *E. coli* enzymes have been reported to catalyze reactions involving nucleotides or nucleosides that could plausibly account for this behavior. UshA is a periplasmic 5′-nucleotidase with additional nucleosidase activity and has been shown to convert nucleotides to nucleosides and free bases under certain conditions[42]. NagD is a cytosolic haloacid dehalogenase-like phosphatase with broad substrate scope, including ribonucleotides[43]. More recently, UmpH has been characterized as a regulated ribonucleotide monophosphatase involved in uridine metabolism[44]. Additionally, the class B acid phosphatase AphA has been shown to act on a variety of phosphate-containing substrates, including nucleotide derivatives[45,47].

The appearance of uracil in these reactions is therefore most consistent with a multi-step process driven by contaminating *E. coli* enzymes rather than direct activity of the TunG protein. This interpretation aligns with the SDS-PAGE results showing the presence of multiple co-purifying proteins and underscores the difficulty of assigning catalytic function in partially purified systems.

Implications for the Identity of the Active Enzyme(s)

Comparison of substrate specificity and metal cofactor preference provides further evidence that the observed activity is unlikely to originate from the TunG protein. Among the three characterized *E. coli* nucleotidases described by Proudfoot et al., SurE, YfbR, and YjjG exhibit distinct biochemical profiles.[41] The rapid turnover of ribonucleotides relative to deoxyribonucleotides, combined with comparable reaction rates for UMP and AMP, rules out YjjG, which does not act on AMP, and YfbR, which is specific for deoxyribonucleotides.

Metal dependence provides additional resolution. The strongest activity observed in the H aliquots occurred in the presence of cobalt, followed by manganese, with magnesium supporting the slowest reactions. This trend closely matches the reported metal preference of YfbR and partially overlaps with that of SurE, while being inconsistent with YjjG, which prefers magnesium.[41] Taken together, the data suggest that the observed activity likely reflects a mixture of endogenous nucleotidases, with enzymes resembling YfbR and SurE contributing most strongly under the tested conditions.

Implications for the Function of the TunG Protein

Although the results do not support a role for the TunG protein as a simple nucleotide monophosphatase under the conditions tested, this negative result is itself informative. Bioinformatic analyses and pathway reconstructions place the TunG protein early in the tunicamycin biosynthetic pathway, where it is unlikely to function as a general metabolic enzyme. Instead, TunG may act on a specialized substrate or generate a transient intermediate that is not stable in isolation.

It is possible that the His tag on the protein is in some way inhibiting its activity to dephosphorylate UMP. This process is highly variable and not every protein can handle having a His tag on it, and the TunG protein may have its active site inhibited by the presence of the His tag due to slight alterations in its conformation.

Another possibility is that the TunG protein produces a high-energy or short-lived species, such as a cyclic nucleotide, that is normally transferred directly to a downstream enzyme in vivo. In the absence of this partner protein, the intermediate may rapidly decompose or revert to starting material, leaving no detectable signature in HPLC-based assays. This type of substrate channeling is well documented in complex biosynthetic pathways and would be consistent with the inability to observe TunG-specific products in vitro.

An alternative explanation is that UMP and related nucleotides are not the true substrates of the TunG protein. If the TunG protein instead acts on a modified nucleotide, sugar-phosphate intermediate, or activated precursor unique to tunicamycin biosynthesis, then assays using common cellular nucleotides would be unlikely to reveal its activity.

VIII. Future Directions and Experimental Improvements

Future work should focus on improving both the biochemical purity of the TunG protein and the relevance of the substrates tested. Additional expression trials using prolonged low-temperature induction (for example, several days at 15 °C) followed by multiple freezing and thawing procedures may improve protein folding and reduce aggregation. Refinement of the lysis procedure, such as combining controlled lysozyme treatment with gentler mechanical disruption, could reduce the release of endogenous nucleotidases while preserving TunG protein solubility.

Incorporation of a protease-cleavable His-tag would allow removal of the affinity tag following purification, addressing the possibility that the tag interferes with TunG protein activity or substrate binding. Tandem purification strategies or negative selection against known *E. coli* nucleotidases could further improve sample purity.

Finally, expanded substrate screening informed by pathway logic, combined with more sensitive detection methods such as mass spectrometry or rapid-quench experiments, may be required to detect unstable or low-abundance intermediates. Co-expression or in vitro reconstitution of the TunG protein with downstream pathway enzymes represents an especially promising avenue for uncovering its true biochemical role.

IX. Conclusion

By narrowing the range of plausible biochemical functions for the TunG protein, this study provides meaningful experimental evidence that refines current models of the tunicamycin biosynthetic pathway. The results presented here strongly support the conclusion that the observed nucleotide turnover arises from co-purified endogenous *E. coli* nucleotidases rather than intrinsic TunG activity, indicating that the TunG protein does not function as a general nucleotide monophosphatase under the conditions tested.

Importantly, the limitations of this study, particularly the persistence of co-purifying enzymes, do not diminish its significance but instead contribute to the identification of TunG's role through a process of elimination. Even in the absence of definitive catalytic activity, the combined analysis of substrate specificity, metal ion dependence, and reaction conditions constrains the functional possibilities for TunG and provides a clearer framework for future investigation.

These findings highlight the critical importance of improved purification strategies and more controlled experimental systems for accurately characterizing pathway-specific enzymes. By refining our understanding of TunG and its place within tunicamycin biosynthesis, this work contributes to broader efforts aimed at engineering tunicamycin-derived compounds with reduced toxicity and enhanced antibacterial efficacy. Such advances are particularly important in the context of the global antimicrobial resistance crisis, where the development of novel or optimized antibiotic scaffolds remains an urgent priority.

Antimicrobial resistance continues to erode the effectiveness of existing antibiotics, underscoring the urgent need to understand and exploit alternative biosynthetic pathways for

drug development. Tunicamycin and its modified analogs represent a promising class of antibiotics whose clinical potential depends on a detailed understanding of their biosynthesis. This study sought to experimentally characterize the function of the TunG protein, a poorly understood enzyme proposed to act early in the tunicamycin biosynthetic pathway.

Recombinant expression and purification of the TunG protein in *E. coli* successfully produced soluble protein, as confirmed by SDS-PAGE analysis. However, these analyses also revealed the presence of co-purifying *E. coli* proteins, indicating that the resulting samples were not enzymatically pure. This lack of purity is particularly challenging because many endogenous *E. coli* proteins, especially nucleotidases, share similar molecular weights and binding properties, allowing them to co-elute with His-tagged TunG protein during nickel affinity purification. As a result, any observed enzymatic activity cannot be definitively attributed to the TunG protein itself, making it difficult to distinguish true TunG protein function from background activity of contaminating proteins. Achieving higher levels of protein purity is therefore essential for accurately determining the biochemical function of TunG, as it would allow enzymatic activity to be definitively attributed to the protein of interest rather than to co-purifying endogenous enzymes. Improvements in cell lysis methods, such as the use of a French press, and the implementation of more stringent purification strategies will be critical for isolating functionally pure TunG protein.

Subsequent HPLC-based activity assays showed nucleotide turnover across multiple substrates and reaction conditions, but comparable activity was observed in both pET^{+} and pET^{-} samples. Together with the observed metal ion preferences, substrate specificities, and

temperature and pH dependencies, these results strongly suggest that the detected activity originated from endogenous *E. coli* nucleotidases rather than from the TunG protein itself.

Comparison of the experimental data with known biochemical profiles of *E. coli* nucleotidases supports this conclusion. The observed activity patterns are inconsistent with YjjG, partially consistent with the SurE protein, and most closely aligned with YfbR-like behavior, particularly with respect to cobalt dependence and ribonucleotide turnover. Additionally, the formation of uracil from uridine is best explained by secondary processing from native cellular enzymes rather than direct TunG catalysis. As such, this work provides compelling evidence that the TunG protein does not function as a general nucleotide monophosphatase under the conditions tested.

Importantly, the absence of a clear TunG-specific activity does not negate its proposed role in tunicamycin biosynthesis. Instead, the results support alternative models in which the TunG protein acts on a specialized or unstable substrate, generates a transient intermediate that requires immediate downstream processing, or functions only within a multi-enzyme complex. These possibilities are consistent with the behavior of enzymes in complex secondary metabolic pathways and highlight the limitations of studying such proteins in isolation.

Future work should focus on achieving higher levels of protein purity, exploring alternative expression systems, and reconstituting the biosynthetic pathway in more native or controlled environments to definitively resolve the TunG protein's function. In particular, implementing alternative affinity purification strategies in which TunG is expressed as a fusion protein with a glutathione-binding tag and purified using glutathione-based affinity chromatography may help reduce co-purification of endogenous proteins and improve isolation

of functionally active TunG protein. More broadly, continued investment in antibiotic research and increased awareness of the clinical and economic consequences of antimicrobial resistance will be essential for driving innovation at both the scientific and policy levels.

Overall, this work refines the functional landscape of the tunicamycin biosynthetic pathway by experimentally excluding several plausible but incorrect models for TunG activity. It establishes a framework for future studies aimed at improving protein purity, identifying biologically relevant substrates, and reconstituting pathway-specific enzyme interactions. By narrowing the range of possible biochemical roles for the TunG protein, this study contributes meaningful experimental insight toward the long-term goal of engineering novel tunicamycin-derived antibiotics capable of addressing the growing threat of antimicrobial resistance.

X. References

[1] Anderson MS, Eveland SS, Price NP. 2000. Conserved cytoplasmic motifs that distinguish sub-groups of the polyprenol phosphate:N-acetylhexosamine-1-phosphate transferase family. FEMS Microbiol Lett. 191(2):169–175. https://doi.org/10.1111/j.1574-6968.2000.tb09335.x

[2] Basics: centrifugal force & centrifuge type – Eppendorf US. 2019 Jul 22. https://www.eppendorf.com/us-en/lab-academy/life-science/cell-biology/basics-in-centrifugation/

[3] Centers for Disease Control and Prevention (CDC). 2019. Antibiotic resistance threats in the United States, 2019. Atlanta (GA): CDC. https://doi.org/10.15620/cdc:82532

[4] Chavan S, Olsson T, Nyman G. 2025. Structure based prediction of selective MraY inhibitors. J Mol Graph Model. 138:109053. https://doi.org/10.1016/j.jmgm.2025.109053

[5] Chen W, Qu D, Zhai L, et al. 2010. Characterization of the tunicamycin gene cluster unveiling unique steps involved in its biosynthesis. Protein Cell. 1(12):1093–1105. https://doi.org/10.1007/s13238-010-0127-6

[6] Colombatti Olivieri MA, Cassmann ED, Jackson MA, Price NPJ, Bannantine JP. 2025. TunR2, a novel mode-of-action tunicamycin-type antibiotic: pharmacokinetics in C57BL/6

mouse and Holstein cattle. PLOS One. 20(7):e0327932.
https://doi.org/10.1371/journal.pone.0327932

[7] Colombatti Olivieri MA, Price NPJ, Jackson MA, Bannantine JP. 2025. Evaluation of the cytotoxicity and antibacterial activity of a synthetic tunicamycin derivative against Mycobacterium avium complex. Front Microbiol. 16.
https://doi.org/10.3389/fmicb.2025.1604400

[8] COVID-19: U.S. impact on antimicrobial resistance, special report 2022. 2022. National Center for Emerging and Zoonotic Infectious Diseases. https://doi.org/10.15620/cdc:117915

[9] Davis JM, Clay H, Lewis JL, Ghori N, Herbomel P, Ramakrishnan L. 2002. Real-time visualization of mycobacterium–macrophage interactions leading to initiation of granuloma formation in zebrafish embryos. Immunity. 17(6):693–702.
https://doi.org/10.1016/S1074-7613(02)00475-2

[10] DIY chemically competent cells: easy 10-step protocol. n.d. Accessed Oct 27, 2025.
https://bitesizebio.com/30145/chemically-competent-cells/

[11] Dubendorf JW, Studier FW. 1991. Controlling basal expression in an inducible T7 expression system by blocking the target T7 promoter with lac repressor. J Mol Biol. 219(1):45–59. https://doi.org/10.1016/0022-2836(91)90856-2

[12] Fuhrman J, Polleys E, Mattaini K. 2024. pET expression system. Biology LibreTexts. https://bio.libretexts.org/Bookshelves/Biotechnology/Encyclopedia_of_Biological_Methods_(Mattaini)/23%3A_pET_Expression_System

[13] Gheibihayat SM, Farahani N, Golichenari B. 2018. Recombinant protein expression in Escherichia coli: what we need to know. Curr Protein Pept Sci. https://doi.org/10.2174/1381612824666180131121940

[14] Heat shock transformation (E. coli) protocol. 2021 Dec 2. https://sharebiology.com/heat-shock-transformation-e-coli-protocol/

[15] Heifetz A, Keenan RW, Elbein AD. 1979. Mechanism of action of tunicamycin on the UDP-GlcNAc:dolichyl-phosphate GlcNAc-1-phosphate transferase. Biochemistry. 18(11):2186–2192. https://doi.org/10.1021/bi00578a008

[16] HisPur Ni-NTA resin user guide. n.d.

[17] Ibrahim HR, Aoki T, Pellegrini A. 2002. Strategies for new antimicrobial proteins and peptides: lysozyme and aprotinin as model molecules. Curr Pharm Des. 8(9):671–693. https://doi.org/10.2174/1381612023395349

[18] Kapp U, Macedo S, Hall DR, Leiros I, McSweeney SM, Mitchell E. 2008. Structure of Deinococcus radiodurans tunicamycin-resistance protein (TmrD), a phosphotransferase. Acta Crystallogr F. 64(Pt 6):479–486. https://doi.org/10.1107/S1744309108011822

[19] Kelly JM, Sterry SJ, Cose S, et al. 1993. Identification of conserved T cell receptor CDR3 residues contacting known exposed peptide side chains from a major histocompatibility complex class I-bound determinant. Eur J Immunol. 23(12):3318–3326. https://doi.org/10.1002/eji.1830231239

[20] Laemmli UK. 1970. Cleavage of structural proteins during the assembly of the head of bacteriophage T4. Nature. 227(5259):680–685. https://doi.org/10.1038/227680a0

[21] Latest global cancer data: cancer burden rises to 19.3 million new cases. 2020.

[22] Macherey-Nagel. 2011. Purification of His-tag proteins.

[23] Murray CJL, Ikuta KS, Sharara F, et al. 2022. Global burden of bacterial antimicrobial resistance in 2019: a systematic analysis. Lancet. 399(10325):629–655. https://doi.org/10.1016/S0140-6736(21)02724-0

[24] Ni-NTA His-tag protein purification. n.d. https://www.biorender.com/template/ni-nta-his-tag-protein-purification

[25] Nonarath HJT, Jackson MA, Penoske RM, Zahrt TC, Price NPJ, Link BA. 2024. The tunicamycin derivative TunR2 exhibits potent antibiotic properties with low toxicity in an in vivo Mycobacterium marinum zebrafish TB infection model. J Antibiot. 77(4):245–256. https://doi.org/10.1038/s41429-023-00694-z

[26] OpenLearn. n.d. Understanding antibiotic resistance. Accessed Oct 30, 2025. https://www.open.edu/openlearn/mod/oucontent/view.php?id=82297&section=_unit3.2.1

[27] Overall CM. 1987. A microtechnique for dialysis of small volume solutions with quantitative recoveries. Anal Biochem. 165(1):208–214. https://doi.org/10.1016/0003-2697(87)90221-1

[28] Petty KJ. 2001. Metal-chelate affinity chromatography. Curr Protoc Neurosci. Unit 5.10. https://doi.org/10.1002/0471142301.ns0510s05

[29] Price NPJ, Hartman TM, Li J, et al. 2017. Modified tunicamycins with reduced eukaryotic toxicity that enhance the antibacterial activity of β-lactams. J Antibiot. 70(11):1070–1077. https://doi.org/10.1038/ja.2017.101

[30] Principles, classifications and applications of centrifuges. n.d. Accessed Oct 27, 2025. https://www.iqsdirectory.com/articles/centrifuge.html

[31] Sapkota A. 2021 May 19. Bacterial transformation: definition, principle, steps, examples. https://microbenotes.com/bacterial-transformation/

[32] Takatsuki A, Arima K, Tamura G. 1971. Tunicamycin, a new antibiotic. I. Isolation and characterization of tunicamycin. J Antibiot. 24(4):215–223. https://doi.org/10.7164/antibiotics.24.215

[33] Troubleshooting His-tagged protein binding to Ni-NTA columns. n.d. Accessed Oct 27, 2025. https://blog.interchim.com/troubleshooting-his-protein-ni-nta-columns/

[34] Tsvetanova BC, Kiemle DJ, Price NPJ. 2002. Biosynthesis of tunicamycin and metabolic origin of the 11-carbon dialdose sugar, tunicamine. J Biol Chem. 277(38):35289–35296. https://doi.org/10.1074/jbc.M201345200

[35] Wang H. n.d. Semi-synthesis and biological evaluations of tunicamycin lipid analogues and investigation of the tunicamycin biosynthetic pathway.

[36] What is HPLC (high performance liquid chromatography)? n.d. Accessed Oct 27, 2025. https://www.shimadzu.com/an/service-support/technical-support/analysis-basics/basic/what_is_hplc.html

[37] Widdick D, Royer SF, Wang H, et al. 2018. Analysis of the tunicamycin biosynthetic gene cluster of Streptomyces chartreusis reveals new insights into tunicamycin production and immunity. Antimicrob Agents Chemother. 62(8):e00130-18. https://doi.org/10.1128/AAC.00130-18

[38] Wyszynski FJ, Hesketh AR, Bibb MJ, Davis BG. 2010. Dissecting tunicamycin biosynthesis by genome mining: cloning and heterologous expression of a minimal gene cluster. Chem Sci. 1(5):581. https://doi.org/10.1039/c0sc00325e

[39] Wyszynski FJ, Lee SS, Yabe T, et al. 2012. Biosynthesis of the tunicamycin antibiotics proceeds via unique exo-glycal intermediates. Nat Chem. 4(7):539–546. https://doi.org/10.1038/nchem.1351

[40] Liu Y, et al. Method of sequence optimization for improved recombinant protein expression using a particle swarm optimization algorithm. US Patent 8,326,547. Issued December 4, 2012.

[41] Proudfoot, Michael, Ekaterina Kuznetsova, Greg Brown, N. N. Rao, Masaru Kitagawa, Hirotada Mori, Alexei Savchenko, and Alexander F. Yakunin. 2004. “General Enzymatic Screens Identify Three New Nucleotidases in Escherichia coli.” Journal of Biological Chemistry 279 (52): 54687–94. https://doi.org/10.1074/jbc.M411023200

[42] Zakataeva, Natalia P. 2021. “Microbial 5′-Nucleotidases: Their Characteristics, Roles in Cellular Metabolism, and Possible Practical Applications.” Applied Microbiology and Biotechnology 105 (20): 7661–81. https://doi.org/10.1007/s00253-021-11547-w

[43] Tremblay, Lee W., Debra Dunaway-Mariano, and Karen N. Allen. 2006. “Structure and Activity Analyses of Escherichia coli K-12 NagD Provide Insight into the Evolution of Biochemical Function in the Haloalkanoic Acid Dehalogenase Superfamily.” Biochemistry 45 (4): 1183–93. https://doi.org/10.1021/bi051842j

[44] Aparecida Gonçalves, Ana Carolina, Tatiana de Mello Damasco Nunes, Erick Parize, et al. 2024. “The Activity of the Ribonucleotide Monophosphatase UmpH Is Controlled by Interaction with the GlnK Signaling Protein in Escherichia coli.” Journal of Biological Chemistry 300 (12): 107931. https://doi.org/10.1016/j.jbc.2024.107931

[45] Thaller, Maria Cristina, Serena Schippa, Alessandra Bonci, Stefania Cresti, and Gian Maria Rossolini. 1997. “Identification of the Gene (aphA) Encoding the Class B Acid Phosphatase/Phosphotransferase of Escherichia coli MG1655 and Characterization of Its Product.” FEMS Microbiology Letters 146 (2): 191–98. https://doi.org/10.1111/j.1574-6968.1997.tb10192.x

[46] Passariello, Claudio, Costantino Forleo, Vanna Micheli, et al. 2006. “Biochemical Characterization of the Class B Acid Phosphatase (AphA) of Escherichia coli MG1655.”

Biochimica et Biophysica Acta (BBA) – Proteins and Proteomics 1764 (1): 13–19. https://doi.org/10.1016/j.bbapap.2005.08.028

[47] UniProt Consortium. n.d. “AphA (Escherichia coli K-12).” UniProt Knowledgebase. Accessed February 8, 2026. https://www.uniprot.org/uniprotkb/P0AE22/entry

[48] Hutchings MI, Truman AW, Wilkinson B. Antibiotics: past, present and future. Trends Microbiol. 2019. https://www.sciencedirect.com/science/article/pii/S1369527419300190

[49] Nicolaou KC, Rigol S. A brief history of antibiotics and select advances in their synthesis. J Antibiot (Tokyo). 2018;71:153–184. https://www.nature.com/articles/ja201762

[50] Gaynes R. The Discovery of Penicillin—New Insights After More Than 75 Years of Clinical Use. Emerg Infect Dis. 2017. https://pmc.ncbi.nlm.nih.gov/articles/PMC5403050/

[51] Davies J, Davies D. Origins and Evolution of Antibiotic Resistance. Microbiol Mol Biol Rev. 2010. https://pmc.ncbi.nlm.nih.gov/articles/PMC2937522/

[52] Hunt D. A Brief History of Antimicrobial Resistance. AMA J Ethics. 2024. https://journalofethics.ama-assn.org/article/brief-history-antimicrobial-resistance/2024-05

[53] World Health Organization. Global action plan on antimicrobial resistance. 2015. https://iris.who.int/bitstream/handle/10665/193736/9789241509763_eng.pdf

[54] O'Neill J. Tackling a crisis for the health and wealth of nations. Review on Antimicrobial Resistance. 2014/2016 (final paper). https://amr-review.org/sites/default/files/AMR%20Review%20Paper%20-%20Tackling%20a%20crisis%20for%20the%20health%20and%20wealth%20of%20nations_1.pdf

[55] World Health Organization. Antimicrobial resistance (Fact sheet). Updated Nov 21, 2023. https://www.who.int/news-room/fact-sheets/detail/antimicrobial-resistance

[56] Murray CJL, Ikuta KS, Sharara F, et al. Global burden of bacterial antimicrobial resistance in 2019: a systematic analysis. Lancet. 2022;399(10325):629–655. https://doi.org/10.1016/S0140-6736(21)02724-0

[57] CDC. Antibiotic Resistance Threats in the United States, 2019. https://www.cdc.gov/antimicrobial-resistance/data-research/threats/index.html

[58] Chen W, Qu D, Zhai L, et al. Characterization of the tunicamycin gene cluster… Protein Cell. 2010. https://pmc.ncbi.nlm.nih.gov/articles/PMC4875072/

[59] Wyszynski FJ, Hesketh AR, Bibb MJ, Davis BG. Dissecting tunicamycin biosynthesis by genome mining. Chem Sci. 2010. https://pubs.rsc.org/en/content/articlelanding/2010/sc/c0sc00325e

[60] WHO. 2023 Antibacterial agents in clinical and preclinical development: an overview and analysis. Published Jun 14, 2024. https://www.who.int/publications/i/item/9789240094000

[61] Manning D, et al. The challenges and opportunities of developing small molecule inhibitors… (includes tunicamycin/MraY selectivity + toxicity discussion). 2023. https://pmc.ncbi.nlm.nih.gov/articles/PMC11250723/

[62] Mashalidis EH, et al. Structures of bacterial MraY and human GPT provide insights… 2020. https://pmc.ncbi.nlm.nih.gov/articles/PMC8351759/

[63] Nonarath HJT, Jackson MA, Penoske RM, Zahrt TC, Price NPJ, Link BA. The tunicamycin derivative TunR2 exhibits potent antibiotic properties with low toxicity… J Antibiot. 2024. https://pmc.ncbi.nlm.nih.gov/articles/PMC11403873/

[64] CDC. COVID-19: U.S. Impact on Antimicrobial Resistance, Special Report 2022. https://www.cdc.gov/antimicrobial-resistance/media/pdfs/covid19-impact-report-508.pdf

[65] WHO. Global antibiotic resistance surveillance report 2025. Published Oct 13, 2025. https://www.who.int/publications/i/item/9789240116337

[66] Price NPJ, Hartman TM, Li J, et al. Modified tunicamycins with reduced eukaryotic toxicity that enhance the antibacterial activity of β-lactams. J Antibiot. 2017. https://www.nature.com/articles/ja2017101

[67] Antimicrobial Resistance Collaborators. (2024). Global burden of bacterial antimicrobial resistance in 2021: A systematic analysis. The Lancet, 403(10440), 1234–1263. https://doi.org/10.1016/S0140-6736(24)01867-1